

TECHNISCHE UNIVERSITÄT MÜNCHEN

Lehrbereich Anorganische Chemie, Lehrstuhl für Bauchemie

**Colloidal behavior of casein biopolymer in  
alkaline solution and its application in  
self-levelling underlayments (SLUs)**

**Hang Bian**

Vollständiger Abdruck der von der Fakultät für Chemie der Technischen Universität München zur  
Erlangung des akademischen Grades eines

**Doktors der Naturwissenschaften (Dr. rer. nat.)**

genehmigten Dissertation.

Vorsitzender:

Univ.-Prof. Dr. Volker A. Sieber

Prüfer der Dissertation:

1. Univ.-Prof. Dr. Johann P. Plank

2. Univ.-Prof. Dr. Johannes Buchner

Die Dissertation wurde am 16.02.2012 bei der Technischen Universität München eingereicht und durch die  
Fakultät für Chemie am 19.03.2012 angenommen.



## Acknowledgement

This thesis is dedicated to my parents. Motivated by their deepest love, I am capable of achieving success in studies and completing this thesis.

First of all, I would like to express my deep gratitude to Prof. Plank for honoring me an opportunity to work on my Ph.D in the chair of Construction Chemicals at TUM. I am grateful of him for offering me such an interesting project for my Ph.D study. Prof. Plank greatly impressed me with his wide knowledge, warm personality as well as the professional attitudes toward scientific work. I am lucky to be his student, receiving his inspiring supervision as well as endless encouragement. I deeply appreciate him for his understanding and consideration at the lowest point of my life. I could not complete my thesis without his important support. Thank you, Prof. Plank!

Many thanks go to Dr. Oksana Storcheva for her kindest help during my graduate study.

I would like to thank Dr. Roland Sieber, Dr. Wolfgang Seidl, Dr. Philip Andres for their supervision and helpful suggestions whenever I met problems during my study.

For the kind technical support, I would like to thank Richard Beiderbeck and Dagmar Lettrich.

For the fruitful cooperation and enlightening discussion, I would like to thank Dr. Bin Yu.

Here, I also would like to express my gratitude to Dr. Marianne Hanzlik for the splendid TEM measurements.

A special thank goes to Tobias Kornprobst for his efforts in translating the summary of this thesis into German.

Warm and heartfelt thanks go to my lab mates, Dr. Markus Gretz, Elina Dubina, GeokBee Serina Ng, Thomas Pavlitschek and Matthias Lesti for the harmonious lab atmosphere and outstanding teamwork. It is a great experience to work with them in the same lab.

Many thanks go to the other group members, Nan Zou, Johanna de Reese, Dr. Mirko Gruber, Friedrich von Hoessle, Dr. Fatima Dugonjic-Bilic, Dr. Christof Schröfl, Dr. Nadia Zouaoui, Dr. Bernhard Sachsenhauser, Vera Nilles, Helena Keller, Michael Glanzer-Heinrich, Ahmad Habbaba, Daniela Michler, Constantin Tiemeyer, Daniel Bülchen, Salami Oyewole Taye, Alex Lange, Markus Meier, Dr. Zongbin Zhao, Yu Jin, Xiaoxiao Du, Lei Lei, Stefan

Baueregger, Maïke Müller, Julia Pickelmann, Timon Echt, and Sebastian Foraita. I have learnt not only the academic knowledge but also the wonderful German culture from them. I will keep the unforgettable memories in heart all my life.

I am thankful for my friends in Munich Sisi, Liyi, Hai Bi, Mingdong, Wei Guo, Qin Guo, Haixia, Hua Li, Peng Li, Kun Wang, Weibin Wang, Xinjiao Wang, Lidong Wang and Lei Lei for the happy time in the past four years.

Lastly, I will give my special thank to my husband Ning Zhang for his endless support and love.

*To my family*

献给我的爸爸妈妈



## Scientific Publications

1. J. Plank, **H. Bian**, Method to assess the quality of casein used as superplasticizer in self-levelling compounds, *Cement and Concrete Research*, 40 (2010) 710-715.
2. B. Yu, **H. Bian**, J. Plank, Self-assembly and characterization of Ca-Al-LDH nanohybrids containing casein proteins as guest anions, *Journal of Physics and Chemistry Solids*, 71 (2010) 468-472.
3. **H. Bian**, J. Plank, Re-association behavior of casein submicelles in highly alkaline environment, submitted 2012 to *Zeitschrift für Naturforschung, Teil B*.
4. **H. Bian**, J. Plank, Effect of heat treatment on the dispersion performance of casein superplasticizer used in dry-mix mortar, submitted 2012 to *Cement and Concrete Research*.

## Conference papers

1. B. Yu, **H. Bian**, J. Plank, Self-assembly and characterization of Ca-Al-LDH nanohybrids containing casein proteins as guest anions, *15th International Symposium on Intercalation Compounds*, Beijing, 2009, 45.
2. **H. Bian**, J. Plank, Quality criteria for casein used in self-levelling compounds, *Annual conference of GDCh-Fachgruppe Bauchemie*, Dortmund, 2010, GDCh-Monography no. 42, 341-348.

## Poster

1. **H. Bian**, J. Plank, Quality criteria for casein used in self-levelling compounds, *Annual conference of GDCh-Fachgruppe Bauchemie*, Dortmund, Germany, 7-8 Oct 2010



## Table of Contents

<b>1 Introduction.....</b>	<b>1</b>
<b>2 Theoretical background .....</b>	<b>3</b>
<b>2.1 Casein protein .....</b>	<b>3</b>
2.1.1 Amino acid .....	3
2.1.2 Casein protein.....	6
2.1.2.1 Chemistry of casein.....	6
2.1.2.2 Ionization of casein .....	10
2.1.2.3 Micellar structure of casein.....	12
2.1.2.4 Interactions occurring in casein micelles .....	13
2.1.2.5 Stability of casein micelle .....	16
2.1.2.6 Technical applications of casein .....	20
2.1.3 Protein purification.....	21
2.1.3.1 Ion exchange chromatography .....	22
2.1.3.2 Size exclusion chromatography .....	24
2.1.3.3 Fast protein liquid chromatography (FPLC).....	24
<b>2.2 Casein superplasticizer .....</b>	<b>26</b>
2.2.1 Superplasticizers.....	26
2.2.2 Casein superplasticizer in self-levelling underlayments (SLUs) .....	30
2.2.2.1 Self-levelling underlayments (SLUs).....	30
2.2.2.2 Current research status of casein superplasticizer in SLUs .....	37
2.2.3 Disadvantages of casein superplasticizer .....	41
<b>2.3 Manufacture of casein.....</b>	<b>41</b>
<b>3 Objective of this work.....</b>	<b>44</b>
<b>4 Materials and methods .....</b>	<b>46</b>
<b>4.1 Materials.....</b>	<b>46</b>
4.1.1 Casein powder .....	46
4.1.2 Preparation of casein dispersions .....	46

4.1.3	Preparation of Ca-depleted casein dispersions.....	47
4.1.4	Preparation of casein dispersions containing NaCl at pH 12.....	47
4.1.5	Preparation of precipitate enriched in $\alpha$ - and $\beta$ -casein.....	48
4.1.6	Preparation of buffers for FPLC.....	48
4.1.7	Preparation of casein samples for FPLC .....	48
4.1.7.1	Preparation for chromatographic analysis.....	48
4.1.7.2	Preparation for large-scale separation of casein.....	49
4.1.8	SLU formulation .....	49
<b>4.2</b>	<b>Methods .....</b>	<b>52</b>
4.2.1	Turbidity.....	52
4.2.2	Transmission Electron Microscopy (TEM).....	52
4.2.3	Atomic absorption spectroscopy (AAS) .....	53
4.2.4	Particle Charge Detector (PCD).....	53
4.2.5	Fast protein liquid chromatography (FPLC) .....	54
4.2.6	Cross-flow filtration desalting.....	58
4.2.7	Atomic Force Microscopy (AFM) .....	59
4.2.8	Mini slump test.....	60
4.2.9	Total organic carbon (TOC) .....	60
4.2.10	Zeta potential.....	61
4.2.11	Moisture analyzer .....	62
4.2.12	Dynamic light scattering (DLS) .....	62
4.2.13	Gel permeation chromatography (GPC) .....	63
4.2.14	Thermogravimetry (TG).....	64
4.2.15	Ion chromatography (IC).....	64
<b>5</b>	<b>Results and discussion .....</b>	<b>66</b>
<b>5.1</b>	<b>Behavior of casein in alkaline solution .....</b>	<b>68</b>
5.1.1	Solubility of casein as a function of pH .....	68
5.1.2	Dissociation and re-association of casein in alkaline solution.....	69
5.1.2.1	Turbidity of alkaline casein solutions .....	69
5.1.2.2	TEM images of casein alkaline solutions .....	70
5.1.2.3	Surface charge of casein in alkaline solution.....	72
5.1.3	Influence of ionic strength on re-association of casein .....	74

5.1.4	The role of calcium in the re-association process .....	75
5.1.4.1	Turbidity of Ca-depleted casein in alkaline solution .....	77
5.1.4.2	Surface charge of Ca-depleted casein in alkaline solution.....	77
5.1.5	Interactions between casein proteins in alkaline solutions.....	79
5.1.6	Schematic for the dissociation and re-association process.....	81
5.1.7	Morphology of casein submicelles and micelles.....	85
5.1.7.1	Morphology of casein submicelles .....	85
5.1.7.2	Assembly of casein in the droplet.....	89
5.1.8	Conclusion.....	98
<b>5.2</b>	<b>Effect of protein composition on dispersing performance of casein superplasticizer.....</b>	<b>100</b>
5.2.1	Dispersing performance of casein superplasticizer .....	100
5.2.2	Quality criteria for dispersion effectiveness of casein .....	104
5.2.2.1	Fluctuation in quality of commercial casein samples .....	104
5.2.2.2	Method to assess the quality of casein superplasticizer.....	105
5.2.3	Conclusion.....	111
<b>5.3</b>	<b>Fractionation and modification of casein superplasticizer .....</b>	<b>113</b>
5.3.1	Casein fractions .....	113
5.3.2	Reconstituted casein superplasticizer.....	114
5.3.3	Modified casein samples .....	118
5.3.4	Conclusion.....	122
<b>5.4</b>	<b>Effect of heat treatment on the casein quality .....</b>	<b>123</b>
5.4.1	Moisture content of heat treated casein .....	124
5.4.2	Dispersion power of heat treated casein.....	125
5.4.3	Anionic charge of heat treated casein.....	127
5.4.4	GPC analysis of heat treated casein .....	130
5.4.5	FPLC analysis of heat treated casein.....	132
5.4.6	Thermal stability of casein superplasticizer .....	135
5.4.7	Conclusion.....	136
<b>6</b>	<b>Summary.....</b>	<b>137</b>
<b>7</b>	<b>Zusammenfassung.....</b>	<b>141</b>

**8 Reference ..... 145**

## Abbreviations

$K_a$	Dissociation constant
$\tau$	Turbidity
bwoc	By weight of cement
c	Concentration
d	Diameter
$\mu\text{eq/g}$	Microequivalent per gram
$\mu\text{L}$	Microliter
$\mu\text{m}$	Micrometer
nm	Nanometer
L	Liter
g	gram
cm	centimeter
mAu	Milli-arbitrary units
MPa	Megapascal
UV/Vis	Ultraviolet/visible
CCP	Colloidal calcium phosphate
PSD	Particle size distribution
DLS	Dynamic light scattering
PCD	Particle charge detector
DSC	Differential scanning calorimetry
TEM	Transmission electron microscopy
AAS	Atomic absorption spectroscopy
SEM	Scanning electron microscope
FPLC	Fast protein liquid chromatography
AFM	Atomic force microscopy
TOC	Total organic carbon
GPC	Gel permeation chromatography
SEC	Size exclusive chromatography
IC	Ion chromatography
TGA	Thermogravimetry
EDTA	Ethylenediaminetetraacetic acid
SLU	Self-levelling underlayment

SP	Superplasticizer
OPC	Ordinary Portland cement
CAC	Calcium aluminate cement
w/c	Water to cement ratio
h	Hour
min	minute
rpm	Rounds per minute
M	Molar (mol/L)
Da	Dalton
mV	Milli volt
S	Siemens
T	Temperatur
t	Time
wt. %	Weight percent
v/v	Volume ratio
R <sub>h</sub>	Hydrodynamic

## Chemical notation

In cement chemistry, chemical formulae are often expressed as sums of oxides, which are usually abbreviated to single letters. For example, C stands for CaO, S stands for SiO<sub>2</sub>, and so forth. The abbreviations most commonly used in cement chemistry are as follows. These standard chemistry notations are used throughout this thesis.

Abbreviation	Chemical formula
C	CaO
S	SiO <sub>2</sub>
A	Al <sub>2</sub> O <sub>3</sub>
H	H <sub>2</sub> O
F	Fe <sub>2</sub> O <sub>3</sub>
f	FeO
K	K <sub>2</sub> O
M	MgO
N	Na <sub>2</sub> O
$\bar{C}$	CO <sub>2</sub>
$\bar{S}$	SO <sub>3</sub>



## 1 Introduction

Milk and milk components are of major significance to the dairy and non-food industries. Due to the unique properties and technological importance, milk proteins have been used extensively in western countries. In Germany, the yield of milk per cow in kg/year has increased steadily, specifically from 1260 kg per cow in 1812 to 3800 kg in 1970, and to 6537 kg in 2003 [1].

Casein is the principle protein in bovine milk, which is mainly responsible for the functionality of milk proteins. Initially, casein was used primarily for industrial application, *e.g.* glue, plastics, paper coating, etc. In the 1960s, casein was upgraded for use as food ingredient to enhance the physical properties and to improve the nutrition of foods [2].

In the construction industry, casein is by far the most widely used dispersant in self-levelling underlayments (SLUs) [3]. It provides excellent dispersing effectiveness and unique self-healing properties on the surface of SLU grouts. Different from synthetic superplasticizers, casein is a natural product from milk. Thus, the quality of casein superplasticizer significantly varies depending on the species of animals, sampling seasons and manufacturing methods, etc. A simple and inexpensive method to assess the quality of casein superplasticizer is required to be developed.

As a chemical admixture, the application of casein can be tracked back to ancient Rome. Despite of that, the working mechanism of casein superplasticizer and its interaction with cement are by far very rarely reported. Little work has been done on the fundamental scientific aspect of casein superplasticizer although it is widely used in the construction industry. This, to a certain extent, limits the improvement in the performance of casein. When added to cement, casein is exposed to alkaline conditions. Therefore, it is of great importance to conduct a fundamental scientific study on the colloidal behavior of casein in alkaline environment.

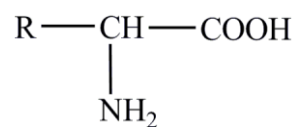
Towards a better understanding of casein superplasticizer, this thesis systematically investigates the colloidal properties of casein and its applications in cementitious materials. It covers several aspects of research, including the “casein proteins in alkaline solutions”, “casein superplasticizer in SLUs”, “fractionated and modified casein superplasticizer” and “effect of heat treatment on the quality of casein superplasticizer”.

## 2 Theoretical background

### 2.1 Casein protein

#### 2.1.1 Amino acid

Amino acids are a group of organic compounds which are composed of a carboxyl group, a primary amino group and a distinctive side chain (R group) bonded to the central carbon atom. The general structure of amino acid can be described as follows,



where R can be H or other aliphatic, aromatic, heterocyclic residues. There are about 300 naturally occurring amino acids, however, only 20 are commonly found as constituents of proteins. These amino acids provide monomeric units from which the polypeptides and proteins are built up. **Table 2.1** shows the most important amino acid constituents of proteins [4].

Amino acids can be grouped into different classifications depending on the properties of side chains. Based on the polar nature of the attached side groups, amino acids can be divided into non-polar and polar amino acids. Depending on the nutritional requirements, amino acids can be classified into essential and non-essential amino acids. Furthermore, based on the nature of metabolic end products, amino acids can be divided into glucogenic amino acids and ketogenic amino acids [5].

In aqueous solutions, amino acids can be present as cations, anions or zwitterions. This is determined by the solution pH, in other words, the different ionization state of amino or carboxyl groups in protein molecules. Ionizable  $-\text{COOH}$  and  $-\text{NH}_3^+$  can be regarded as weak acids in solution, and their protonic equilibrium is described as follows:



Each of the ionizable groups on amino acids complies with the same principles that apply to weak acid, as follows:



The above equation can be further converted to Henderson-Hasselbalch equation:  $\text{pH} = \text{pK}_a + \text{Log} ([\text{A}^-]/[\text{HA}])$ . For carboxyl groups, it can be written as:  $\text{pH} = \text{pK}_1 + \text{Log} ([\text{COO}^-]/[\text{COOH}])$ . For amino groups, it can be written as:  $\text{pH} = \text{pK}_2 + \text{Log} ([\text{NH}_2]/[\text{NH}_3^+])$ . Although both  $-\text{COOH}$  and  $-\text{NH}_3^+$  are weak acids,  $-\text{COOH}$  is much stronger than  $-\text{NH}_3^+$ . Therefore,  $\text{pK}_1$  is always smaller than  $\text{pK}_2$ .

According to above equations, when  $\text{pH} = (\text{pK}_1 + \text{pK}_2)/2$ , then the amino acid carries an equal amount of ionizable groups which possess the opposite charges, and therefore bears zero net charge. In this case, the amino acid is present as zwitterion in solution. This pH is the so called isoelectric point (pI) at which an amino acid is electrically neutral.

At lower pH ( $\text{pH} < \text{pK}_1$ ), carboxylic acid groups carry zero charge, whilst amino groups carry positive charges. Therefore, amino acid possesses protons, and is present as cations in aqueous solution. Likewise, the amino acid carries electrons, and is present as anion when solution pH is higher than  $\text{pK}_2$ .

Generally, the dissociation constants ( $\text{pK}_a$ ) of amino acids can be determined by a titration method. For example, **Figure 2.1** shows the titration curve of alanine [6]. It describes the equivalents of NaOH consumed by titrating alanine (aq) from pH 0 to pH 14. The cation, zwitterions and anion forms of alanine are also displayed in the figure.

**Table 2.1** Amino acids with their corresponding three and one letter symbols [4].

	Glycine (Gly. G)		L-Methionine (Met. M)		L-Aspartic acid (Asp. D)
	L-Alanine (Ala. A)		L-Serine (Ser. S)		L-Glutamic acid (Glu. E)
	L-Valine (Val. V)		L-Threonine (Thr. T)		L-Lysine (Lys. K)
	L-Leucine (Leu. L)		L-Cysteine (Cys. C)		L-5-Hydroxy-lysine
	L-Isoleucine (Ile. I)		L-4-Hydroxy-proline		L-Histidine (His. H)
	L-Proline (Pro. P)		L-Tyrosine (Tyr. Y)		L-Asparagine <sup>a</sup> (Asn. N)
	L-Phenylalanine (Phe. F)		L-Glutamine <sup>a</sup> (Gln. Q)		L-Arginine (Arg. R)
	L-Tryptophan (Trp. W)				

<sup>a</sup> When no distinction exists between the acid and its amide then the symbols (Asx, B) and (Glx, Z) are valid.

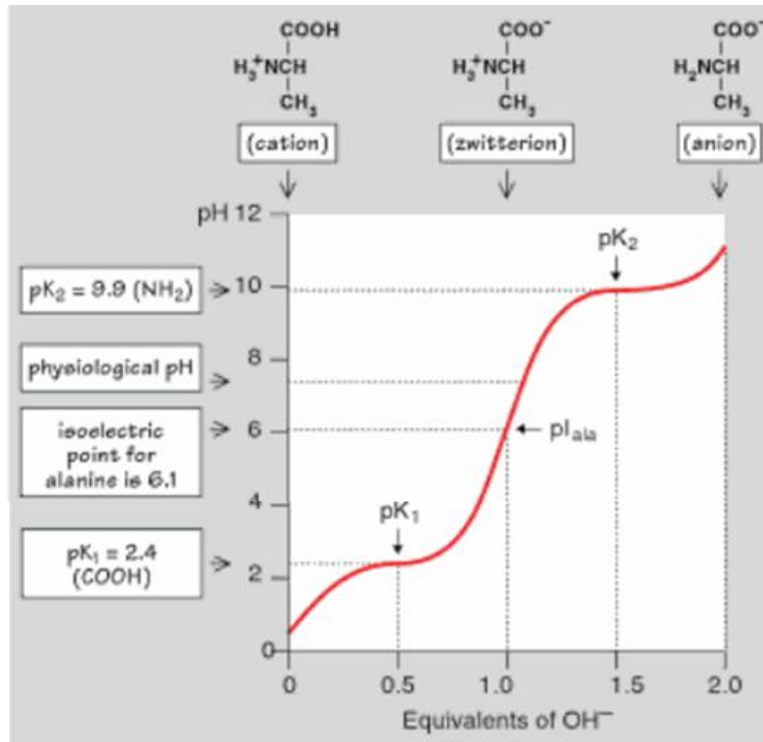


**Figure 2.1** Titration curve of alanine [6].

## 2.1.2 Casein protein

Proteins are regarded as the main constituent of all living matter. They perform multiple functions and play the critical role in biology. Proteins are formed through amide linkage, from the building block amino acid. In some cases, covalently bound hetero constituents can also be involved into proteins. For example, casein protein contains phosphoric acid esters of serine and threonine residues [4].

### 2.1.2.1 Chemistry of casein

Casein is a biopolymer obtained by acid precipitation from milk, which accounts for approximately 80 wt.% of the milk protein content. For many years, casein was believed to be a homogeneous protein, *i.e.* consisted of only one molecular species. Only in the early years of the 20th century, casein protein was proven to be heterogeneous, namely to be composed of a group of different phosphoproteins [7]. The three major protein fractions are  $\alpha$ -,  $\beta$ - and  $\kappa$ -casein, each possessing different





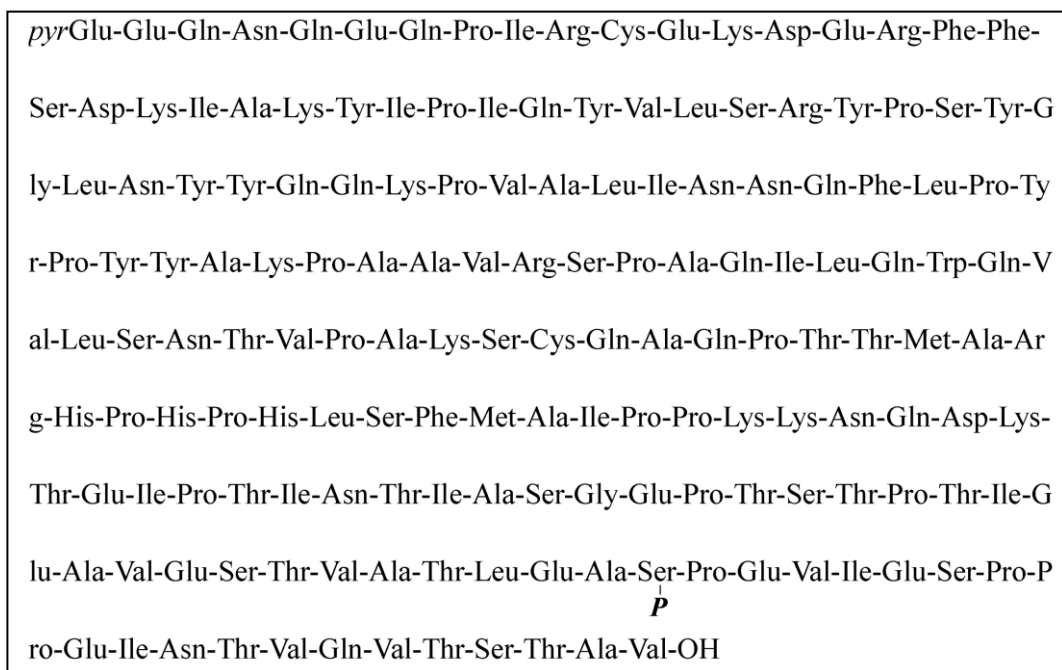


**Figure 2.5** The primary sequence of bovine  $\kappa$ -casein [8].

The  $\alpha$ - and  $\beta$ -casein fractions contain large hydrophobic domains in molecules, possessing highly hydrophobic nature. However,  $\kappa$ -casein is a glycoprotein containing an acidic (charged) carbohydrate section, thus it is much more hydrophilic [10]. Towards a better understanding of casein proteins, some of their properties are summarized and listed in **Table 2.2**. Also shown are the properties of  $\gamma$ -casein which is a minor fraction in casein protein, occurring naturally as a result of proteolysis of  $\beta$ -casein by plasmin.

**Table 2.2** Casein protein fractions and their properties [11].

Protein fraction	Percentage of skim milk protein	Molecular weight (g/mol)	Isoelectric point (pH)
$\alpha$ -casein	45 - 55	23,000	4.1
$\beta$ -casein	25 - 35	24,100	4.5
$\kappa$ -casein	8 - 15	19,000	4.1
$\gamma$ -casein	3 - 7	30,650	5.8 - 6.0

### 2.1.2.2 Ionization of casein

Casein molecules carry net negative charge at milk pH (6.7) due to the deprotonation of amino acid residues. Specifically,  $\alpha$ -casein has a net charge of -24,  $\beta$ -casein has -13, whereas  $\kappa$ -casein due to the phosphorylation deficiency in its molecule, possesses a net charge of only -3 at pH 6.7. The net charge of casein proteins varies at different solution pH.

Casein has an average isoelectric point (pI) of 4.6, at which proteins start to precipitate from milk. At pH > 4.6, casein is present as anions in solution. Whereas at pH < 4.6, casein is present as cations. The dissociation constants of side groups in casein proteins have been summarized and listed in **Table 2.3**, from which  $\kappa$ -casein is omitted because its content in casein proteins is rather low and contributes little to the overall charge of casein. Additionally, the side groups contained in cysteine and phosphoserine are also not displayed in the table. That is because the former exists in the form of disulfide bonds in casein, while the latter is associated with calcium in the alkaline pH [12].

**Table 2.3** Overview of amino acids with acidic and basic side groups present in casein [12].

amino acid	type of side group	pK of side group <sup>a</sup>	no. of residues (values between brackets indicate the no. of residues located in the hydrophobic areas)		
			$\alpha_{s1}$ -casein <sup>b</sup>	$\alpha_{s2}$ -casein <sup>c</sup>	$\beta$ -casein <sup>d</sup>
glutamic acid	carboxylic acid	4.5	25 (10)	24 (0)	19 (2)
aspartic acid	carboxylic acid	4.0	7 (4)	4 (0)	4 (1)
tyrosine	phenol	9.6	10 (10)	12 (3)	4 (3)
lysine	$\epsilon$ -amino	10.5	14 (7)	24 (1)	11 (2)
histidine	imidazole	6.4	5 (2)	3 (0)	5 (2)
arginine	guanidine	>12.5	6 (4)	6 (1)	4 (2)

<sup>a</sup> Values from ref 37. <sup>b</sup> Values are for  $\alpha_{s1}$ -CN B-8P (31); hydrophobic areas contain residues 1–44 (37), 90–110, and 140–190 (31). <sup>c</sup> Values are for  $\alpha_{s2}$ -CN A-11P; hydrophobic area contains residues 90–120 (31). <sup>d</sup> Values  $\beta$ -casein A<sup>2</sup>-5P; hydrophobic areas contain residues 55–90 and 130–209 (31).

### 2.1.2.3 Micellar structure of casein

Casein exists in milk in the form of colloidal particles, so called “micelles”. These micelles are composed of protein molecules and inorganic constituents, mainly calcium and phosphate, and their diameters were found to range between 50 and 500 nm (on average is about 120 nm) [13]. Towards a better understanding of casein micellar structure, a variety of models have been developed since the 1960s [14,15,16]. The two most widely accepted models were proposed by WALSTRA (1984) and HOLT (1992), respectively [17,18].

WALSTRA proposed that the casein micelles are built of roughly spherical submicelles ( $d = 12 - 15$  nm), each having 20 - 25 casein molecules. These submicelles are kept together by hydrophobic interactions between the proteins, and by calcium phosphate linkages. A hairy layer consisting of  $\kappa$ -casein protrudes from the surface of the submicelles and is responsible for the stability of the micelles. There are two types of sub-micelles. One mainly consists of  $\alpha$ - and  $\beta$ -caseins, which is hydrophobic and present in the interior of the micelle. Another type consists of  $\alpha$ - and  $\kappa$ -caseins, which is more hydrophilic and located near the outside of the micelle. As a consequence, the micelles are fairly stable in dairy milk. **Figure 2.6** shows the structure of casein micelles from the submicelle model.

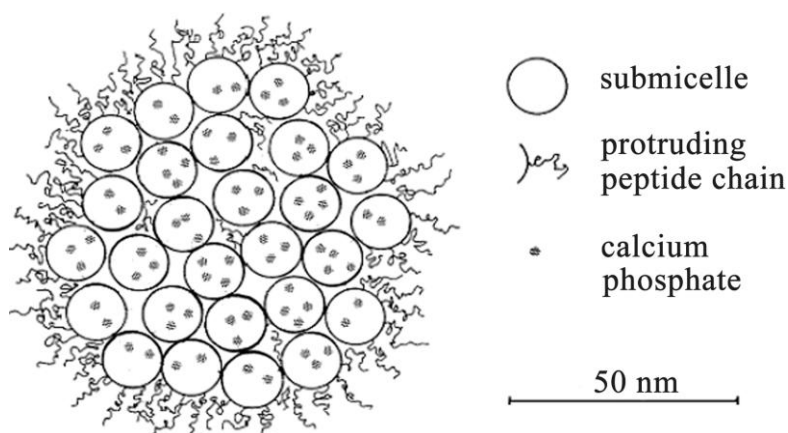


**Figure 2.6** Model of casein micelle as proposed by WALSTRA [17].

Although the submicellar structure of casein micelles has been widely accepted, another alternative model which differs mainly in the internal structure of the micelle was presented by HOLT in 1992 [19]. He depicted casein micelles as a tangled web of flexible casein molecules, from which a gel-like structure is formed. Micro granules of colloidal calcium phosphate are interspersed through the casein phosphate center, whereas the hydrophilic region of  $\kappa$ -casein extends to form the hairy layer. This model structure suggests a more homogeneous protein matrix in the casein micelle, as shown in **Figure 2.7**.

While the debate still continues, it is commonly believed that the proposed models are oversimplified. The submicelles should not be seen as identical, perfect, and hard spheres [20]. The actual micelle might have a structure which is somewhat between the models from WALSTRA and HOLT.

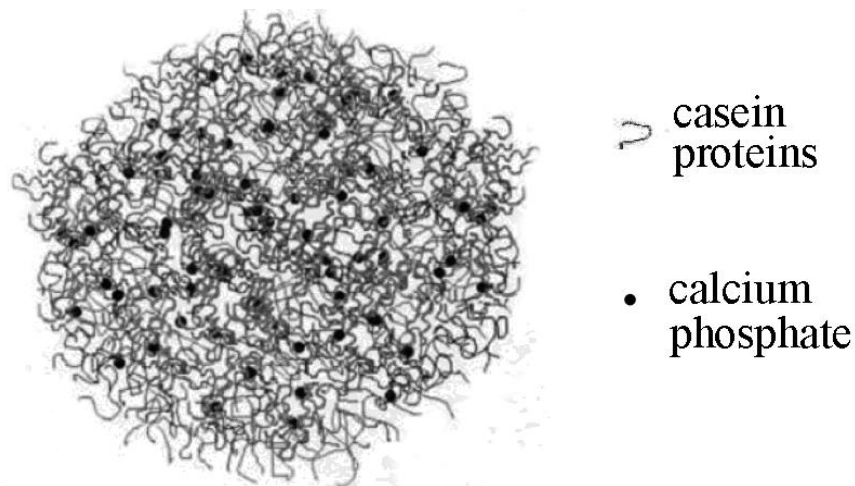


**Figure 2.7** Model of casein micelle as proposed and modified by HOLT et al. [19].

#### 2.1.2.4 Interactions occurring in casein micelles

##### 2.1.2.4.1 Hydrophobic interaction

Hydrophobic force plays a significant role in protein stability. It arises mainly because water exhibits decreased entropy as a result of the occurrence of apolar amino acid

residues in the solvent [21]. According to the calculation of HILL and WAKE [22], caseins are among the most hydrophobic of all proteins, thus it is not unexpected that these apolar residues are somewhat clustered in  $\alpha$ - and  $\beta$ -caseins, as well as in  $\kappa$ -casein. Previous studies revealed that the hydrophobic interactions are of great importance in the formation of casein micelles [23]. The apolar region on the surface of casein molecules is available for interactions with other protein molecules. From the energy aspect, it is favorable for these residues to cluster with similar residues from other molecules. This endows caseins with a strong tendency to associate, and thus the hydrophobic core of the micelle is formed (mainly from  $\alpha$ - and  $\beta$ -caseins). The amphiphilic nature of  $\kappa$ -casein allows it to interact hydrophobically with  $\alpha$ -casein and meanwhile to provide a hydrophilic surface on the micelle, which inhibits the growth of hydrophobic core in casein micelles. As a consequence, a stable casein micelle is formed.

#### **2.1.2.4.2 Electrostatic repulsion**

Compared to hydrophobic interactions, electrostatic repulsion is a long-range force, a significant factor which has been identified in studies of protein interactions. The electrostatic repulsion is critical for close packing and proper formation of micelles/aggregates [23]. It defines the extent of association and inhibits the further growth of casein micelles.

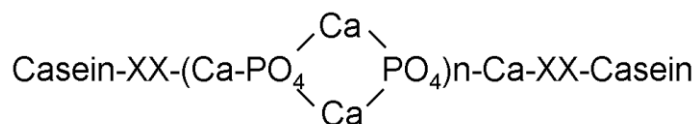
The electrostatic repulsion is greatly influenced by the surface charge of casein. For instance, increasing the pH of solution facilitates an increase in the charge casein proteins carry, therefore causing a decrease in the particle size of casein micellar structure. Additionally, the electrostatic repulsion will be influenced if the surface charge is modified via chemical reactions, *e.g.* conversion of positively charged lysine residues to neutral or negatively charged derivatives, introduction of negatively charged sites by iodination of tyrosine residues to the di-iodo form, etc. These

modifications effectively increase the net negative charge of casein proteins, thereby reducing their tendency of aggregation [24].

#### **2.1.2.4.3 Calcium phosphate binding**

Calcium phosphate binding is also an essential factor in maintaining the integrity of casein micellar structure. In casein micelles, proteins are cross-linked through the binding between their ester phosphate groups and inorganic calcium phosphate, resulting in the formation of colloidal calcium phosphate (CCP) clusters. For many years, the nature of CCP was believed to be inorganic calcium phosphate salt, namely  $\text{Ca}_9(\text{PO}_4)_6$ . In 1986, HOLT obtained the precipitate consisting mainly of peptides and CCP, revealing the latter contains primarily serine phosphate and glutamine residues. Based on that, he concluded that the CCP region in principle contains most of the phosphoserine residues of casein [20, 25]. These phosphoserine residues provide potential sites for linkage between casein and CCP, as is shown in **Figure 2.8**.

The importance of CCP in governing the micellar structure of casein was subject to extensive investigations in past years. Unfortunately, these studies did not reach a consistent conclusion, and the debate still continues. Some earlier research revealed that the calcium phosphate is an essential component which binds casein micelles. The addition of calcium chelating agents will lead to the extensive micellar disintegration due to the disruption of calcium phosphate ion pairs [26]. Whereas, MADADLOU et al. argued that colloidal calcium phosphate plays only a minor role in the formation and structural features of casein micelles since the calcium content in casein is rather low [27]. Further investigations are required to clarify the actual function calcium plays in maintaining the integrity of the casein micelle.



*XX= phosphoserine group or carboxylate*

**Figure 2.8** The type of linkage possible in colloidal calcium phosphate [23, 26].

### 2.1.2.5 Stability of casein micelle

During the past decades, extensive research has been carried out to determine the stability of casein micelles in different environments. The aggregation and disintegration of casein micelles have been demonstrated in those previous studies.

#### 2.1.2.5.1 Heat induced change in casein micelle

Compared to most other proteins, casein proteins are very stable against heating due to their deficiency in tertiary structure. However, the micellar structure of casein is susceptible to heat treatments [28, 29, 30, 31]. LE et al. reported a heating induced change in particle size distribution of casein micelles both in the absence and in the presence of whey proteins [32]. Dynamic light scattering measurement indicated a bimodal distribution in casein dispersion, where the large-diameter mode is ascribed to heat-induced casein micellar aggregation. On the other hand, nanoparticle tracking analysis provided visual information on submicron particles and thereby confirmed the onset of aggregation phenomena. PANOUILLE et al. studied the aggregation of micellar casein particles in polyphosphate [33]. The rate of gelation process was found to increase clearly with increasing the heating temperature. The structure of formed gel was further studied by cryo-electron microscopy, where the aggregates consisting of branched connected spheres were observed as shown in **Figure 2.9**.

It should be noted that the stability of casein micelles can be influenced by many other factors, among which medium solvent is the most significant one.

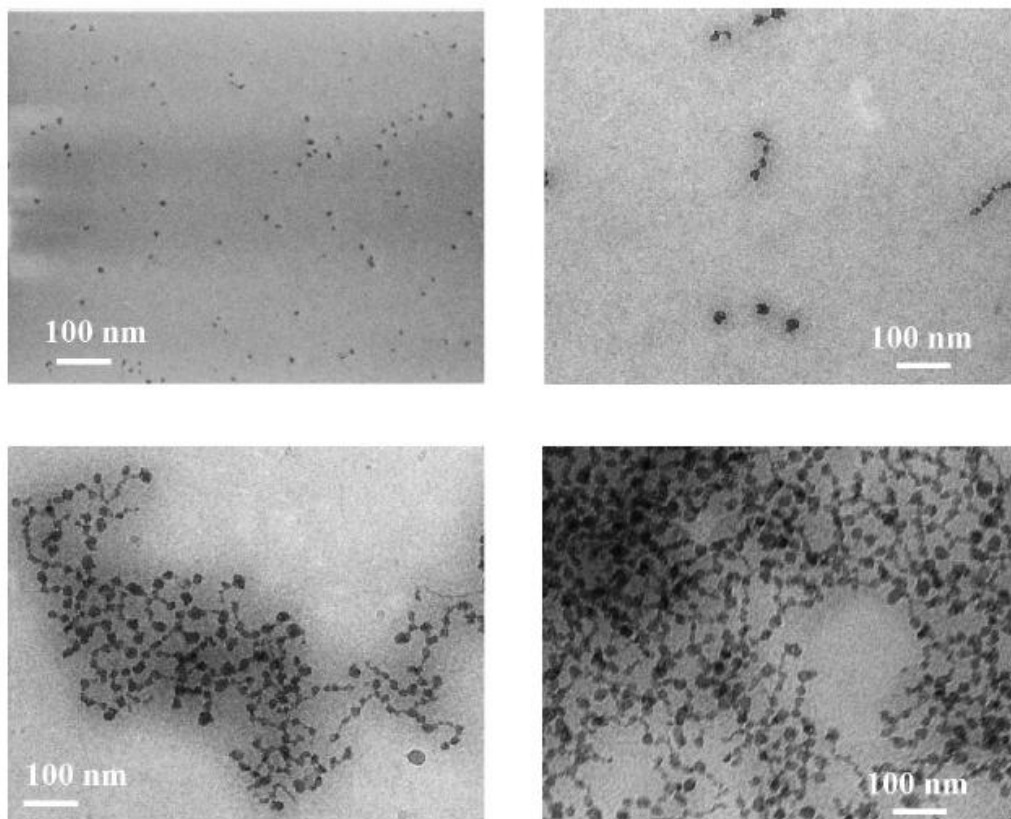


**Figure 2.9** Cryo-electron microscopic images of frozen-hydrated casein samples, monitoring casein aggregation after (a) 7 h (b) 15 h (c) 19 h and (d) 27 h of a 16 g/L casein solution heated at 80 °C [33].

#### 2.1.2.5.2 Solvent-mediated change in casein micelle

The micellar structure of casein is greatly subjected to the surrounding medium, namely the solvent. For many years, the contribution of various solvents to the structural change in casein micelle has been the subject of extensive investigations. O'CONNELL et al. revealed the dissociation of casein micelles at 65 °C in 1:1 (v/v) mixture of milk and 65% ethanol [34]. This change in micelle was ascribed to the interactions between casein proteins and the solvent, and to the increase in solvent quality on the addition of ethanol at high temperature. MCGANN et al. reported that the white appearance of milk was reduced severely on the addition of 6 M urea [35]. This phenomenon was believed to derive from the dissociation of casein micelles into particles which are on average considerably smaller. However, it is noted that the

micellar change induced by urea is dependent on the intermediate concentration. For example, addition of 3.5 M urea was reported to render the gelation and precipitation of casein proteins, which are mainly composed of  $\alpha$ -casein [36].

### 2.1.2.5.3 Pressure induced change in casein micelle

Previous studies have shown that the micellar structure of casein is related to the environmental pressure [37, 38, 39]. GEBHARDT et al. investigated the pressure-decomposed casein micelle, indicating that the native micelles dissociated into subunits on a 20 nm scale at pressures between 50 and 250 MPa, as shown in **Figure 2.10** [37]. This has been attributed to the reduced electrostatic and non-polar interactions occurring in casein micelles. Furthermore, the pressure-release study revealed that the subunits only partially recovered to the native state of casein micelles, suggesting that the pressure induced change in casein micelle is not fully reversible. Additionally, hydrostatic pressure was also used to induce dissociation of casein micelles. A high hydrostatic pressure of 250 to 310 MPa was found to promote extensive disruption of the casein micelles [38].

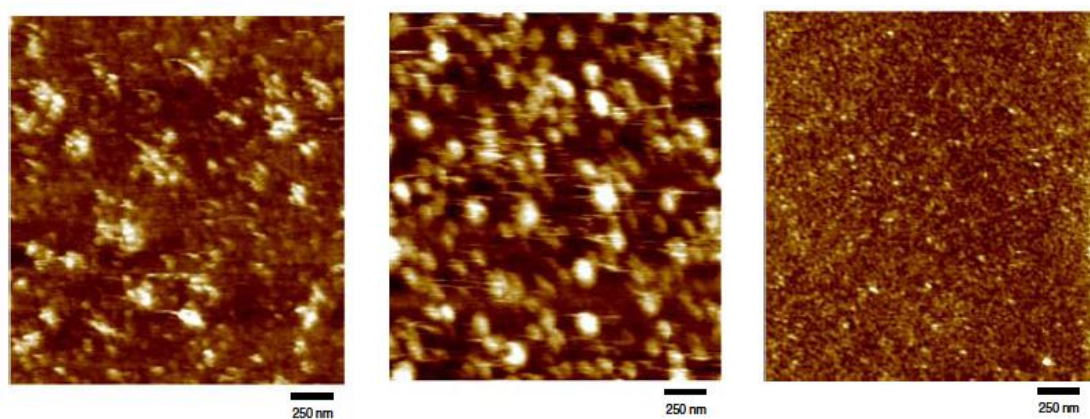


**Figure 2.10** AFM images of pressure-treated casein micelles. **Left:** intact micelles,  $P < 50$  MPa; **middle:** compact reconstituted micelles,  $120$  MPa  $< P < 240$  MPa; **right:** mini-micelles,  $P > 280$  MPa [37].

### 2.1.2.5.4 pH induced change in casein micelle

The influence of pH on the micellar structure of casein is among the most significant. The extensive aggregation of casein micelles and the subsequent precipitation which occur at pH 4.6 (isoelectric point of casein) are a classic example. Under alkaline conditions, the structure of the casein micelle has also been widely studied [12, 40, 41, 42, 43, 44]. VIAL et al. reported on the disruption of casein micelles at pH > 9, and proposed that the underlying mechanism is based on the increased solubility of casein at alkaline pH [12]. They suggest that the decreased content of calcium phosphate clusters would increase the solvent quality, leading to reduced cohesive interaction between the hydrophobic regions of casein proteins and accordingly an increased solubility of casein micelles. However, MADADLOU argued there is only a minor amount of calcium in casein, and thus the calcium phosphate cluster could not play such an important role in determining the structural stability of casein micelles [43].

Additionally, LIU and GUO revealed an association of casein molecules into micelles over a broad pH range of 5.5 - 12 [44]. Using fluorescent technique together with DLS and turbidity measurements, a more compact casein micellar structure at low pH and a looser structure at high pH have been shown. It is worth mentioning that those previous studies contradict each other. Therefore, the alkaline induced change in casein micelles and the underlying mechanism are still under debate.

#### **2.1.2.5.5 Calcium chelating agent induced change in casein micelle**

The calcium phosphate linkage between proteins is essential for maintaining the integrity of the casein micelle [45, 46, 47, 48]. Thereby, removal of calcium from casein is likely to result in the disintegration of the micelle structure. It has been reported that in the presence of a calcium chelating agent such as EDTA- $\text{Na}_2$ , calcium and phosphate ions diffused out of casein micelles, resulting in a reduction of micellar stability [49]. Sodium polyphosphate is another commonly used calcium chelating agent. Using scattering and turbidity measurements, PITKOWSKI et al. studied the

dissociation of casein after the addition of polyphosphate. It was found that the casein micelle either became completely disintegrated or remained intact, in other words, this dissociation of casein micelle induced by calcium chelation was a cooperative process. Furthermore, the dissociation kinetics were closely related to the ratio of calcium chelating agent to casein proteins. The proportion of undissociated casein micelles decreased linearly with increasing the above ratio till a critical value was reached, where all casein micelles were dissociated [50].

#### **2.1.2.6 Technical applications of casein**

Casein, as the principle protein in dairy milk, is commonly used as ingredient in foods. It can modify the physical properties of food products, such as foaming, whipping, emulsification, texture, and so on [51]. Nevertheless, casein also finds broad industrial applications owed to the multiple functions it possesses [52, 53, 54]. Due to its amphiphilic nature, casein can easily form a protein film at interfaces. This provides casein with good emulsifying and stabilizing properties, thus promoting its application as surfactant. Due to the lack of a secondary structure, casein proteins consisting of mostly random coil polypeptides show high molecular flexibility, which enables the intermolecular interactions and as such facilitates its good film forming and coating properties. Therefore, casein can be used for paper coating, painting, leather finishing, etc. Additionally, casein finds application in the manufacture of plastics, textile fibers, in production of ethanol, and so on [55]. A list of the principle uses of casein in technical areas is shown in **Table 2.4**.

In the construction field, casein is generally used as a dispersant, specifically as a superplasticizer in cementitious materials [56]. It provides excellent dispersing effectiveness in mortar and greatly improves the workability of cement and concrete. Therefore, casein plays a significant role in the market of dry-mix mortar admixtures. More detailed information on the application of casein superplasticizer in building materials will be presented in **2.2.2**.

**Table 2.4** Principle technical applications of casein [55].

Product	Applications	Properties
Coating	Paint, ink, leather finishing, textile coating.	Adhesion, film forming ability, good processability, bond strength, water resistance obtained by crosslinking, good mechanical property, strength, water resistance obtained by crosslinking, stability of interface, surface tension, stability of interface.
Adhesive	Glue	
Plastic	Plastics, fiber, film/foil in packaging application.	
Surfactant	Emulsifier, detergent.	
Superplasticizer	Cement admixture	

### 2.1.3 Protein purification

High purity is essential for the characterization of structure, function and interaction of proteins. In the early days, proteins were commonly separated according to their solubility variation in different solvent media. For example, the addition of salts (*e.g.* salting out with ammonium sulfate), organic solvents (*e.g.* precipitation with ethanol or acetone), or variation of solution pH (*e.g.* isoelectric precipitation), these alterations help proteins to be separated from other impurities [57, 58, 59, 60]. Nowadays, chromatographic methods are more often used for the purification of proteins [61, 62, 63, 64]. The basic procedure of chromatography is to partition the protein molecules between two phases, namely the mobile phase and the stationary phase. In general, the stationary phase is packed into a column, through which the mobile phase is pumped. The chromatography of proteins employs small spherical beads of modified cellulose, acrylamide or coated silica as the column materials (stationary phase) [65]. Different proteins interact differently with these column

materials. Therefore, proteins can be separated according to their size, charge, hydrophobicity, and so forth. Up till now, the chromatographic purification has become the most widely used method of proteins separation. In the following section, several commonly used chromatographic techniques of protein purification are introduced.

### 2.1.3.1 Ion exchange chromatography

Ionic interaction is the basic principle used for the protein separation by ion exchange chromatography. Ion exchange columns are packed with resins that carry positive or negative charges at a certain pH, which retards the elution of proteins with opposite charge [66, 67, 68, 69, 70]. **Figure 2.11** illustrates the principle of ion-exchange chromatography [71], where a matrix with positive charges is used as an example. Negatively charged proteins are eluted by increasing the ionic strength of the buffer. Specifically, the proteins with a net negative charge adsorb onto the positively charged resins. In the process of elution, the counter ions (*e.g.*  $\text{Cl}^-$ ,  $\text{CH}_3\text{COO}^-$ ) contained in the buffer compete against negatively charged proteins for the binding sites on the column. With increased concentration of counter ions in the buffer solution (mobile phase), the proteins bound can be gradually replaced and are eluted from the chromatography column (stationary phase). The association of proteins and column materials is determined by solution pH, ionic strength, etc.

As is shown in **Figure 2.12**, a typical ion-exchanger is an insoluble matrix, to which the functional ionogenic groups are covalently bound, resulting in the formation of electrically charged surface. Depending on the composition of the matrix, ion exchangers can be divided into several groups, including ion-exchange cellulose, ion-exchange polydextran, synthetic resins, inorganic exchangers, etc [72].

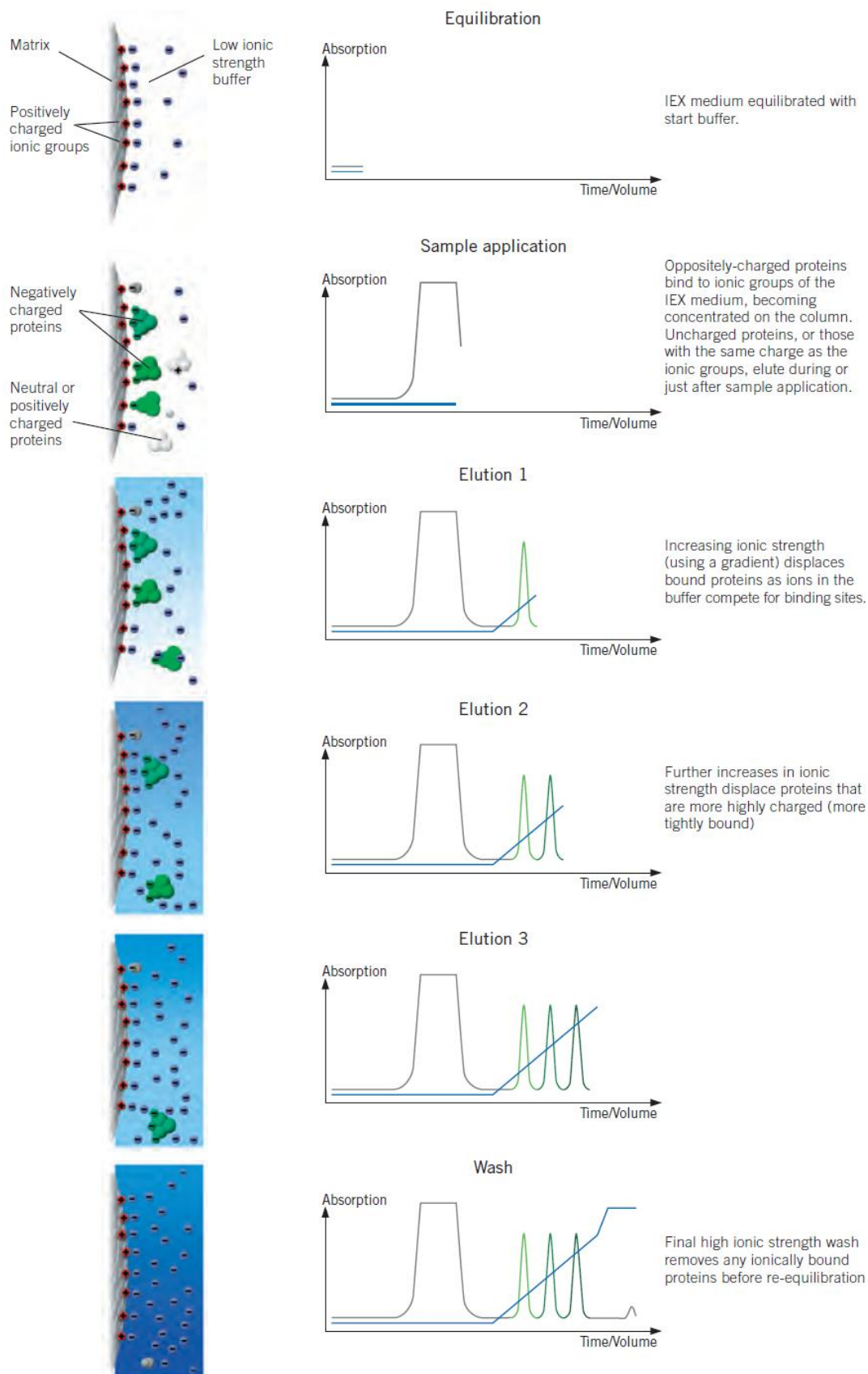


**Figure 2.11** Principle of anion exchange separation of proteins [71].

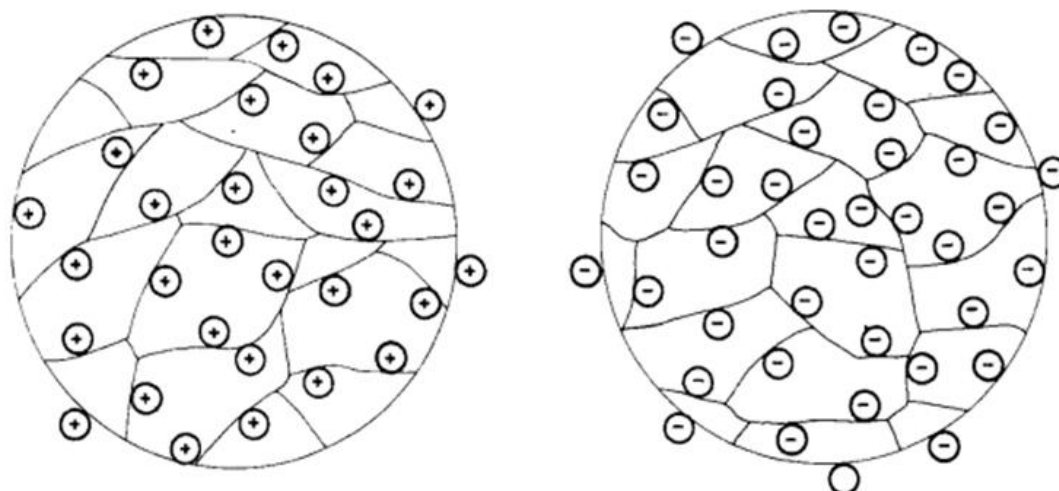


**Figure 2.12** Schematic representation of positively charged (left) and negatively charged (right) resins used in ion exchange chromatography. The lines illustrate the cross-linked polymer matrix [72].

### 2.1.3.2 Size exclusion chromatography

Size exclusion chromatography (SEC) is also termed as gel permeation chromatography (GPC). SEC separates proteins based on their Stokes radius, which refers to the radius of a hard sphere that diffuses at the same rate as the molecule. In SEC, the column is packed with porous beads of slightly different pore sizes. During elution, proteins of smaller size enter the holes in the beads and travel slowly through the channels in the column, thus they are retarded in elution. In contrast, proteins with a Stokes radius too large to enter the holes in the beads pass quickly through the column, accordingly, they are washed out at a shorter retention time. The column materials used in SEC are often composed of polymers, such as agarose, dextran, polyacrylamide, etc. Through crosslinking, a three dimensional network is formed from these polymers, thus resulting in the formation of porous media. The pore sizes of SEC media are determined by the degree of crosslinking.

### 2.1.3.3 Fast protein liquid chromatography (FPLC)

The conventional chromatographic techniques face the problems of long analysis time and low resolution of protein separation. To provide a more biocompatible chromatographic method, Pharmacia (now GE Healthcare) developed fast protein liquid chromatography (FPLC) in 1982. After step-by-step improvements, FPLC nowadays allows a high resolution of fractionated components, and most importantly, a dramatically reduced separation time for protein purification [73, 74, 75, 76]. FPLC systems have been built up based on diverse principles, *e.g.* ion exchange, size exclusion, hydrophobic interaction, reverse phase, etc. The columns are able to accommodate much higher protein loadings than the conventional chromatographic techniques [77].

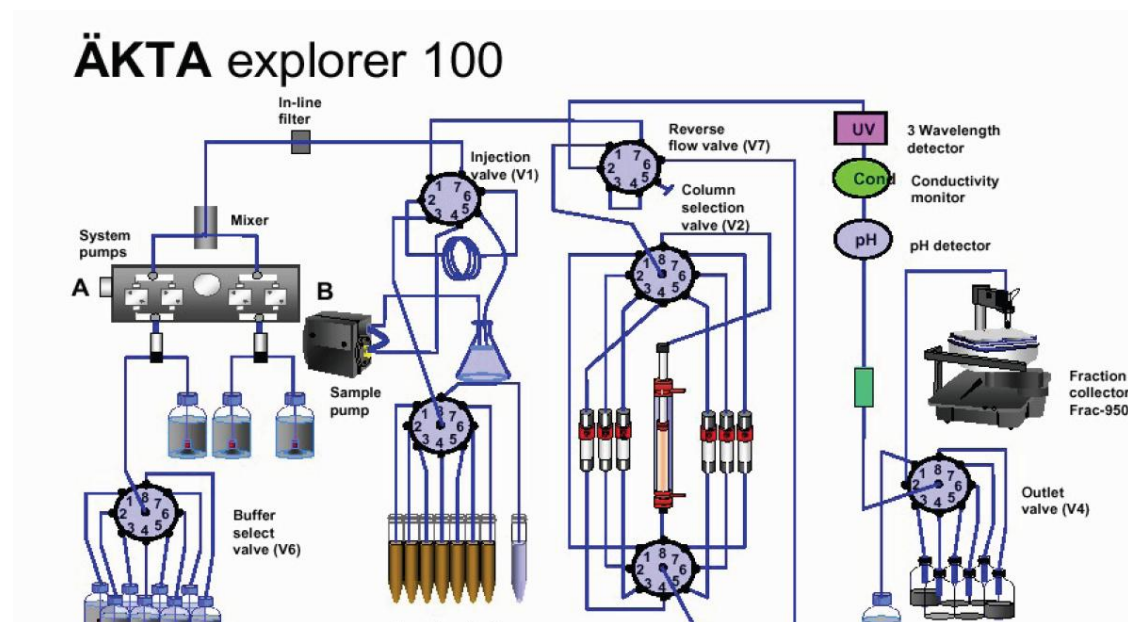


**Figure 2.13** Schematic diagram of FPLC instrument “Äkta explorer 100” (GE Healthcare).

A standard FPLC system is mainly composed of high-precision system pumps, a sample pump, an analytical column, several valves, a detection system (UV/Vis spectrophotometer, conductivity meter, pH meter) and a fraction collector. The entire FPLC system is driven by a software control interface. During the measurement, the sample is either supplied manually by using a sample loop or applied automatically by

the sample pump. After being pumped through the injection valve, the samples are loaded to the analytical column and fractionated on the column. Depending on their distinct characteristics, the signals of eluted components are detected. Lastly, the different protein fractions are monitored and collected in the collectors. A widely used configuration of a FPLC system is shown in **Figure 2.13**.

## 2.2 Casein superplasticizer

### 2.2.1 Superplasticizers

Superplasticizers (SPs) belong to the category of water-reducing agents. They are widely used in cementitious materials such as grouts, mortars and concrete mixes [78, 79, 80, 81, 82]. SPs are also known as high-range water reducing agents. Their function is to reduce the water-to-cement ratio and to provide enhanced fluidity [83]. In the 1960s, SPs were originally developed in Germany and Japan. Up till now, a variety of SPs has been developed, *e.g.*  $\beta$ -naphthalenesulfonate formaldehyde condensates (BNS), sulfonated melamine formaldehyde condensates (PMS), and acetone–formaldehyde–sulfite (AFS) condensate. These SPs are linear polymers containing sulfonic acid groups at regular intervals, which are neutralized by calcium or sodium counter ions. Since the 1980s, application of a new generation of polycarboxylate (PC) superplasticizers has been widely studied [84,85,86,87]. They are comb-like copolymers consisting of negatively charged backbone with carboxylic groups. At the backbone chain, various side chains are grafted, *e.g.* polyethylene oxide unit. Although PCs are not as tolerant to different cements like polycondensates, they can achieve high fluidity at very low water to cement ratios (as low as 0.15) and provide slump retention over a prolonged period of time. Finally, in the 1990s superplasticizers based on “small molecules” were introduced [88]. They consist of an anionic anchor group which allows the molecule to adsorb onto the surface of cement hydrates, and a non-ionic, non-adsorbing side chain, typically made of polyethylene oxide units. The chemical structures of these different types of superplasticizers are

shown in **Figure 2.14**.

Additionally, a great diversity of bio-admixtures is applied in the cement industry nowadays. Compared to above mentioned SPs, bio-admixtures are quite expensive. But due to the good performance and unique properties they provide, these microbial biopolymers are still commonly used in industry. **Table 2.5** depicts the major biopolymers and biotechnological products used in this field [3].

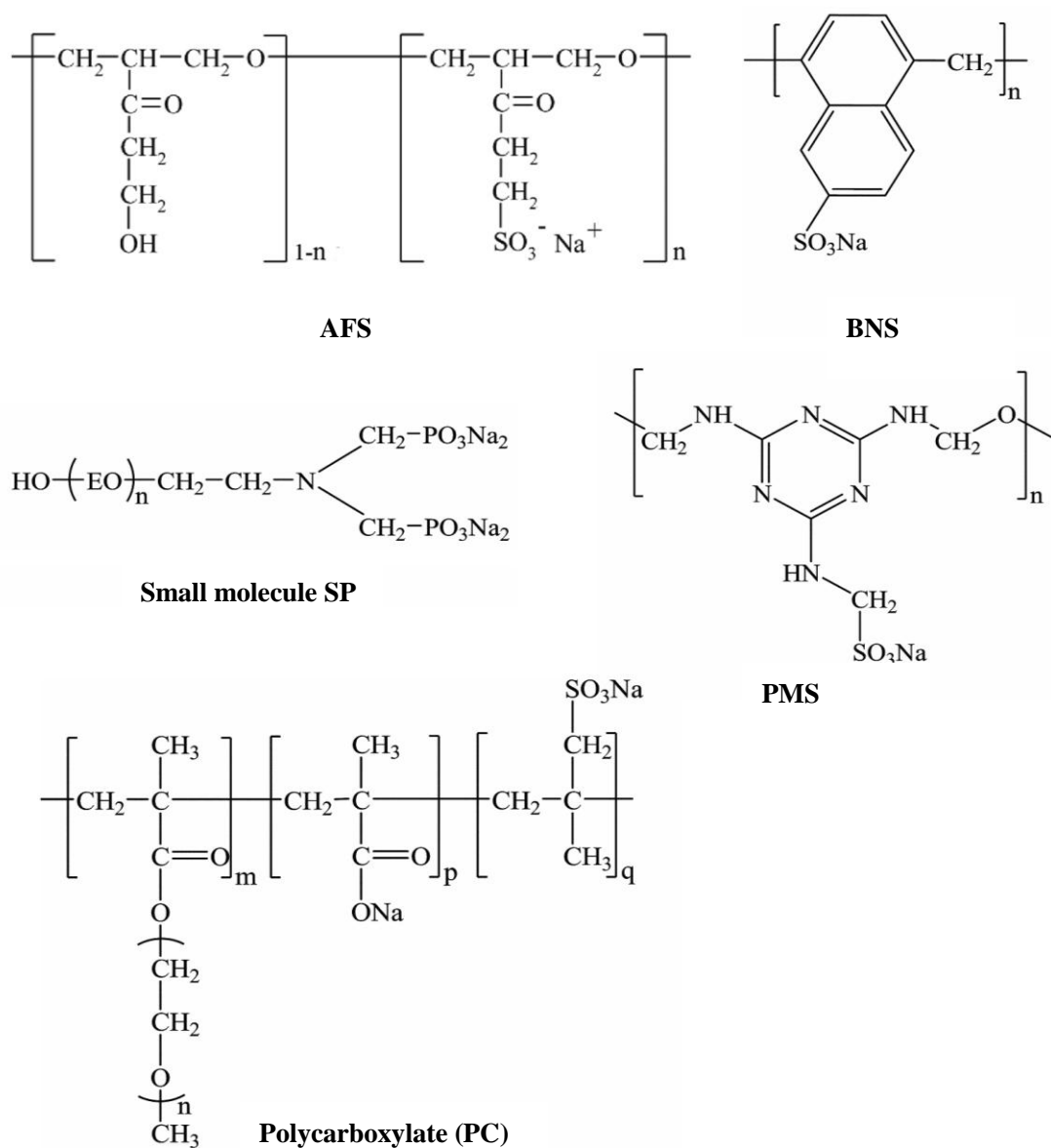


**Figure 2.14** Chemical structures of different types of superplasticizers.

**Table 2.5** Bio-admixtures used in dry-mix mortars [3].

Product	Annual consumption (metric tonnes)
Cellulose ethers	100,000
Starch and derivatives	30,000
L (+)-Tartaric acid	10,000
Casein	5,000
Xanthan gum	250
Welan gum	100
Succinoglycan	50

In cementitious systems, the chemical admixtures perform their functions through several ways, which involve physico-chemical interactions with hydrating cement phases [89, 90, 91, 92]. In general, cement paste becomes agglomerated due to the attractive forces existing between cement particles. When superplasticizer is added in the paste, the adsorption of anionic polymers neutralizes the attractive forces, giving the cement particles a highly negative charge so that they repel each other. Thus, the cement paste is well dispersed and its workability is greatly improved. AFS, PMS and BNS belong to the superplasticizers introducing electrostatic repulsion to cement.

However, for some types of superplasticizers, such as PC, the dispersion mechanism is related more to a steric hindrance effect. When adsorbed on cement particles, the grafted side chain of polymer would hinder the flocculation of particles. In this way, the large agglomerates are dispersed into smaller ones, accordingly a significant increase in the workability of cement paste is achieved [93]. **Figure 2.15** describes the different ways in which admixtures and cement hydration products interact [94]. The illustration shows the solid/solution interface on a hydrating cement particle.

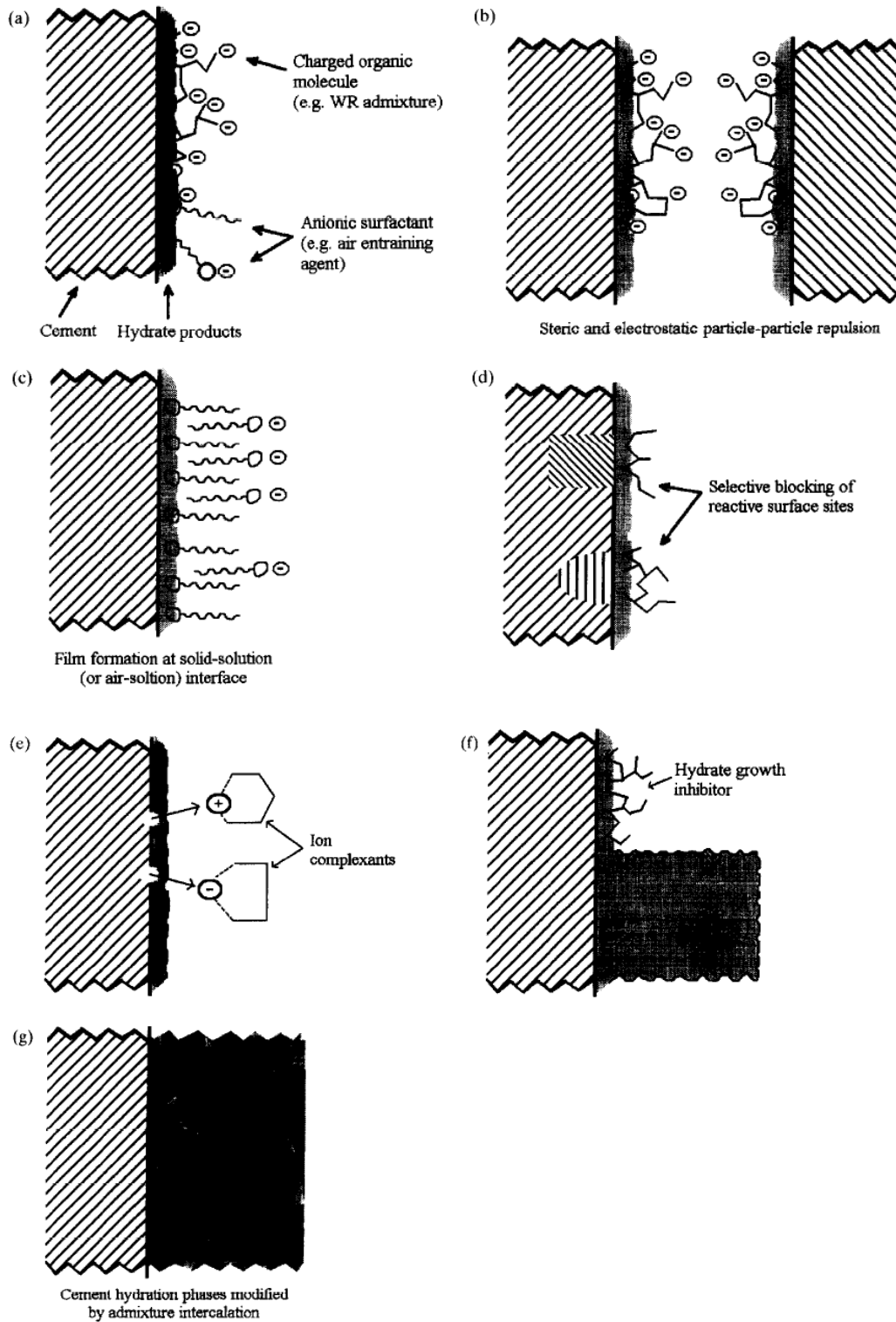


**Figure 2.15** Schematic illustration of different physico-chemical effects occurring upon interaction of chemical admixtures and cement particles at the interface cement/pore solution. (a) adsorption of superplasticizer molecules at the interface; (b) particle-particle repulsion due to electrostatic forces and steric hindrance; (c) layered

molecular organization from adsorption of superplasticizer at the interface; (d) preferential adsorption of chemical admixtures on specific surface sites; (e) complexation and solubilization of ionic species; (f) hydrate crystal nucleation and growth inhibition by adsorbed admixture; (g) intercalation of chemical admixture in cement hydrate products with structural alteration [94].

### **2.2.2 Casein superplasticizer in self-levelling underlayments (SLUs)**

The application of casein as admixture can be tracked back to ancient Rome. At that time, builders added various organic additives to mortars to adjust certain mortar properties. For example, the addition of sugar, fruit syrup and blood extended the workability time of mortars. The addition of malt, beer and urine could improve the durability and frost resistance, etc. Casein as well as some casein contained products were in general used as plasticizer or stiffening agent, which could improve the workability or adjust the consistency of cementitious mortars [95]. In the past decades, the introduction of synthetic polymeric additives caused some of the natural organic additives to gradually disappear. However, casein due to its excellent plasticizing effect at low dosage and good compatibility with retarders in cement based grouts, still plays a significant role on the market for self-levelling underlayments (SLUs).

#### **2.2.2.1 Self-levelling underlayments (SLUs)**

Self-leveling underlayments (SLUs) are commonly used to level floors and to cover cracks prior to the installation of a finish flooring [96, 97, 98, 99]. They are marked by good flow characteristics, self-levelling as well as fast setting/drying properties. Compared to other “normal” grouts, the application of SLU materials helps to save working time and to reduce heavy labor at construction sites (**Figure 2.16**) [100].

Basically, there are two types of SLUs, one is based on cement and the other is based on gypsum [101]. Cement based SLU materials generally possess high compressive strength. They can strongly adhere to concrete substrates, thus providing a higher

internal strength. In comparison to cement based SLUs, gypsum based materials in general weigh less and cost less. However, they are more susceptible to the environmental moisture. Under humid conditions, gypsum based SLUs soften and may become more brittle after redrying. Therefore, for wet environment they are not recommended by manufacturers.



**Figure 2.16** Comparison of conventional floor screed placement technique (left) and of self-levelling cement mortar (right) [100, 102].

In practice, a ternary binder system based on special hydraulic binders, such as ordinary Portland cement (OPC), calcium aluminate cement (CAC) and anhydrite, is most often used in the industry [103, 104]. **Table 2.6** shows a typical formulation of a ternary binder based self levelling underlayment.

#### **2.2.2.1.1 Portland cement**

Portland cement clinker is in principle produced by heating a mixture of raw materials typically calcium carbonate (limestone or chalk) and aluminosilicate (clay or shale) [105, 106, 107]. The clinker obtained is then mixed with a few percent of calcium sulfate to adjust the setting time, and afterwards is finely ground to produce cement powder. Joseph Aspdin, the inventor, named it Portland cement because the hardened cement material resembles the stone from quarries near Portland in England [108].

The composition of Portland cement is rather complicated, but basically it contains four main constituents as shown in **Table 2.7**.

**Table 2.6** Typical formulation of a ternary binder based self-levelling underlayment [109].

Component	Function	weight %
Portland cement (CEM I 42,5 R)	binder	18.5
High alumina cement (ca. 40 % Al <sub>2</sub> O <sub>3</sub> )	binder	11.5
CaSO <sub>4</sub> (synthetic anhydrite)	binder	6.5
Quartz sand (0.1 to 0.315 mm)	aggregate	41
CaCO <sub>3</sub> filler (10 to 20 µm)	filler	19.4
Casein or polycarboxylate ether	superplasticizer	0.4
Vinylacetate-ethylene copolymer	redispersible powder	2
KNaC <sub>4</sub> H <sub>4</sub> O <sub>6</sub> · 4H <sub>2</sub> O or Na <sub>3</sub> C <sub>6</sub> H <sub>5</sub> O <sub>7</sub> · 2H <sub>2</sub> O	hydration retarder	0.4
Li <sub>2</sub> CO <sub>3</sub> (particle size < 40 µm)	accelerator	0.1
Cellulose ether	water retention agent	0.05
Polyglycol	defoamer	0.15
Water (for 100 weight % dry mortar)		20

**Table 2.7** Clinker composition of Portland cement.

Mineral	Chemical formula	Oxide composition	Abbreviation
Tricalcium silicate (alite)	$\text{Ca}_3\text{SiO}_5$	3CaO SiO <sub>2</sub>	C <sub>3</sub> S
Dicalcium silicate (belite)	$\text{Ca}_2\text{SiO}_4$	2CaO SiO <sub>2</sub>	C <sub>2</sub> S
Tricalcium aluminate	$\text{Ca}_3\text{Al}_2\text{O}_4$	3CaO Al <sub>2</sub> O <sub>3</sub>	C <sub>3</sub> A
Tetracalcium aluminoferrite	$\text{Ca}_4\text{Al}_n\text{Fe}_{2-n}\text{O}_7$	4CaO Al <sub>n</sub> Fe <sub>2-n</sub> O <sub>3</sub>	C <sub>4</sub> AF

C<sub>3</sub>S and C<sub>2</sub>S, the two silicates, are the main hydraulic phases which together constitute about 70-80 % of the cement. Upon hydration, C<sub>3</sub>S reacts very quickly with water, which is responsible for the development of early strength. Whereas, C<sub>2</sub>S hydrates and hardens slowly, thus contributing little to the early strength occurring in the first 28 days. But C<sub>2</sub>S provides much of the final strength. After one year, the final strength obtained from C<sub>3</sub>S and C<sub>2</sub>S are comparable under comparable conditions.

It has been reported that the hydration mechanisms for C<sub>3</sub>S and C<sub>2</sub>S are very similar [110]. Both calcium silicates give the same hydration products, which are calcium silicate hydrate (C-S-H) and calcium hydroxide. The latter is also known as Portlandite.

C<sub>3</sub>A is the most abundant alumina-containing clinker phase in Portland cement. It can constitute between 2 and 15 % of the total cement clinker. Upon hydration, Al(OH)<sub>4</sub><sup>-</sup> and OH<sup>-</sup> ions which are diffused out of C<sub>3</sub>A react with Ca<sup>2+</sup> and SO<sub>4</sub><sup>2-</sup> present in the cement pore solution, producing hydrous calcium trisulfoaluminate (ettringite). C<sub>3</sub>A reacts with water rapidly, leading to an immediate stiffening of cement paste, which is known as flash set. In general, gypsum, the set-controlling agent is added to prevent such undesirable process. Compared to calcium silicates, C<sub>3</sub>A contributes less to the strength development of cement, and makes concrete susceptible to sulphate attack.

Tetracalcium aluminoferrite ( $C_4AF$ ) constitutes 5-15 % of the Portland cement. The composition of the ferrite phase can be described as a limited solid solution between  $C_2F$  and  $C_6A_2F$ , with  $C_4A_xF_{(1-x)}$ ,  $0 < x < 0.7$  [111]. The hydration rate of ferrite appears to be variable, which is attributed to variations in its composition. The contribution of ferrite to the total strength of cement is insignificant.

**Figure 2.17** shows a typical cement grain, where the appearances of different cement clinker phases are characterized by an optical microscope. Specifically,  $C_3S$  hexagonal crystals are observed in cross section, about 10  $\mu\text{m}$  in length.  $C_2S$  crystallizes in rounded shape with multidirectional lamellae, about 7-10  $\mu\text{m}$  in length. On the other hand, tricalcium aluminate ( $C_3A$ ) appears as gray triangle- or ladder-shaped crystals. The calcium aluminoferrite ( $C_4AF$ ) forms a continuous matrix which surrounds the other mineral crystallites.

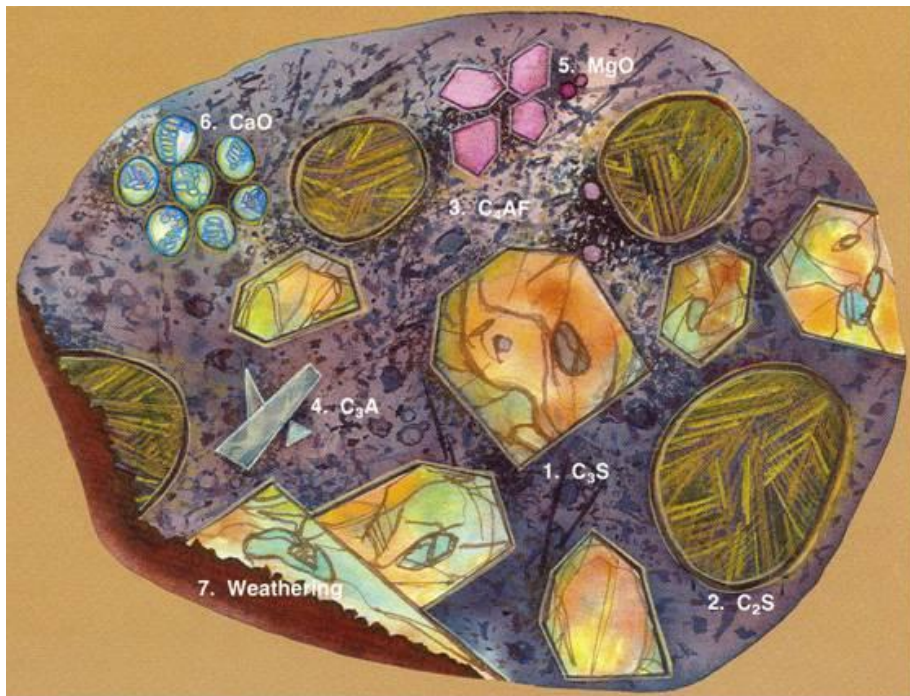


**Figure 2.17** Schematic drawing of the constituents of Portland cement clinker (grain size 30  $\mu\text{m}$ ); the clinker was etched with 1,2-cyclohexanediamine-N,N,N',N'-tetraacetic acid-di-sodium salt (CDTA). Adapted from Cement Microscopy, Halliburton Services, Duncan, OK.

### 2.2.2.1.2 Calcium aluminate cement (CAC)

CAC is produced by heating a mixture of raw materials, typically calcium carbonate (limestone) and bauxite or other low-SiO<sub>2</sub> aluminous materials. Similar to Portland cement, CAC also contains calcium oxide, aluminium, silicon, and iron. However, their compositions are rather different as is shown in **Figure 2.18** [112, 113]. CAC belongs to the group of alumina-abundant cements. The commonly used dark grey/black variety contains 35-40 % Al<sub>2</sub>O<sub>3</sub>, whilst the white CAC variety has Al<sub>2</sub>O<sub>3</sub> contents ranging from 50-80%.

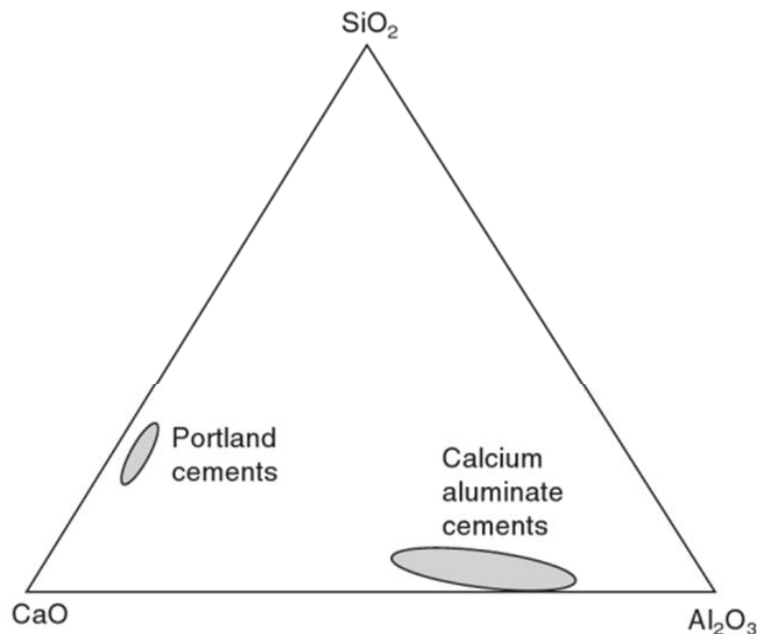


**Figure 2.18** Compositional range of calcium aluminate cements in comparison to Portland cement [112].

The phase composition of commercial CACs varies significantly. But the common feature of these cements is they consist primarily of monocalcium aluminate (CA), which is the principle hydraulic phase responsible for the strength development of CAC. Mayenite (C<sub>12</sub>A<sub>7</sub>) is another main reactive phase, which contributes to the adjustment of the setting time of cement. Other phases such as melilite, belite, ferrite, etc. make up a certain amount of the total cement clinker. The hydration reaction of CAC is rapid, accompanied by considerable evolution of heat. At low temperature, the

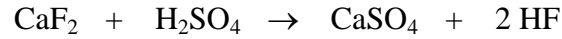
major hydration product of CAC is  $\text{Ca}[\text{Al}(\text{OH})_4]_2 \cdot 6\text{H}_2\text{O}$  ( $\text{CAH}_{10}$ ). Above 15 °C, the intermediate phase ( $\text{C}_2\text{AH}_8$ ) is formed along with  $\text{CAH}_{10}$ . A further higher temperature promotes the formation of stable  $\text{C}_3\text{AH}_6$  from the early stage of hydration [114, 115, 116, 117].

CAC is marked by its rapid strength development, good resistance to chemical attack (*e.g.* sulfate, acid), as well as its abrasion resistant properties. But CAC is considerably more expensive as compared with Portland cement. Therefore, it is commonly used as one component in mixed binder systems to bring special properties to concrete or mortars.

### 2.2.2.1.3 Anhydrite

Anhydrous calcium sulfate ( $\text{CaSO}_4$ ) is called anhydrite. The natural anhydrite generally originates from supersaturation of aqueous solutions in shallow seas. It possesses a rhombic dipyramidal structure, often in association with gypsum deposits. Anhydrite, always crystalline, can either be sparry (anhydrite spar), coarse to close grained, or even rod shaped. Very pure anhydrite is bluish white, but usually it is gray with a bluish tinge. Natural anhydrite is rich in mineral resources, but its reactivity is very low. Unless being very finely ground, the natural anhydrite does not react with water.

Synthetic anhydrite is mainly produced as a by-product of hydrofluoric acid. During its production, calcium fluoride is treated with sulfuric acid, resulting in the precipitation of calcium sulfate (see **Equation 2.1**). Unlike the natural material, synthetic anhydrite is composed of very small primary crystals. These crystals are agglomerated to form secondary particles with high specific surface area. Therefore, this synthetic anhydrite is highly reactive with water as compared to natural anhydrite. In flooring materials, synthetic anhydrite is added as a component to ternary binder systems including OPC and CAC [118, 119, 120, 121].



**Equation 2.1** Production of hydrofluoric acid and synthetic anhydrite (by-product).

According to the specific use and requirements, SLUs are modified by different organic additives, including retarders, stabilizers, defoamers, redispersible powder, etc. Among them, the most important additives are superplasticizers (casein or polycarboxylate) which act as water reducing agent, supporting the self-levelling and self-smoothing properties of the mortars.

#### 2.2.2.2 Current research status of casein superplasticizer in SLUs

In self-levelling underlayments (SLUs), casein stands out above all other superplasticizers because it provides excellent flow properties, as well as a unique self-healing effect on the surface of the grout (see **Figure 2.19**).

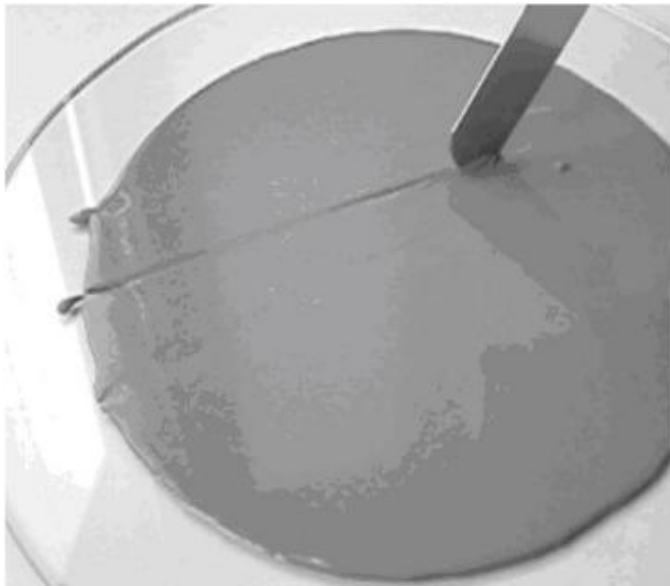
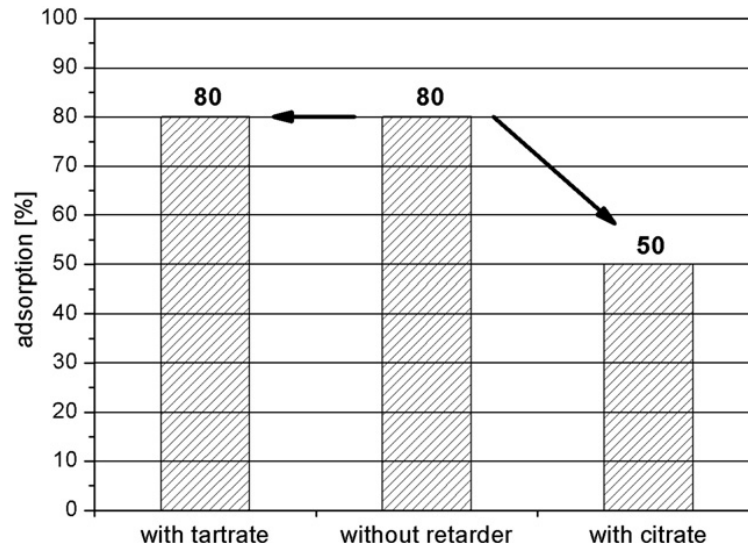


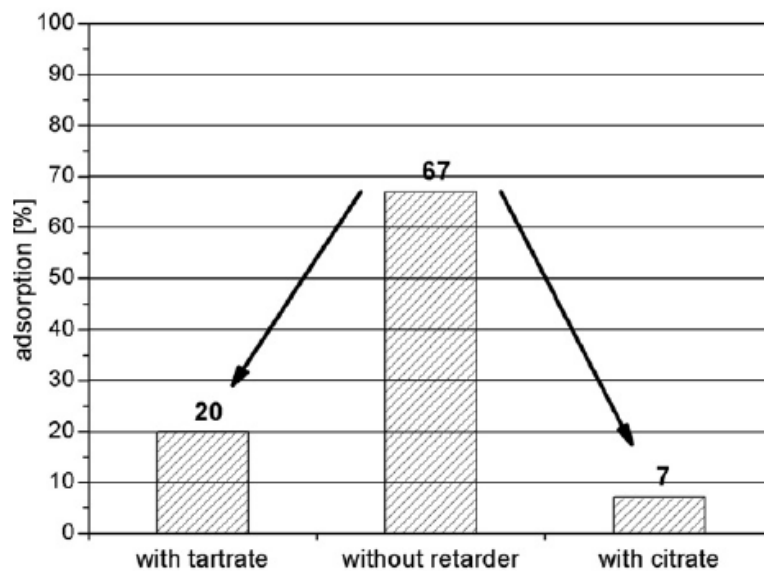
**Figure 2.19** Demonstration of the self-healing property of a casein based SLU grout [100].

Although casein has a long history of application, the systematic investigation on the performance of casein superplasticizer in SLUs only occurred very recently. In 2008, PLANK et al. studied the compatibility of superplasticizers (polycarboxylate, casein) with retarders (tartrate, citrate) in SLUs [122]. As is shown in **Figure 2.20**, in the presence of retarders, adsorption of casein superplasticizer on the ternary binder system remained at high levels. In contrast, polycarboxylate was found to hardly adsorb, especially in the presence of citrate. These results were believed to be related to the charge properties of superplasticizers in cement pore solution. Specifically, casein was revealed to possess a high anionic charge density in cement pore solution, which facilitated its higher adsorption affinity to the binder surface and thus a better dispersing effectiveness in mortar. Whereas, the anionic charge density of polycarboxylates was found to be relatively low. In SLU paste, polycarboxylate would adsorb only after the retarders possessing a higher anionic charge density have adsorbed. This study demonstrated the excellent compatibility of casein superplasticizer with other additives in the ternary binder system.

Furthermore, PLANK et al. isolated the pure  $\alpha$ -,  $\beta$ - and  $\kappa$ -casein fractions from whole casein, and characterized the single proteins with respect to their charge properties, adsorption behavior and the dispersing effectiveness in SLU pastes [109]. The study revealed that  $\alpha$ -casein is the most functional fraction responsible for the outstanding plasticizing effect of casein. It adsorbed on cement in the highest amount, whereas  $\beta$ -casein showed medium and  $\kappa$ -casein the lowest adsorption.



Superplasticizer:  
Casein



Superplasticizer:  
Polycarboxylate

**Figure 2.20** Adsorption of superplasticizers in a SLU formulation in the absence and presence of tartrate and citrate [122].

Additionally, DE GASPARO. et al. studied the distribution of casein superplasticizer in the Portland cement and calcium aluminate cement dominated SLU formulation [123]. Using selective additive staining along with in-situ observations of fluorescence development, the localization and quantification of chemical additives present in the SLU were clearly revealed. Under hot-dry climate conditions, it was found that casein migrated greatly with evaporation induced water flow, resulting in strong skin enrichment at the surface. As a consequence, casein superplasticizer

formed a film at the surface of the hardened grout, which accordingly increased the surface hardness significantly. In contrast, under humid conditions, casein showed almost no fractionation in the mortar layer. The detailed results are displayed in **Figure 2.21**. This finding helps to gain new insights into the dynamics of water transport within the SLU during curing.

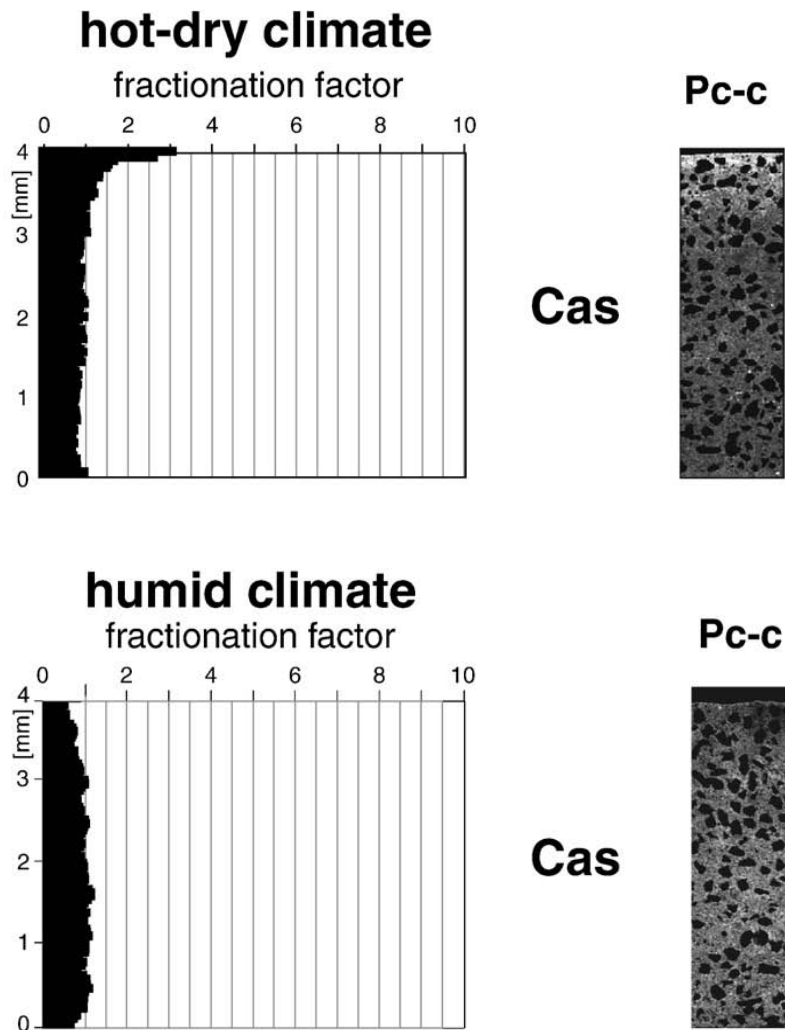


**Figure 2.21** Quantitative distribution diagrams of casein in a Portland cement dominated SLU formulation. The skin of the samples was cured under hot-dry (top) and humid (bottom) climate conditions, respectively [123].

Despite of these above studies, the working mechanism of casein superplasticizer in SLUs is still poorly understood. Little work has been done on the interaction of casein

proteins and cement. This is not conducive to the further development of casein superplasticizer in the construction industry. Further fundamental research on the casein/binder interaction is required.

### **2.2.3 Disadvantages of casein superplasticizer**

Over the past decades of application, some disadvantages of casein based superplasticizers have been reported. In the late 1970s, the malodour in buildings where casein was used as additive to improve the flowability of concrete, was reported for the first time. In 1984, the accumulation of malodorous amines was reported [124], which led people to believe that some kinds of bacteria may have attacked the casein proteins in concrete. In 1988, the bacteria from deteriorated concrete materials containing casein were isolated, identified and characterized [125]. Two bacteria species, namely *Clostridium bifermentans* and *Clostridium sporogenes*, were found to be dominant in concrete materials, which may be fertilized by casein proteins. This study gave a clear indication of the origin of infected buildings.

Another major problem which severely bothers the formulators is that the quality of casein superplasticizer can vary greatly. Depending on a series of factors, such as species of animals, sampling season and manufacturing method, widely fluctuant plasticizing effects were observed for caseins of different batches. Therefore, the industry has to spend enormous cost for quality assessment of random samples before delivery can be made.

## **2.3 Manufacture of casein**

Casein is generally produced by precipitation from dairy milk. During the past decades, a number of methods for the production of casein have been established and were improved, *e.g.* cryoprecipitation precipitation, ethanol precipitation, etc. [2]. Among them, acid precipitation and rennet coagulation are two principal methods which are widely used for casein manufacturing on an industrial scale.

Acid casein is produced from skim milk by acid precipitation, usually with lactic, hydrochloric and sulphuric acid. In Europe, hydrochloric acid has been the most commonly used acid for production of acid casein. Acid casein is insoluble in water but becomes soluble in alkaline solution, where caseinate is believed to be formed.

Rennet casein is produced when *chymosin* (the milk-clotting enzyme extracted from the stomachs of young calves) was added into milk, where casein proteins were found to coagulate and congeal into a solid mass. Rennet casein is insoluble in water and alkaline solutions, but becomes soluble after being treated with polyphosphate. Most of the rennet casein is used for production of cheese. Its properties are significantly different from those of acid caseins.

In general, commercial casein powder is produced according to the following processing steps (**Figure 2.22**). Firstly, casein proteins are precipitated from skim milk. Then, the precipitated mixture is heated to expel the moisture, and also to coagulate the casein curd formed. Furthermore, the casein curd is dewheyed and washed with pure water. After dewatering and drying, the moisture content of casein is greatly reduced. Lastly, the casein particles are milled, blended and bagged for sale [51].

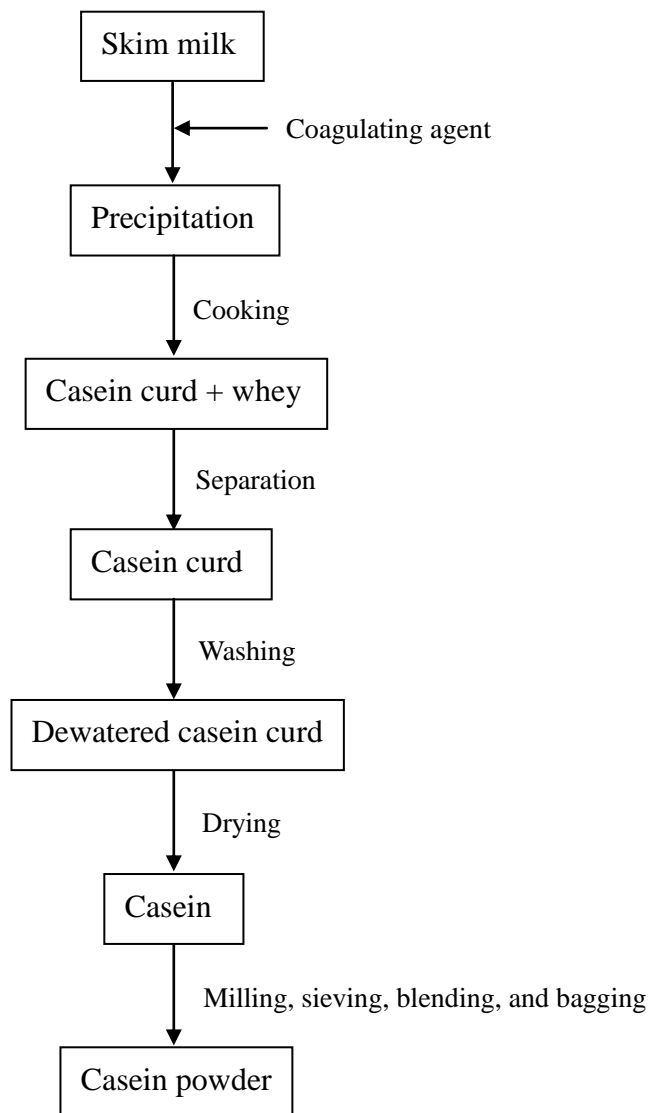


**Figure 2.22** The main processing steps involved in the production of casein [51].

### **3 Objective of this work**

Casein being a natural biopolymer is consumed in annual quantities of approximately 5000 tons in the construction industry. There, it has been used as a major admixture in cementitious building materials for decades. In spite of its long history of application, the working mechanism of casein superplasticizer is still unknown. Additionally, the applicators of casein repeatedly have reported about huge fluctuations in the quality which poses a major problem for them. The industry has to routinely test every casein sample extensively and assess its performance before application. Unfortunately, this testing process is very time consuming and a significant amount of mortar specimens have to be prepared which presents a considerable time and cost factor.

This thesis targets to investigate the working mechanism of casein superplasticizer in self-levelling underlayments, and to develop a fast and inexpensive method to determine the quality of casein superplasticizer. As is well known, casein in Portland cement-based building materials is principally exposed to highly alkaline environments. Thus, understanding the structure of the casein micelles under alkaline pH will help to understand the working mechanism and performance of casein superplasticizer. In the thesis, firstly the behavior of casein micelles in alkaline environment is to be characterized. In this context, the colloidal properties of casein in alkaline solutions of varied pH as well as the morphology of dried casein deposit will be investigated.

Secondly, the commercial caseins from different quality batches will be subjected to an in-depth study. The biochemical composition of caseins and their interactions with cement are to be characterized. In this context, a fast and accurate method of analyzing this biopolymer and assessing its quality will be developed. Meanwhile, the working mechanism of casein superplasticizer in SLUs will be further confirmed.

Aiming to determine the functional component in superplasticizer, casein will be fractionated using chromatographic method in the third part of this chapter. The obtained individual proteins are to be characterized with respect to their dispersing effectiveness and self healing properties in SLU pastes. Furthermore, the performance of recombined casein and chemical-treated casein superplasticizer will be investigated.

It is known that the structure and quality of casein superplasticizer are influenced by many factors. In the last part of this chapter, the heat induced change in casein occurring during its production is to be investigated. Casein superplasticizers subjected to various heat treatments will be characterized with respect to the charge property, chemical structure, dispersing effectiveness, and so forth. This context helps to optimize the manufacturing conditions of casein superplasticizer.

## 4 Materials and methods

### 4.1 Materials

#### 4.1.1 Casein powder

Bovine casein used in this thesis is provided by Ardex GmbH, Witten/Germany, manufactured by acid (HCl) precipitation from milk. The chemical components of the casein sample are listed in **Table 4.1**. Elemental analysis showed the composition (wt.%) as follows: 48.53 % C, 7.34 % H, 13.42 % N, 29.15 % O, 0.61 % S, 0.20 % Ca and 0.75 % P. Additionally, a specific surface area of 1,523 cm<sup>2</sup>/g was determined for casein powder using the Blaine method. The bulk density was found to be 1.31 g/cm<sup>3</sup>.

**Table 4.1** Chemical components of the commercial casein sample.

Component of Casein	
Moisture (%)	11.4
Protein (%)	85.4
Ash (%)	1.8
Lactose (%)	0.1
Fat (%)	< 1.3
Sodium (%)	< 0.1
Calcium (%)	< 0.1

#### 4.1.2 Preparation of casein dispersions

Casein/water suspensions were prepared simply by dispersing acid casein powder into deionized water. Casein dispersions of varied pH were subsequently obtained by adding concentrated NaOH (aq) to the aqueous casein suspensions. The resultant

dispersions were allowed to stand at room temperature for 1 hour, and subjected to no further treatment before use. Casein concentration used in this study was adjusted to 1 g/L with deionized water. A pH glass electrode (BlueLine 14 pH from Schott, Mainz/Germany) was applied to examine the pH values over a range of 8 - 12. Whereas, the achievement of pH 13 and 14 were verified using the calculation of OH<sup>-</sup> activity in casein dispersions, which prevents the inaccurate pH meter reading caused by alkaline error. To study the colloidal behaviour of casein at extreme alkaline condition, casein powder was dispersed in 4 M NaOH (aq) and the resulting dispersion was designated as “casein pH > 14”.

#### **4.1.3 Preparation of Ca-depleted casein dispersions**

Ca-depleted casein was prepared as follows: 3 g of casein powder was dissolved in 200 mL of 0.8 M urea (Merck, Darmstadt/Germany), to which 0.3 g of EDTA-Na<sub>2</sub> 2H<sub>2</sub>O (Merck, Darmstadt/Germany) were added. The resultant solution was stirred for 2 hours at room temperature and afterwards centrifuged at 9,600 rpm for 5 min. Next, the produced supernatant was dialyzed using cross flow filtration to remove the urea and salt. The concentrated and dialyzed sample was then lyophilized in a laboratory freeze dryer, finally resulting in the dried Ca-depleted casein.

The same preparation procedure applied to casein (see section 4.1.2) was used here to produce Ca-depleted casein solutions at pH 12, 13, 14 and > 14.

#### **4.1.4 Preparation of casein dispersions containing NaCl at pH 12**

0.08 g, 0.87 g and 2.33 g of NaCl salt (Merck, Darmstadt/Germany) were added into 10 mL of casein solutions of pH 12 ( $c_{\text{casein}} = 1$  g/L), resulting in solutions with ionic strength of 0.15 M, 1.5 M and 4 M, respectively. This way, the NaCl-containing casein solutions possess the same ionic strength as the above mentioned casein solutions of pH 13, 14 and > 14 (see section 4.1.2). It should be mentioned that the volume change of the solutions due to the addition of NaCl was ignored.

#### **4.1.5 Preparation of precipitate enriched in $\alpha$ - and $\beta$ -casein**

According to a previous study [126], 4 g of casein powder were dissolved in 40 mL of ultra pure water and heated moderately to 35 °C. The pH of the resultant solution was adjusted to 7.0 - 7.5 by dropwise addition of dilute NaOH (aq). After that, 5 M calcium chloride (aq) were added until the concentration of  $\text{Ca}^{2+}$  reached 0.25 M. The obtained viscous solution was allowed to be incubated for a few hours. Lastly, a white precipitate enriched in  $\alpha$ - and  $\beta$ -casein was produced by the centrifugation of above solution at 9,600 rpm for 5 min.

The supernatant obtained from above centrifugation was strongly enriched in  $\kappa$ -casein, which would be used for the large-scale purification of  $\kappa$ -casein later (see 4.1.7.2).

#### **4.1.6 Preparation of buffers for FPLC**

For FPLC analysis of caseins, an imidazole/HCl buffer containing 3.3 M urea was used. To obtain eluent buffer A, 1.362 g of imidazole (Merck, Darmstadt/Germany) and 198 g of urea were dissolved in 900 mL of ultra pure water under stirring. The pH of the solution was adjusted to 7.0 by carefully adding diluted hydrochloric acid. After that, 2 mL of 3-mercapto-1,2-propanediol (Merck, Darmstadt/Germany) and ultra pure water were added until the total volume of the solution reached 1000 mL. This way, an eluent buffer A containing 20 mM imidazole, 3.3 M urea and 0.2 % (v/v) 3-mercapto-1,2-propanediol was obtained. Preparation of the eluent buffer B was done in the same manner. The only difference was that it additionally contained 0.5 M NaCl.

#### **4.1.7 Preparation of casein samples for FPLC**

##### **4.1.7.1 Preparation for chromatographic analysis**

100 mg of casein, 720 mg of urea, 5 mg of EDTA and 2 mg of dithiothreitol (Merck,

Darmstadt/Germany) were dissolved in 2 mL of buffer A, to which 0.1 mL of 3-mercapto-1,2-propanediol were added. The pH of above solution was adjusted to 7 by addition of diluted ammonia. Prior to use, the solution was filtered through a 0.2  $\mu\text{m}$  Millipore membrane (Macherey-Nagel, Düren/Germany) to remove insoluble particles which disturb the chromatography process.

#### **4.1.7.2 Preparation for large-scale separation of casein**

According to a previous study [126], 1.5 g of casein powder, 4.3 g of urea, 50 mg of EDTA and 60 mg of dithiothreitol were dispersed in 12 mL of buffer A, which was followed by the addition of 0.5 mL of 3-mercapto-1,2-propanediol. The pH of above solution was adjusted to about 7 by dropwise addition of diluted ammonia. After centrifugation for 20 min, the obtained supernatant was filtered through a syringe filter to remove the large particles, resulting in an opaque solution enriched in  $\alpha$ - and  $\beta$ -casein.

Preparation of a  $\kappa$ -casein enriched sample was described in **4.1.5**.

#### **4.1.8 SLU formulation**

For performance testing of the casein samples, a simplified SLU mortar formulation was used in this thesis (see **Table 4.2**). The formulation is based on a ternary binder system with a water to binder ratio of 0.25. The physical properties of the binders used in this study are shown in **Table 4.3**. The chemical compositions of the binders are displayed in **Table 4.4**, **Table 4.5** and **Table 4.6**.

**Table 4.2** SLU model formulation used in the thesis.

Component	Supplier	Function	Wt. %
Ordinary Portland cement (CEM I 42.5 R)	Milke	binder	47.3
Calcium aluminate cement (approx. 40 wt.% Al <sub>2</sub> O <sub>3</sub> )	Kerneos	binder	32.8
CaSO <sub>4</sub> (synthetic anhydrite)	Solvay	binder	19.1
Li <sub>2</sub> CO <sub>3</sub> (particle size < 40 μm)	Chemetall	accelerator	0.3
Sodium potassium tartrate (KNaC <sub>4</sub> H <sub>4</sub> O <sub>6</sub> 4H <sub>2</sub> O)	Merck	retarder	0.4
Casein	Ardex	superplasticizer	0.12
Water (for 100 wt.% dry mortar)			25.0

**Table 4.3** Physical properties of binders used in the SLU formulation.

Binder	Particle size (D <sub>50</sub> )	Density	Specific surface area
Ordinary Portland cement	11.08 μm	3.18 g/cm <sup>3</sup>	3392 cm <sup>2</sup> /g
Calcium aluminate cement	10.03 μm	3.20 g/cm <sup>3</sup>	3225 cm <sup>2</sup> /g
CaSO <sub>4</sub>	3.24 μm	2.96 g/cm <sup>3</sup>	6010 cm <sup>2</sup> /g

**Table 4.4** Oxide composition of ordinary Portland cement (CEM I 42.5 R) sample [127]

Oxide	Content (wt.%)
SiO <sub>2</sub>	23.7
Al <sub>2</sub> O <sub>3</sub>	3.8
CaO	64.1
Fe <sub>2</sub> O <sub>3</sub>	1.4
SO <sub>3</sub>	2.6
MgO	0.7
K <sub>2</sub> O	0.7
TiO <sub>2</sub>	0.1
Na <sub>2</sub> O	0.1

**Table 4.5** Oxide composition of calcium aluminate cement sample [128]

Oxide	Content (wt.%)
Al <sub>2</sub> O <sub>3</sub>	39.1
CaO	36.9
Fe <sub>2</sub> O <sub>3</sub>	15.8
SiO <sub>2</sub>	4.8
TiO <sub>2</sub>	1.7
MgO	0.8

**Table 4.6** Chemical composition of CaSO<sub>4</sub> (synthetic anhydrite)

Constituent	Content (wt.%)
CaSO <sub>4</sub>	97.0
CaF <sub>2</sub>	1.9
Ca(OH) <sub>2</sub>	0.7

## 4.2 Methods

### 4.2.1 Turbidity

The turbidity of casein dispersions was measured by transmission of light at 600 nm wavelength using a SpectroFlex 6100 photometer (WTW, Alès/France). A 1 cm path-length quartz cuvette was used in the measurement. The turbidity was calculated using the following equation:

$$\tau = -\frac{1}{L} \ln \frac{I}{I_{\text{ref}}}$$

where  $I$  and  $I_{\text{ref}}$  are the intensities of transmitted light for casein dispersions and water reference, respectively.  $L$  is the path length of cuvette. All the measurements were conducted at room temperature.

### 4.2.2 Transmission Electron Microscopy (TEM)

TEM images were recorded on a JEM 100 CX microscope (JEOL Ltd., Tokyo/Japan) equipped with a tungsten cathode. For sample preparation, casein dispersions were adsorbed onto a thin carbon support for 30 s, followed by washing and negatively staining for 1 min in 1 wt.% ammonium molybdate. The examination was carried out under an accelerating voltage of 100 kV.

### 4.2.3 Atomic absorption spectroscopy (AAS)

The calcium content in casein was determined by atomic absorption spectrophotometry (Perkin Elmer 1100 B, Überlingen/Germany). For sample preparation, 6 M urea was used as solvent to achieve a 1 g/L casein solution, to which an excessive amount of EDTA-Na<sub>2</sub> 2H<sub>2</sub>O ( $c_{\text{EDTA}} 5 \times 10^{-4}$  M) was added to disrupt the bound between calcium and phosphate.

### 4.2.4 Particle Charge Detector (PCD)

This method involves a titration with standard polyelectrolyte titrants to evaluate the colloidal charge content of aqueous samples. The basic principle is the reaction of oppositely charged polymeric materials and the charged surfaces. When aqueous solutions of cationic and anionic polymers are mixed, a neutralization reaction will occur. An indicator, in this case the potentiometric detector, is able to detect the equivalent point of reaction. **Figure 4.1** shows the section view of a particle charge detector [129].

Anionic charge density of casein particles in dispersions was measured using a PCD-03 particle charge detector (BTG M ütek GmbH, Herrsching/Germany). Cationic poly diallyl dimethyl ammonium chloride (polydadmac) (BTG M ütek GmbH, Herrsching/Germany) was used as counter polymer for polyelectrolyte titration. In each experiment, 10 mL of casein solution were filled into the measuring cell and titrated with 0.001 N polydadmac solution until the charge equivalent point was reached. Afterwards, the specific anionic charge density of casein was calculated according to the following equation,

$$q = \frac{V \cdot c}{w} \times 10^6$$

where  $q$  is the specific anionic charge density ( $\mu\text{eq/g}$ ),  $V$  is the consumed volume of polydadmac solution during titration,  $c$  is the concentration of polydadmac (0.001 N,

equivalent to 0.001 eq/L),  $10^6$  is a calculation factor for the unit of charge density in  $\mu\text{eq/g}$  and  $w$  is the mass of casein contained in the suspension.

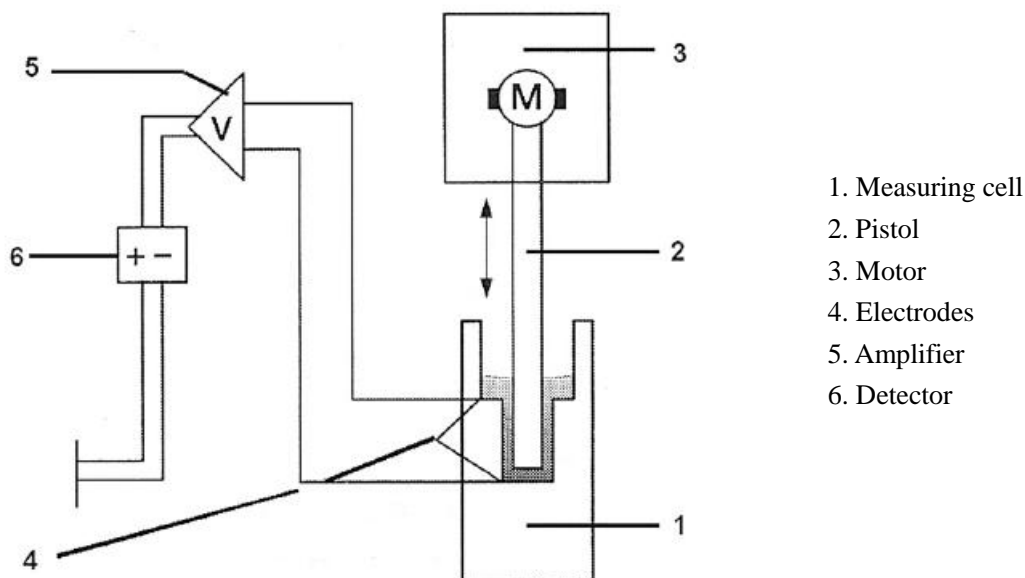


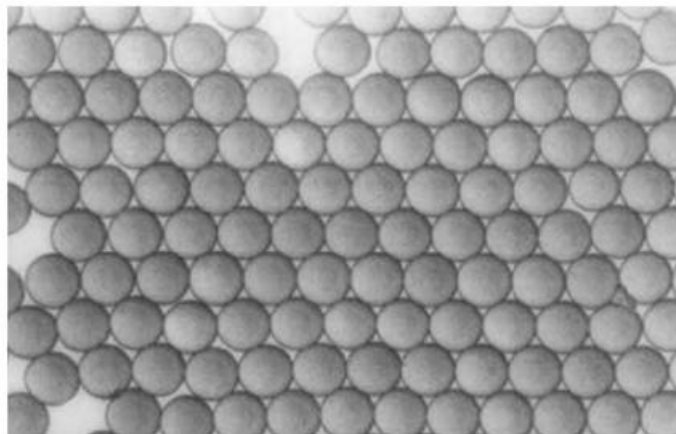
**Figure 4.1** Schematic drawing of charge titration device [129].

#### 4.2.5 Fast protein liquid chromatography (FPLC)

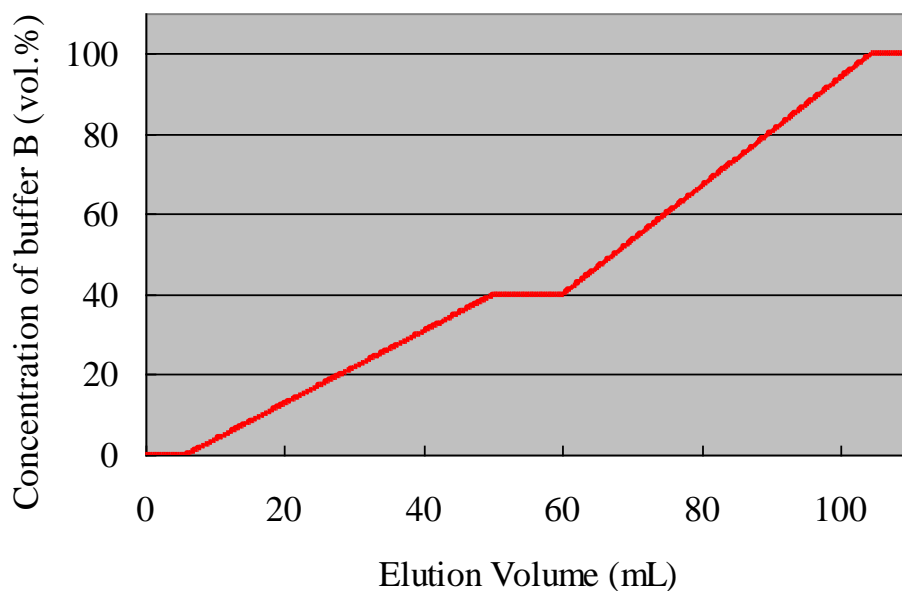
An ÄKTA Explorer (GE Healthcare Munich/Germany) is used as FPLC system in this work. 1 mL Resource Q column (GE Healthcare Munich/Germany) is used as ion exchange media for the analysis of casein proteins, which are based on 15  $\mu\text{m}$  monodisperse, rigid polystyrene/divinyl benzene beads with substituted quaternary ammonium groups. The uniformity and stability of beads allow a high flow rate at low back pressure. **Figure 4.2** shows the monodisperse particles in Resource column. The pore size distribution of the column media is balanced to give high capacities for peptides, proteins, and oligonucleotides [71, 130]. Absorption at 280 nm was monitored by a UV detector.

The preparation methods of the elution buffers and casein sample have been described in section 4.1.6 and 4.1.7. In the measurement, the casein sample is injected into a 100  $\mu\text{L}$  loop on the injection valve. To separate and detect the single protein fractions in

casein, it is necessary to assure that the elution peaks from different fractions are clearly separated and no cross contamination occurs between each other. To meet this requirement, a specific chromatographic protocol has been designed in this work. The elution gradient is shown in **Figure 4.3**. The detailed steps are listed in **Table 4.7**.



**Figure 4.2** Optical micrograph of Source Q monodisperse particles [130].

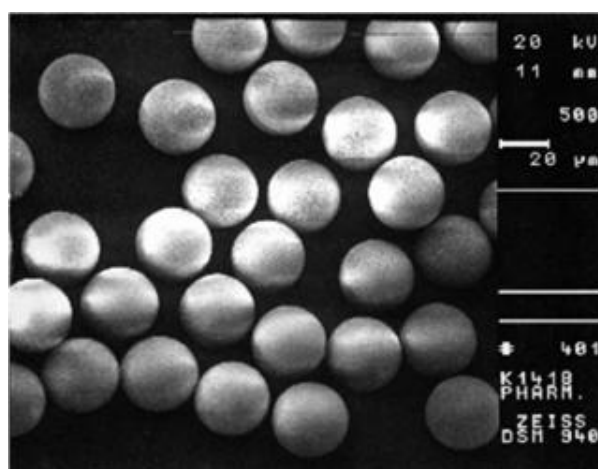


**Figure 4.3** Elution gradient for the FPLC separation of casein proteins.

**Table 4.7** Chromatographic protocol for the FPLC separation of casein proteins.

Volume (mL)	Procedures/parameter
0	Injection of sample to 100 $\mu$ L loop Sample load to column
0 - 5	Wash out the unbound sample Flow rate = 0.5 mL/min
6 - 51	Linear gradient 0-40% (v/v) buffer B Flow rate = 2 mL/min
52 - 61	Platform 40% buffer B (v/v) Flow rate = 2 mL/min
62 - 107	Linear gradient 40%-100% (v/v) buffer B Flow rate = 2 mL/min

For large-scale separation of casein fractions, Source 30Q is used as the column media. It is packed with 30  $\mu$ m monodisperse, rigid polystyrene/divinyl benzene beads, designed for fast, preparative purification of biomolecules. The larger particle size slightly reduces the resolution of chromatograms, but it allows a larger flow rate and a higher loading of protein samples. **Figure 4.4** depicts the monodisperse Source 30 beads [131].

**Figure 4.4** Electron micrograph of monodisperse Source 30 beads [131].

The chromatographic protocol used for the large-scale separation of casein fraction was adopted from the previous study [126]. The elution gradients for the separation of  $\alpha$ - and  $\beta$ -casein and for the purification of  $\kappa$ -casein are shown in **Figure 4.5** and **Figure 4.6**, respectively.

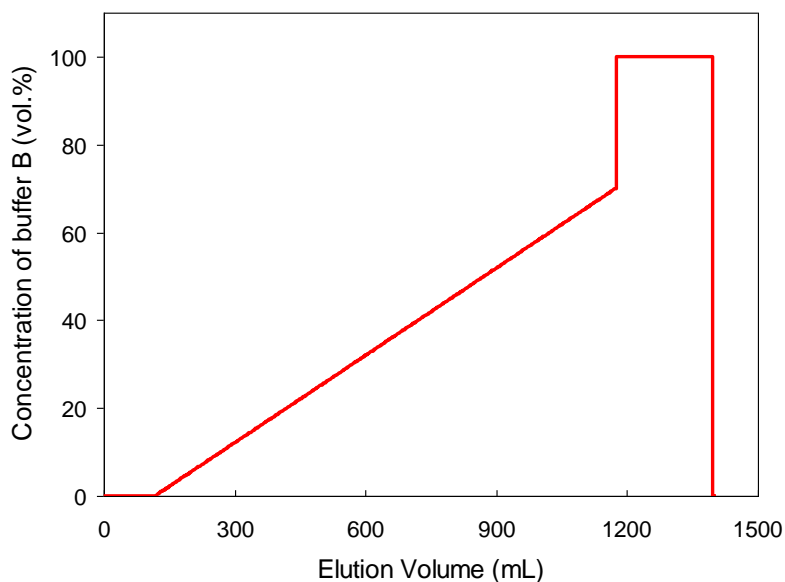


**Figure 4.5** Elution gradient for large-scale separation of  $\alpha$ - and  $\beta$ -casein proteins.

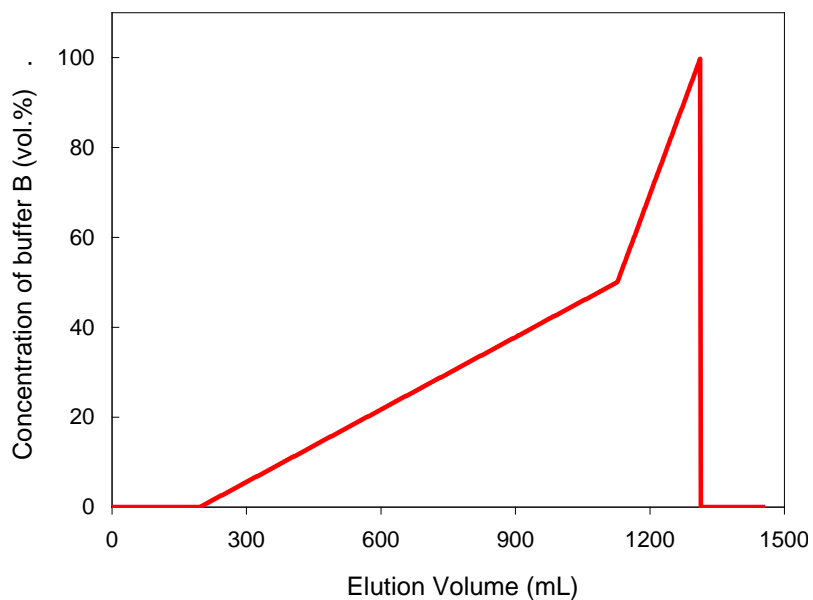


**Figure 4.6** Elution gradient for large-scale separation of  $\kappa$ -casein proteins.

#### 4.2.6 Cross-flow filtration desalting

The desalting of casein fractions resulting from the chromatographic separation is achieved using a cross-flow filtration system (Quixstand, from GE Healthcare, Munich/Germany) which is a commonly used type of filtration in chemical and biochemical engineering. **Figure 4.7** shows the principle of cross-flow filtration and the structure of ultrafiltration membrane [132]. The protein solutions are being pumped in a circuit through a hollow fiber cartridge (UFP-3-C-3X2MA, 3 kDa molecular weight cut-off) in the Quixstand system under a pressure between 0.207 and 0.275 MPa. Ultra pure water is used for the dialysis to remove urea and salts. After an exchange of 8 sample volumes of ultra pure water, the casein solution is almost salt free. The concentrated and dialyzed protein samples are then lyophilized in a laboratory freeze dryer overnight.

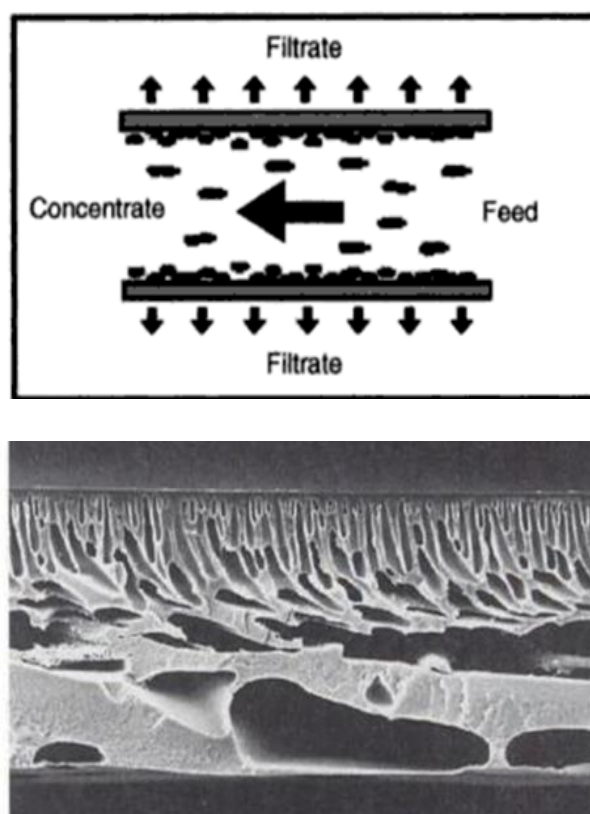


**Figure 4.7** Top: principle of cross-flow filtration; bottom: ultrafiltration membrane with skin layer and support structure [132].

### 4.2.7 Atomic Force Microscopy (AFM)

AFM belongs to the family of high resolution scanning microscopes. It uses the distance dependence of the force between a fine tip and a surface. The working principle of AFM is based on measuring the force by recording the deflection of a cantilever that carries the tip. The major forces derive from van der Waals, electrostatic, hydrophobic, hydrophilic and capillary interactions [133,134]. **Figure 4.8** displays a commercial AFM system with double photo detector. The tip is mounted on a flexible cantilever. When attracted or repelled by the sample, the deflection of cantilever is measured. A laser beam is focused at the end of the cantilever and reflected to two photodiodes, numbered 1 and 2 [135].

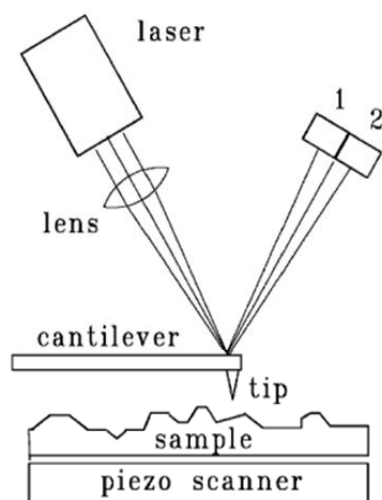


**Figure 4.8** Experimental set-up for atomic force microscopy (AFM) [135].

In this thesis, AFM images were acquired using a Nanoscope IIIa scanning probe microscope (Veeco Instruments, Mannheim/Germany). The microscope was operated in tapping mode using a Si cantilever with a resonance frequency of 320 kHz, a driving amplitude of 1.25 V at a scan rate of 1.0 Hz, and a tip radius of less than 10 nm. For sample preparation, a drop of casein solution ( $c_{\text{casein}} = 1 \text{ g/L}$ ) possessing pH 12 was placed onto a well cleaned silicon substrate (Wacker AG, Burghausen/Germany) which was allowed to dry in  $\text{N}_2$  flow for 30 min. The sample

was then placed on the AFM stage and imaged in air.

#### 4.2.8 Mini slump test

Flowability of cement paste was measured versus time according to EN 12706. Generally, tartrate is dissolved in the mixing water prior to the slump loss test. Then, the dry mortar was added into above water in 1 min. After standing for another 1 min, the mortar was mixed manually at a constant speed for 2 min. The resulting cement paste was poured into a slump cone with an internal diameter of 30 mm and a height of 50 mm. The cone was lifted up and after 30 s the diameter of paste flow was determined by vernier caliper. In some experiments, a smaller mini slump cone with an inner diameter of 14 mm and a height of 25 mm was used to reduce the consumption of superplasticizer. The two types of slump cone used in this study are shown in **Figure 4.9**.

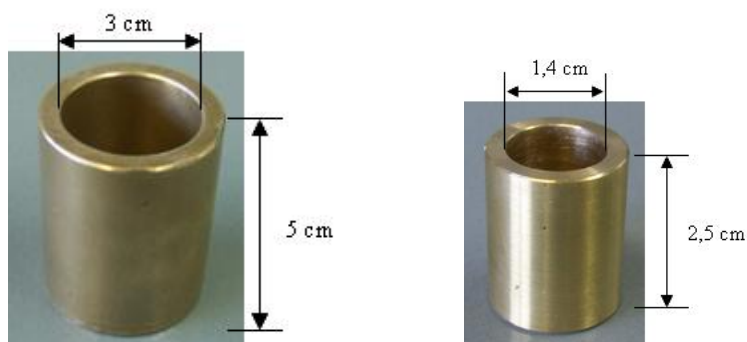


**Figure 4.9** The slump cones used in slump loss measurements.

#### 4.2.9 Total organic carbon (TOC) analysis

In order to measure the adsorption behavior of casein superplasticizer on cement particles, the total organic carbon content in cement pore solution was determined. Specifically, a cement pore solution was produced by centrifugation of the cement paste at 9,600 rpm for 10 min. Prior to measurement, the pore solution was diluted and acidified with 0.65%  $\text{HNO}_3$  (aq) in order to prevent the formation of  $\text{CaCO}_3$  precipitate. Casein content was then measured by TOC analyzer using a High TOC II

instrument (Elementar, Hanau/Germany). The method is based on the combustion of organic compounds and further detection of CO<sub>2</sub> with infrared analysis. Adsorbed amount of superplasticizer was calculated by subtracting the remaining casein concentration in the cement filtrate from initial casein concentration.

#### 4.2.10 Zeta potential measurement

Zeta potentials were determined using a DT 1200 Electroacoustic Spectrometer (Dispersion Technology, Inc., Bedford Hills/USA). This instrument measures a vibration current induced by an acoustic wave which causes the aqueous phase to move relative to the cement particles. From that, a potential difference which can be measured is designated as zeta potential [136]. **Figure 4.10** depicts the surface of a positively charged particle. The counter ions in solution are adsorbed on the particle surface due to the electrostatic attraction. The concentration of counter ions gradually decreases with the distance from the surface. As a consequence, the electric potential decreases with distance. When the particle moves through solution, the counter ions move with it as well. The plane separating the tightly bound liquid layer from the surrounding liquid is called slipping plane. The electric potential at the slipping plane is called zeta potential [137].

In this work, the influence of casein on the zeta potential of binder particles was measured on ordinary Portland cement only, due to premature setting of the ternary SLU system which does not allow zeta potential measurements. A water to cement ratio of 0.5 was used in the measurement. Firstly, the ionic background of cement filtrate was determined, which would be automatically subtracted from the zeta potential values in the experiment. An aqueous casein solution ( $c_{\text{casein}} = 5 \text{ wt.}\%$ , pH = 12) was titrated stepwise to the cement slurry. As a consequence, the zeta potential of cement particles was attained as a function of casein dosage [138].

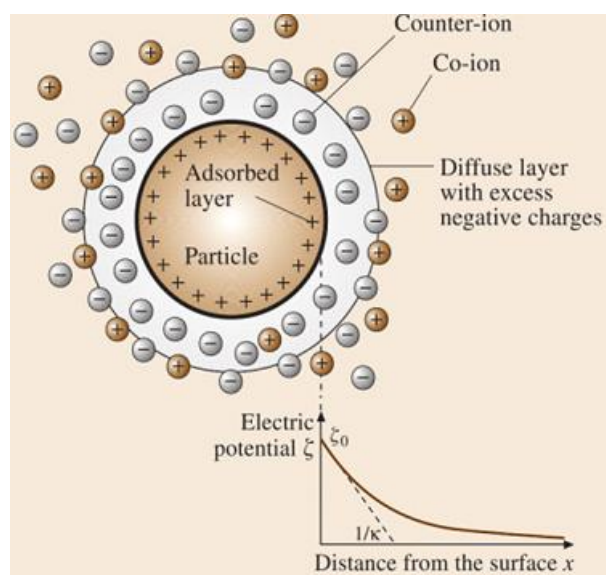


**Figure 4.10** Schematic illustration of electrical double layer and the electric potential near the solid surface [137].

#### 4.2.11 Moisture analysis

The moisture content of casein samples was analyzed using a moisture analyzer Sartorius MA35 (Sartorius AG, Göttingen/Germany). In the experiment, about 1 g of casein powder was placed in an aluminum pan and dried at 120 °C to a constant weight. The data reported for moisture content was the average of three measurements.

#### 4.2.12 Dynamic light scattering (DLS)

DLS measurements were conducted on a Malvern Zetasizer Nano ZS (Malvern Instruments, Herrenberg/Germany) where a He-Ne laser with a wavelength of 632.8 nm is used as light source. The back scattering angle is set to 173 ° and the temperature is stabilized at 25 °C. The particle size distribution was obtained by CONTIN analysis. The measurement was carried on 1 g/L of casein solution at pH 12. Prior to use, the sample solution was filtered by a 0.45 μm Millipore membrane (Macherey-Nagel, Düren/Germany). **Figure 4.11** presents a schematic drawing for the DLS

measurement on a Zetasizer device.

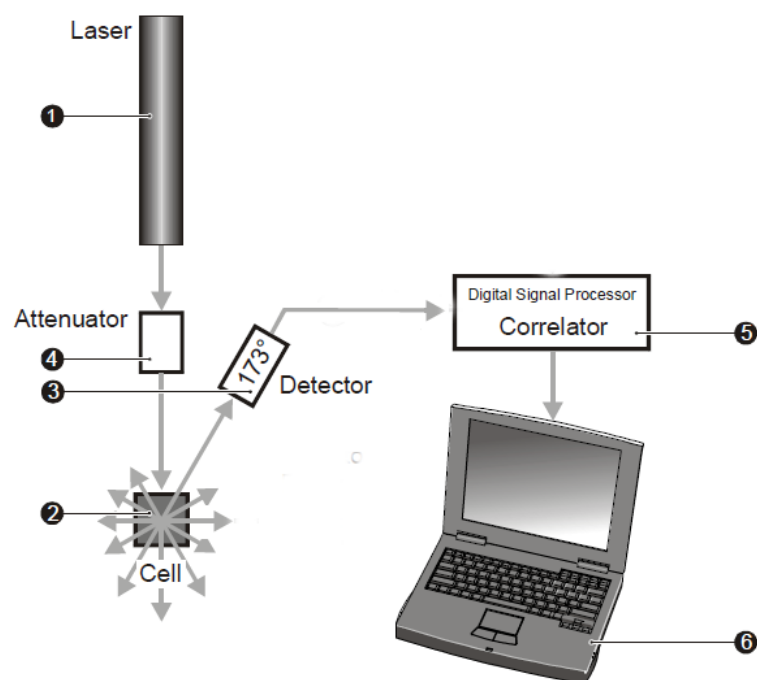


**Figure 4.11** Schematic diagram for the particle size measurement on a Malvern Zetasizer [139].

#### 4.2.13 Gel permeation chromatography (GPC)

Size exclusion chromatography (Waters Alliance 2695 from Waters, Eschborn/Germany) equipped with RI detector 2414 (Waters, Eschborn/Germany) and a three angle dynamic light scattering detector (mini Dawn from Wyatt Technologies, Santa Barbara/USA) was used. Prior to application on the columns, the solution was filtered through a 0.2  $\mu\text{m}$  filter. Casein sample was separated on a Ultrahydrogel<sup>TM</sup> precolumn and three Ultrahydrogel<sup>TM</sup> columns (120, 250 and 500; Waters, Eschborn/Germany). Molecular weights ( $M_w$  and  $M_n$ ) and radius ( $R_h(z)$ ) of casein were determined using a 0.1 M aqueous  $\text{NaNO}_3$  solution (adjusted to pH 12.0 with NaOH) as an eluent at a flow rate of 1.0 mL/min. The value of  $dn/dc$  used to calculate  $M_w$  and  $M_n$  for casein was 0.181 mL/g [140].

#### 4.2.14 Thermogravimetry (TG)

Thermal stability of casein powder was investigated by thermogravimetry using a NETZSCH STA 409 CD instrument (NETZSCH Gerätebau GmbH, Selb, Germany) in a nitrogen atmosphere at a heating rate of 10 °C /min.

#### 4.2.15 Ion chromatography (IC)

The remaining content of tartrate in cement pore solution was determined using ion chromatography (ICS-2000 apparatus, Dionex, Idstein/Germany). An IonPac AS 11 column is used as analytical column in the measurement. It is an anion-exchange column, which allows fast gradient screening of inorganic anions and organic acid anions present in the sample. **Figure 4.12** shows the structure of column material packed in IonPac AS 11. The substrate for column is a 13  $\mu\text{m}$  diameter microporous resin bead, which is composed of a cross-linked core (ethylvinylbenzene crosslinked with 55% divinylbenzene) and an anion-exchange layer (quaternary ammonium functional groups) attached to the surface. The unique structure of the column makes it ideal for the determination of organic acids and inorganic anions at comparable concentrations [141].

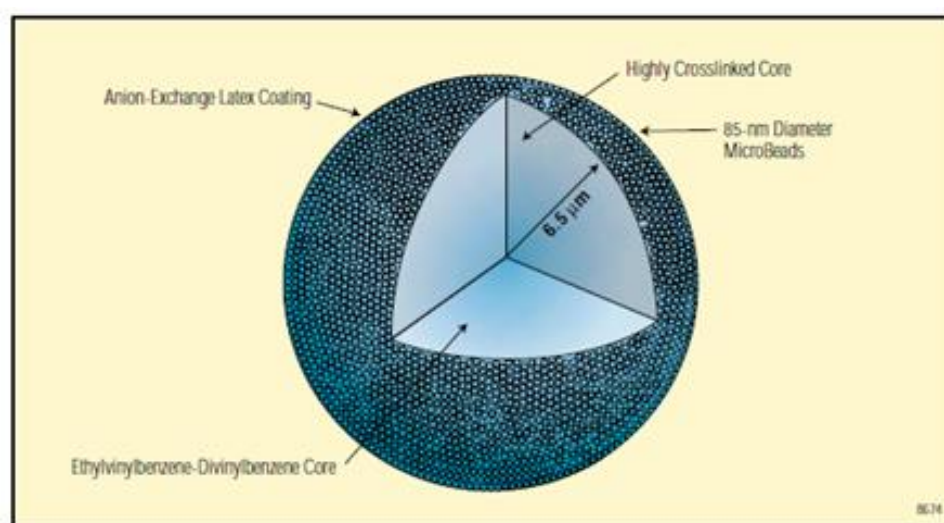


**Figure 4.12** Structure of an IonPac AS 11 packing particle [141].

Prior to measurement, the filtrate of SLU paste containing the admixtures was diluted and acidified with 0.65%  $\text{HNO}_3$  (aq) in order to prevent the formation of  $\text{CaCO}_3$  precipitate. KOH was used as the standard eluent in each measurement. **Figure 4.13** shows the elution gradient used in this work.

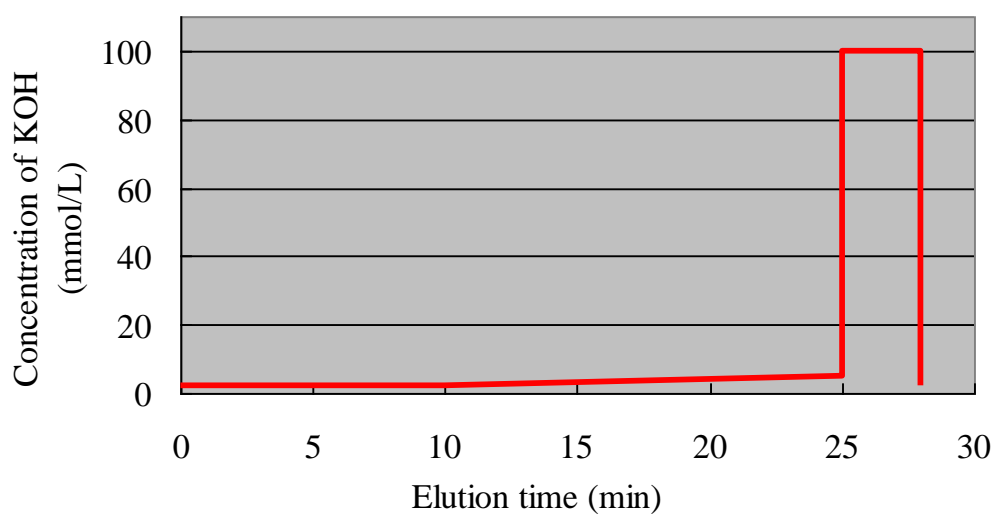


**Figure 4.13** Elution gradient for the ion chromatography separation of tartrate anion.

## 5 Results and discussion

This section is composed of four parts.

In the first part, the behavior of casein in alkaline solutions and in dried state was investigated. The dissociation and re-association of casein was characterized as a function of solution pH, from which the role calcium played in maintaining the integrity of micelles was discussed. A potential mechanism involved in above processes was proposed based on an analysis of interactions occurring between the casein proteins. From a dried deposit, the morphology of submicelles and assembled casein proteins was visualized by microscopic studies.

Secondly, the performance of casein superplasticizer in self-levelling underlayments (SLUs) was subjected to an in-depth study. The dispersing effectiveness of casein superplasticizer along with its surface charge property, adsorption behavior, and the stability of cement particles were systematically investigated. Additionally, a simple and inexpensive method for determining the quality of casein superplasticizer was proposed. Commercial casein products of different batches were characterized with respect to their dispersing power in SLUs. To find out the correlation between the different compositions of the casein samples and their performance, fast protein liquid chromatography (FPLC) as well as dynamic light scattering (DLS) measurements were carried out. Based on these findings, criteria for assessing the quality of casein to be used as superplasticizer in SLUs are proposed.

Thirdly, the performance of individual casein proteins in SLUs was investigated, from which the fraction possessing the highest dispersing effectiveness and unique self-healing property in cement paste was determined. A casein sample recombined from individual proteins was prepared and characterized, aiming to find out the difference of original casein and reproduced casein superplasticizer. Furthermore, a

chemically treated casein superplasticizer was produced. Its compatibility with a SLU formulation was investigated.

In the last part of this chapter, the influence of heat treatment on the quality of casein superplasticizer was investigated. The heat induced physical and chemical changes occurring in casein during its manufacturing process were simulated and analyzed using various techniques. The goal was to explore the influence of heating temperature and exposure time on the denaturation of casein molecules.

## 5.1 Behavior of casein in alkaline solution

### 5.1.1 Solubility of casein as a function of pH

The solubility of casein powder in water and in aqueous NaOH solutions of varied pH was examined and the corresponding photos are presented in **Figure 5.1**. Casein appeared rather insoluble in deionized water and at pH 8, where powder deposits were left at the bottom of the sample vials. In aqueous solution of pH 10, the powder was partially dissolved, but a flocculant layer of sediment could be observed at the bottom. As pH increased further, stable and homogeneous dispersions were formed, which demonstrates good solubility of casein powder in highly alkaline solutions.

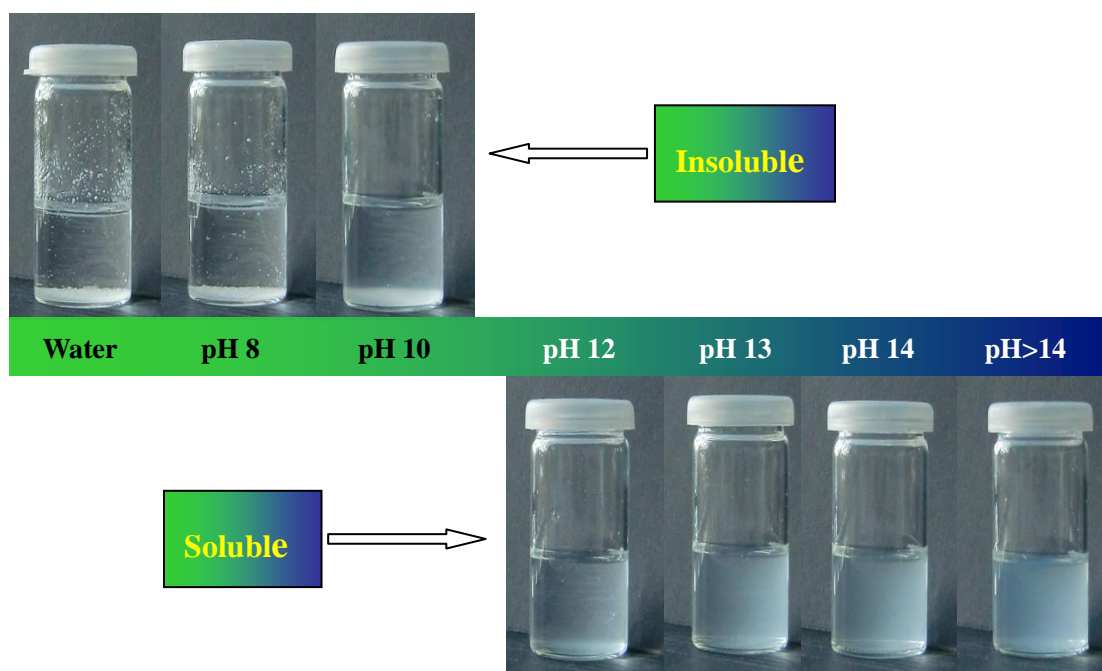


**Figure 5.1** Photos of casein dispersions in water and in aqueous NaOH solutions of varied pH.

The above observation suggests that casein can be well dissolved in strongly alkaline fluids. This finding is in good agreement with industry experience where all applications of casein products require them to be dispersed using an alkali first. According to the literature, caseinate can be produced at alkaline pH as outlined in **Figure 5.2** [51]. In this work, sodium hydroxide is used to dissolve casein powder,

therefore, sodium caseinate is supposed to be produced in solution. Thus, it is more accurate to describe the sample as sodium caseinate. However, to avoid confusion, the term “casein in alkaline solution” is still used in the context instead of caseinate. This is also well accepted in previous publications [12, 43, 44].

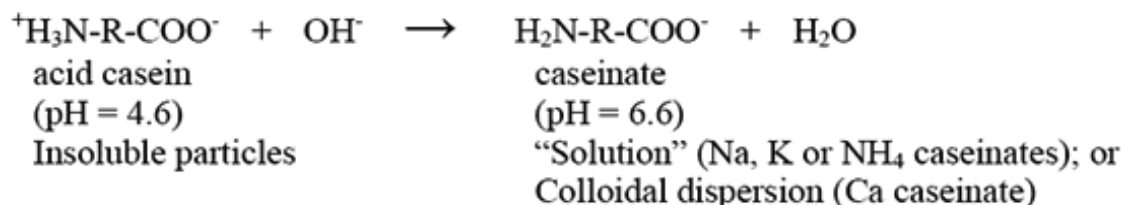


**Figure 5.2** Simple equation showing the reaction of casein with alkali, where R represents the casein protein.

However, it should be noted that casein dispersions at highly alkaline pH (pH 12 - pH > 14) did not show identical appearances in the photographs. There seemed to be a tendency for the solution to become more turbid at higher pH. Towards a better understanding of casein micellar behavior in highly alkaline environment, further investigations have been launched and the results will be discussed in the following.

## 5.1.2 Dissociation and re-association of casein in alkaline solution

### 5.1.2.1 Turbidity of alkaline casein solutions

Turbidity measurement as an indicator of protein aggregation is advantageous for comparative assessment of samples [142]. In this study, the turbidity of casein solutions over a pH range of 12 to > 14 has been determined. In **Figure 5.3**, the turbidity values were found to be constant for casein solutions of pH 12 and 13. There, the intensities of transmitted light achieved 92 % as compared to the deionized water reference. Therefore, rather low turbidity values have been obtained at pH 12 and 13, which according to a previous study is attributed to a disruption of casein micelles in solution [12]. As pH increased to 14, the turbidity of casein dispersion slightly

increased to  $0.1 \text{ cm}^{-1}$ , which according to previous studies correlates with an alteration of the micellar structure in solution [143]. Most likely, the subunits disrupted from micelles start to re-associate, and a slight aggregation occurs in casein solution of pH 14. Furthermore, a sharp increase in turbidity has been observed as pH exceeded 14, which is assumed to arise from an increase in the extent of aggregation [144].

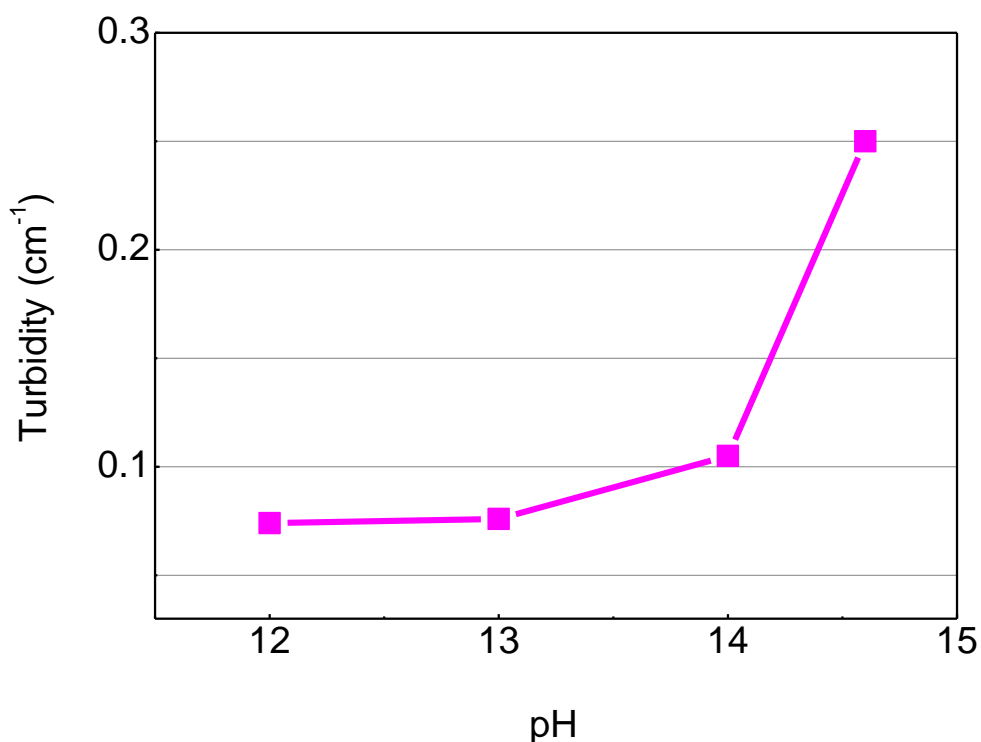


**Figure 5.3** Turbidity of casein solutions as a function of pH ( $c_{\text{casein}} = 1 \text{ g/L}$ ).

#### 5.1.2.2 TEM images of casein alkaline solutions

Above speculation has been confirmed by TEM measurements of casein solutions. As shown in **Figure 5.4**, negatively stained casein particles are visible as bright areas in the micrographs. The diameter of casein particles at pH 12 and 13 was found to be around 10 nm, which is comparable to the reported size of casein submicelles. There is no evidence for the existence of large casein micelles or aggregates in the micrographs, indicating that the casein micelles have been completely dissociated into submicelles at pH 12 and 13. These observations agree well with the low turbidity values of corresponding casein solutions.

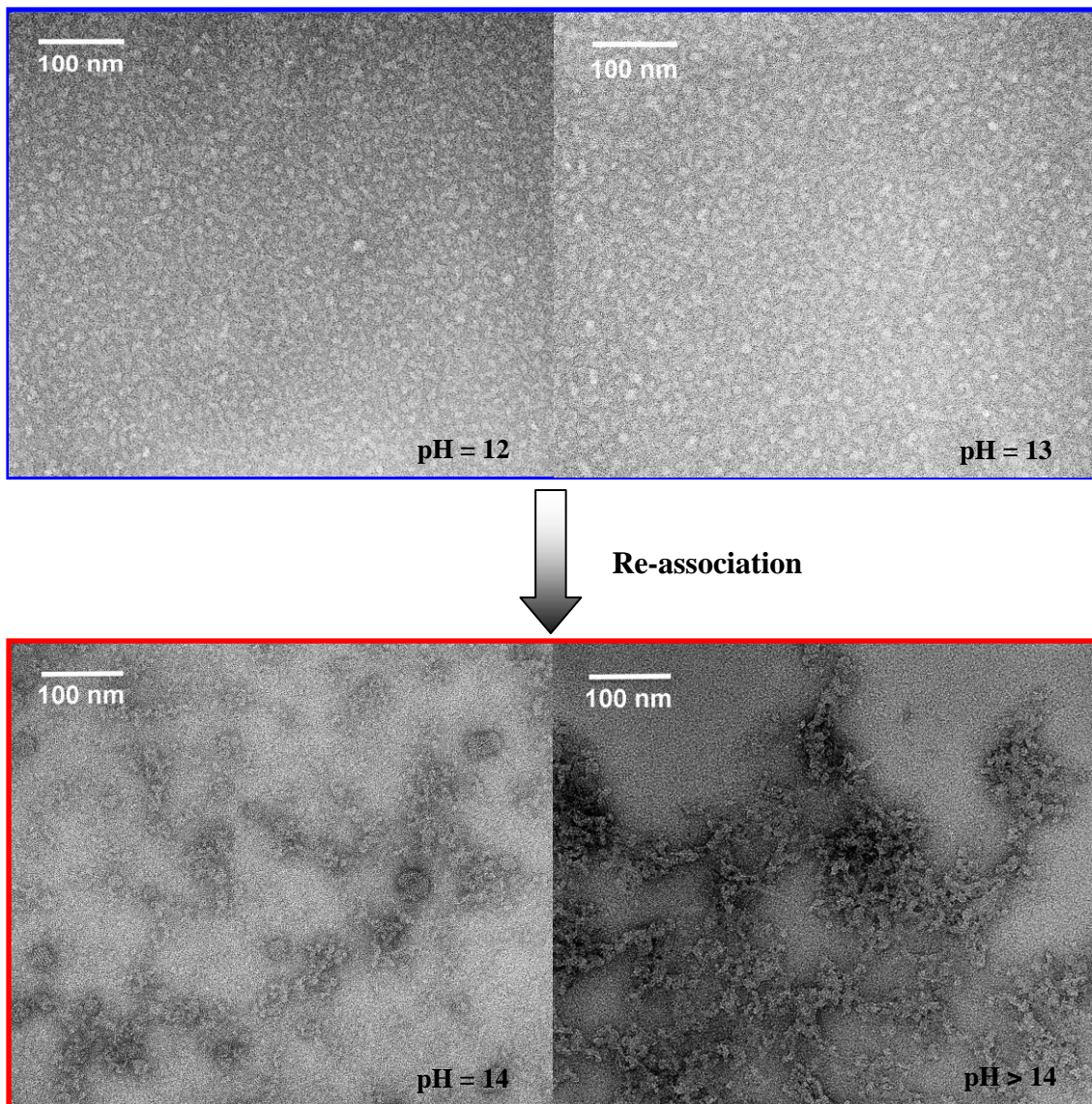


**Figure 5.4** Transmission electron micrographs from casein dispersions ( $c_{\text{casein}} = 1 \text{ g/L}$ ) at varied alkaline pH: casein submicelles appeared as dominant species at pH 12 and 13; as pH increased to 14, a slight tendency for submicelle association was observed; as pH exceeded 14, an extensive association of casein submicelles occurred, resulting in the formation of network aggregates.

As pH increased to 14, a tendency for submicelles to aggregate occurred. Larger particles are occasionally observed in the micrograph, which explains the slight increase in the turbidity result. Furthermore, as pH exceeded 14, a progressive aggregation of submicelles is observed on the image, where cross-linked network

aggregates are formed through association of casein submicelles, explaining the sharp increase in the turbidity curve. These TEM images confirm the initial alkaline-induced dissociation of casein micelles and subsequent re-association of submicelles at very high pH.

### 5.1.2.3 Surface charge of casein in alkaline solution

The charge property of colloidal materials or surfaces can be characterized using polyelectrolyte titration [145, 146, 147]. The basic principle of this method is the complexation of oppositely charged polyelectrolytes and charged surfaces or particles. The charge of a sample can then be calculated according to the consumption of standard polyelectrolyte and the stoichiometry assumed for this complexation reaction. In this thesis, the above method is used to evaluate the surface charge of casein particles as described in the experimental section (4.2.4). It is worth mentioning that the detected charges derive from the surface of casein particles rather than the individual protein molecules. Especially when an aggregated structure is formed in solution, the surface charge density of the particles supposedly decreases with increased association. This is because some charged amino acid groups may be embedded in the particle interior, consequently, they are not able to contribute to the overall surface charge of the particle. Here, the surface charge of casein particles in solutions of varied pH was characterized, aiming to further examine the re-association process as mentioned above.

In general, due to the deprotonation of amino acid residues in casein proteins, the protein molecule surface is negatively charged in alkaline solution. For example,  $=\text{NH}_2^+$  in arginine is neutralized to  $=\text{NH}$  and the  $-\text{COOH}$  group in glutamic acid is converted to  $-\text{COO}^-$  [148]. The extent of deprotonation increases with increased pH. As a consequence, the surface charge of casein particles is supposed to increase gradually with pH. **Figure 5.5** depicts the anionic charge density of casein particles at varied alkaline pH. In an aqueous solution of pH 12, the charge density was revealed

to be  $-1,894 \mu\text{eq/g}$ , demonstrating a highly charged surface of the casein particle. As pH increased to 13, the charge density increased and reached a maximum value of  $-2,141 \mu\text{eq/g}$ , which is ascribed to a larger extent of deprotonation of the amino acid residues. However, further increase in pH did not lead to the expected increase in the charge density of the casein particles. In contrast, the titration experiments revealed rather different results at  $\text{pH} \geq 14$ . The charge densities were found to decrease by 25.2 % and 28.0 % as compared to the maximum value at pH 13, reaching  $\sim 1,600$  and  $\sim 1,500 \mu\text{eq/g}$  for casein particles at pH 14 and  $\text{pH} > 14$ , respectively. These results suggest that association of casein proteins occurs in highly alkaline environments ( $\text{pH} \geq 14$ ), which is consistent with the above turbidity and TEM analysis.

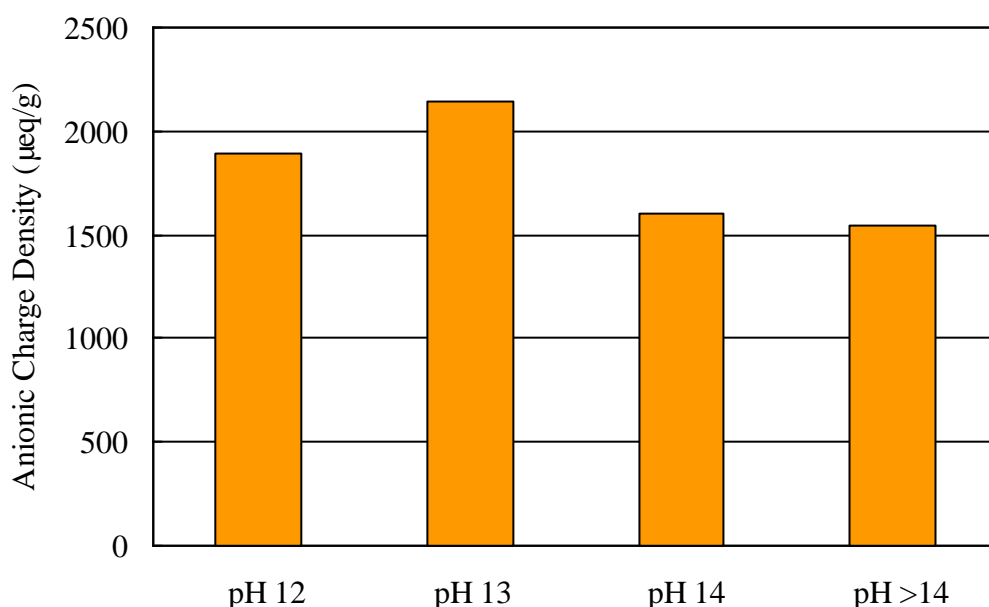


**Figure 5.5** Anionic charge density of casein particles as a function of solution pH ( $c_{\text{casein}} = 1 \text{ g/L}$ ).

To sum up above results, the casein micelles dissociate into submicelles over a pH range of 12 to 13. However, as pH goes up to extreme alkaline conditions, namely  $\text{pH} \geq 14$ , dissociation of the casein micelles is not only halted, but in fact reversed to produce aggregated structures.

### 5.1.3 Influence of ionic strength on re-association of casein

High concentrations of NaOH (aq) have been employed to achieve the desired pH, which accordingly induced a large variation in the ionic strength of casein solutions. Therefore, one can argue that the assembly behavior of casein may be caused by the increase in ionic strength in solution, instead of the alkaline pH only. To clarify that and demonstrate the role ionic strength plays in the association, alkaline casein solutions with different contents of NaCl were prepared according to the procedure mentioned in 4.1.4. Specifically, the ionic strengths of the solutions containing NaCl were adjusted to correspond with the NaOH concentrations in casein solutions of pH 13, pH 14 and pH > 14, respectively. The turbidity measurements on these NaCl-containing solutions were subsequently performed and the results obtained are shown in **Figure 5.6**. For comparison, the turbidity of casein solutions containing merely NaOH is displayed as well.

From the figure, the turbidity of NaCl-containing casein solutions increases very slightly with ionic strength. Specifically, the turbidities were revealed to be 0.07, 0.09 and 0.11  $\text{cm}^{-1}$  at ionic strengths of 0.15, 1.5 and 4 M, respectively. The addition of NaCl did not result in much increase in turbidity of the alkaline casein solutions. However, alkaline casein solutions containing only NaOH, at the same ionic strength, appeared to be more turbid than NaCl-containing solutions. The turbidity was found to dramatically increase by 229 % as ionic strength increased from 0.15 M to 4 M, reaching a maximum value of 0.25  $\text{cm}^{-1}$ . These results indicate that association of casein submicelles is dominantly related to a rise in solution pH. The increase in ionic strength contribute only slightly.

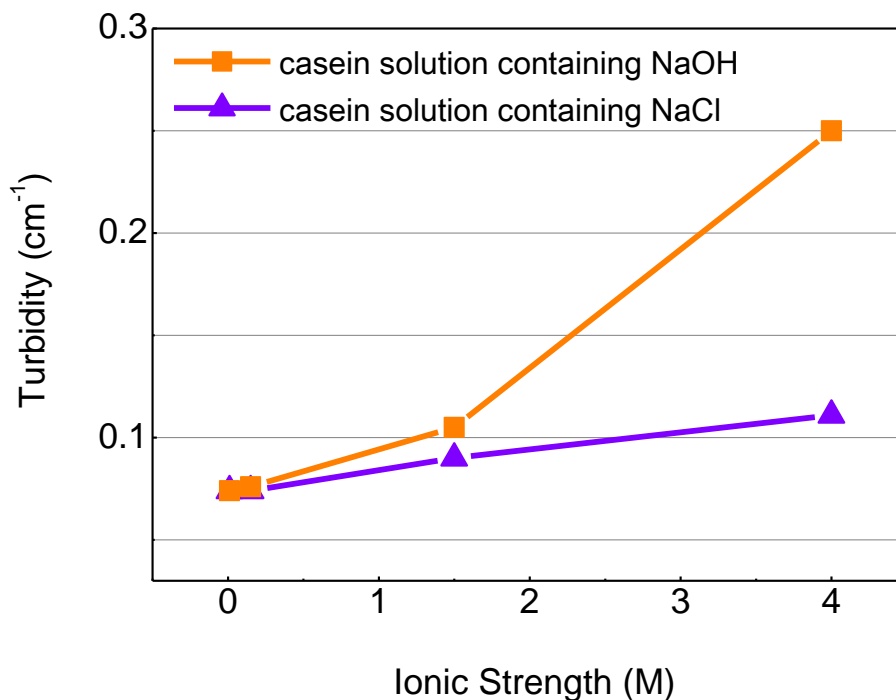


**Figure 5.6** Turbidity of alkaline casein solutions as a function of ionic strength. Triangle: casein solution with different NaCl contents ( $c_{\text{casein}} = 1 \text{ g/L}$ ,  $\text{pH} = 12$ ); Square: casein solution with different NaOH contents ( $c_{\text{casein}} = 1 \text{ g/L}$ ,  $\text{pH} = 12 - \text{pH} > 14$ ).

#### 5.1.4 The role of calcium in the re-association process

Calcium is known to play a function in maintaining the integrity of casein micelles. It generally binds on the phosphoserine group of casein, forming the calcium phosphate linkage between submicelles. In this section, the importance of calcium in the re-association process of casein submicelles is examined through a study of calcium-depleted casein. The removal of calcium was carried out according to the procedure mentioned in 4.1.3. The residual content of calcium in the Ca-depleted casein solution ( $c_{\text{Ca-depleted casein}} = 1 \text{ g/L}$ ) was found at 0.2 mg/L. This is significantly less as compared to 1.6 mg/L of calcium in the original casein solution ( $c_{\text{casein}} = 1 \text{ g/L}$ ). The method for determination of the calcium content is described in 4.2.3.

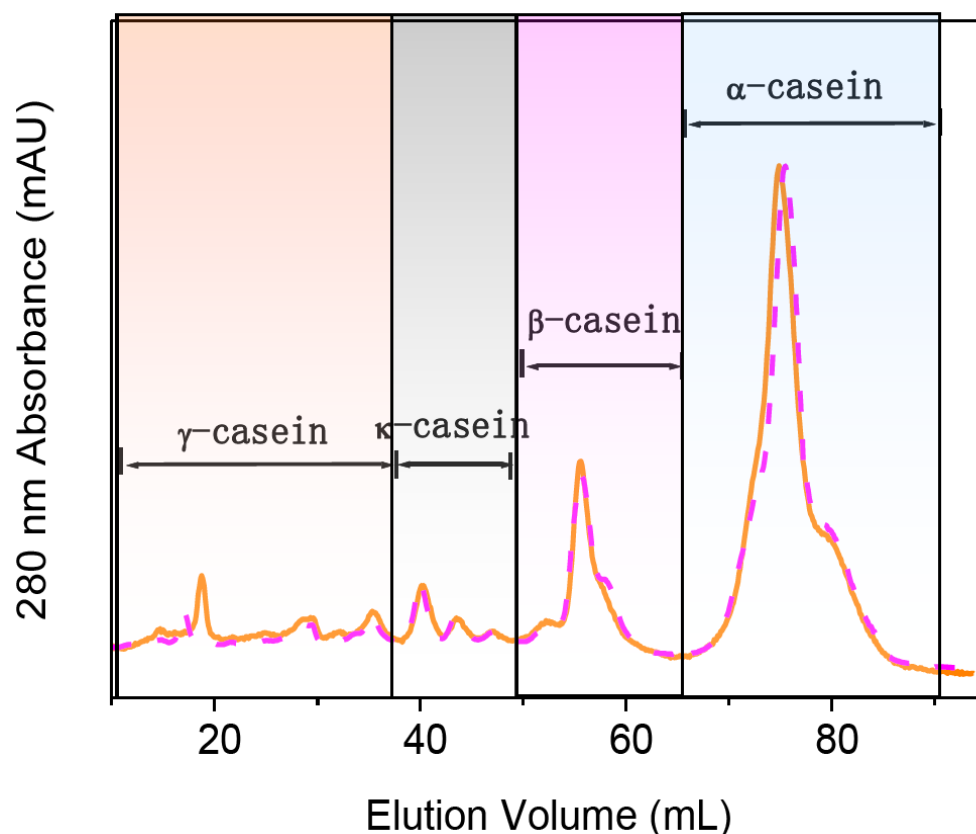


**Figure 5.7** FPLC profiles of casein (solid line) and Ca-depleted casein (dashed line), characterized on ion exchange column Resource Q.

A chromatographic analysis of Ca-depleted casein was performed by ion exchange FPLC and the result is shown in **Figure 5.7**. For comparison, the elution profile of original casein is also displayed. According to previous publications [126, 149], the elution peaks have been identified and assigned to different casein fractions. Specifically, the first peaks of substances eluted at 0–10 mL are ascribed to unbound proteins and some chemicals added during sample preparation. The elution profiles occurring at ~36 – 47 mL correspond to a group of protein species called  $\kappa$ -casein. The family of  $\beta$ -casein proteins eluted from ~48 mL to 60 mL elution volume whereas the  $\alpha$ -casein protein appeared from ~61 mL to 85 mL elution volume. From the figure, the absorbance peaks of Ca-depleted casein appeared to be highly identical to those of original casein. It indicates the removal of calcium did not influence the structure and composition of protein molecules.

#### 5.1.4.1 Turbidity of Ca-depleted casein in alkaline solution

The turbidity dependency of Ca-depleted casein on alkaline pH was characterized and the obtained results are shown in **Figure 5.8**. Similar to original casein (see **Figure 5.3**), the turbidity of Ca-depleted casein increased with solution pH. But, the increase is much less. Specifically, the turbidity of Ca-depleted casein solution was found less than  $0.1 \text{ cm}^{-1}$  at  $\text{pH} > 14$ , in contrast to  $0.25 \text{ cm}^{-1}$  for original casein as shown in **Figure 5.3**. This suggests that only slight aggregation occurs in the Ca-depleted casein solutions at highly alkaline pH.

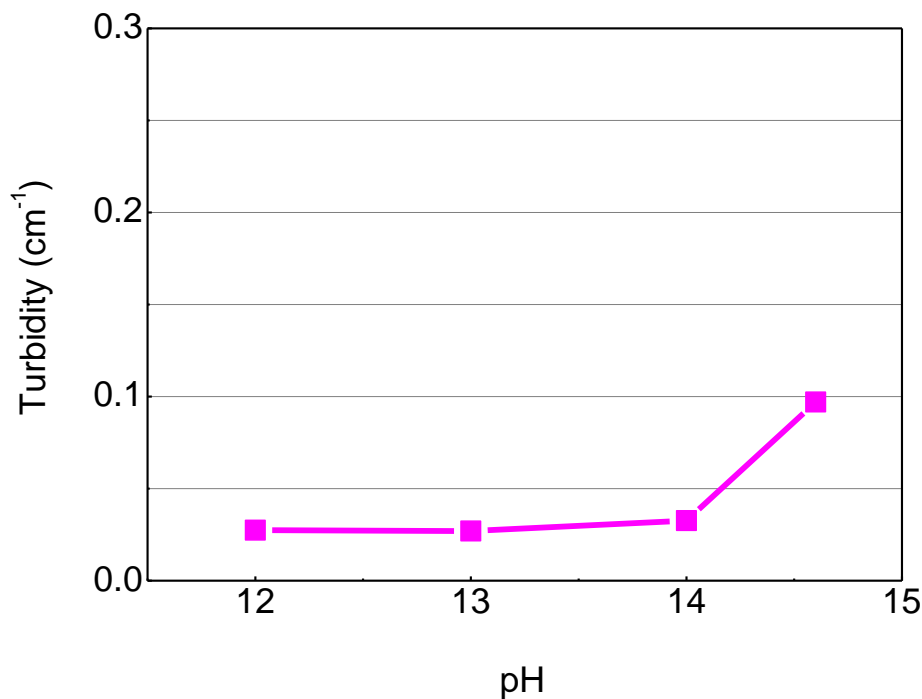


**Figure 5.8** Turbidity of Ca-depleted casein solutions as a function of pH ( $C_{\text{Ca-depleted casein}} = 1 \text{ g/L}$ ).

#### 5.1.4.2 Surface charge of Ca-depleted casein in alkaline solution

Additionally, the surface charge of Ca-depleted casein was determined and the results are shown in **Figure 5.9**. At pH 12 and 13, the anionic charge densities of Ca-depleted casein were comparable to those of original casein, though slightly higher (see **Figure**

5.5). Whereas at pH 14 and pH > 14, unlike original casein, the charge density values of Ca-depleted casein did not show a progressive decrease, instead they remained at high levels. Based on the discussion in section 5.1.2.3, the surface charge properties of casein particles are able to reflect the aggregation of casein submicelles in highly alkaline environments. Here, the relatively high charge density of Ca-depleted casein simply suggest a decreased association tendency of submicelles. Evidently, these results are in good agreement with the turbidity analysis.

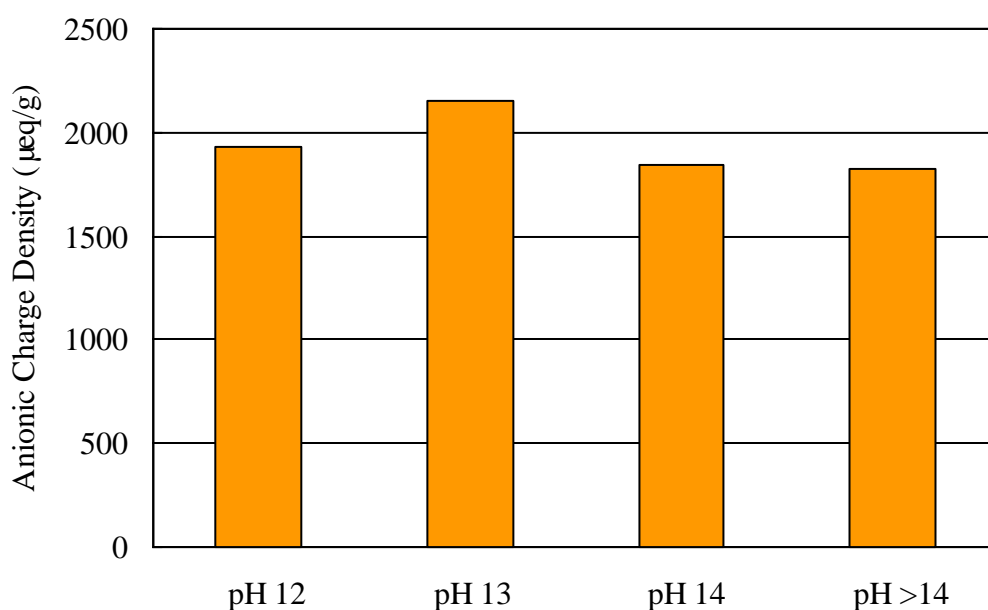


**Figure 5.9** Anionic charge density of Ca-depleted casein as a function of solution pH ( $c_{\text{Ca-depleted casein}} = 1 \text{ g/L}$ ).

Above results reveal that the removal of calcium from casein leads to a decreased tendency for the association of submicelles. In other words, calcium was proven to play an important role in the formation of large aggregated structures of casein proteins. This may be related to a reduction in the calcium phosphate linkage between proteins in Ca-depleted casein. Towards a better understanding of the above findings, the interactions between casein proteins in alkaline solution need to be systematically analyzed. A detailed discussion is shown in the next section.

### 5.1.5 Interactions between casein proteins in alkaline solutions

Although the dissociation of casein micelles in alkaline environment was observed before [12], the re-association of casein submicelles under extreme alkaline pH has never been reported elsewhere. It is widely accepted that the micelle structure of casein is mainly governed by a balance of electrostatic repulsion, hydrophobic attraction as well as the calcium phosphate linkage between casein molecules [17]. An analysis of the interactions between casein proteins in the micellar structure may throw a light on the mechanism of this unexpected re-association process.

#### 5.1.5.1 Electrostatic repulsion

The electrostatic repulsion between casein proteins is principally governed by the electric charges carried by molecules, and the charges are mainly dependent on the deprotonation extent of amino acid residues in proteins. In casein molecules, most of the amino acids possess  $pK_a$  values of less than 10.5. According to the Henderson-Hasselbalch equation, these residues should be completely deprotonated in an aqueous solution of pH 13. The most basic amino acid in casein is arginine which possesses a  $pK_a$  of 12.5 (see **Table 2.3**), but it accounts for only 2.4 % of the casein protein. Over the pH range used in this work, the deprotonation extent of amino acids in casein has been maintained at high levels and should not vary significantly after pH 13. Therefore, the electric charges carried by casein molecules should not greatly increase in the highly alkaline solutions.

However, the binding of positively charged calcium phosphate onto casein phosphoserine groups can partially neutralize the negative charge of proteins [150], thus facilitating a reduction in the electrostatic repulsion between casein proteins. With increased solution pH, the binding of calcium phosphate to phosphoserine groups increases dramatically due to a higher equilibrium binding constant at higher pH [151]. Consequently, the electrostatic repulsion between casein proteins will be

greatly reduced in highly alkaline environment, which may promote a tendency for casein submicelles towards large associated structures.

#### **5.1.5.2 Hydrophobic interaction**

Hydrophobic effects are among the most general and complicated of the chemical binding forces, which can be moderated by pH, temperature, ionic strength of solutions, etc. In this study, the hydrophobic interaction between casein proteins in principle may be connected with (1) an alternation in the surface charge of casein molecules in alkaline environments and (2) an increase in the ionic strength of solutions due to the use of high concentration of NaOH. As mentioned above, the negative charges carried by each casein molecule are diminished by an increased number of calcium phosphate binding at higher pH, which accordingly prompts an increase in the hydrophobic region of protein molecules. These newly exposed hydrophobic regions presumably facilitate an enhancement in the hydrophobic interaction between casein molecules. On the other hand, the ionic strength of casein solutions surely increases with increasing pH, which slightly strengthens the hydrophobic interactions between proteins. Therefore, the association of casein proteins at higher pH is reinforced. The influence of ionic strength on the micellar structure of casein will be discussed in further detail in section **5.1.3**.

#### **5.1.5.3 Calcium phosphate linkage**

Based on above discussion, calcium phosphate is believed to play an important role in the re-association process of casein submicelles. It moderates the interactions between proteins by neutralizing the negative charge on casein molecules. As a result, the electrostatic repulsion is weakened and the hydrophobic interaction is strengthened in highly alkaline environment. Additionally, casein molecules can be cross-linked through the calcium phosphate binding [152], thus forming a phosphoserine – calcium phosphate – phosphoserine linkage between proteins, which has been described as

micellar calcium phosphate (MCP) in some reports. MCP can be greatly built up in highly alkaline conditions due to an increased equilibrium constant at higher pH [153]. Eventually, re-association of casein submicelles occurs and a large aggregated structure will be formed in highly alkaline solutions.

For calcium-depleted casein (see section **5.1.4**), the negative charges on protein molecules are not much neutralized by calcium phosphate, accordingly, the electrostatic repulsion and hydrophobic attraction between submicelles can not be significantly moderated. Furthermore, MCP linkages are hardly established between casein proteins. As a consequence, the association of casein submicelles is severely impeded. This well explains the reduced association tendency of casein submicelles in Ca-depleted casein solutions.

#### **5.1.6 Schematic for the dissociation and re-association process**

In **Figure 5.10** and **Figure 5.11**, a schematic for dissociation of casein micelles and subsequent re-association of submicelles in alkaline solutions is presented. The competition between electrostatic repulsion, hydrophobic attraction as well as calcium phosphate linkage between proteins eventually determines the micellar behavior of casein.

Generally, native casein appears as micelle-like particle, where spherical submicelles are held together by hydrophobic interaction and calcium phosphate linkages (**Figure 5.10a**). When casein is dissolved in alkaline solution,  $\text{OH}^-$  ions can diffuse into the micelle due to its loose and porous nature [154]. This results in the deprotonation of amino acid residues and allows the negative charge of proteins to attain high values. At pH 12 and pH 13, electrostatic repulsion occurring between the proteins exceeds the attractive forces provided by calcium phosphate linkages and hydrophobic interactions between the proteins. Hence, the casein micelle starts to disrupt and negatively charged submicelles are dissociated out (**Figure 5.10b** and **Figure 5.10c**).

This is believed to be the mechanism for the formation of so called “sodium caseinate”, which has been reported to be composed of about 15 casein molecules and to possess an average diameter of about 11 nm [155]. These submicelles are considered as the fundamental structural units comprising casein micelle.

However, the casein submicelles start to re-associate when an extremely alkaline pH is adjusted (**Figure 5.11**). Specifically, when the solution pH is raised to  $\geq 14$ , negative charges on casein molecules are greatly neutralized due to the binding of positively charged calcium phosphate onto phosphoserine residues in casein. Thus, on the one hand the electrostatic repulsion between submicelles is diminished; on the other hand, the hydrophobic attraction associated with newly exposed hydrophobic regions in casein molecules is certainly enhanced. Meanwhile, the phosphoserine - calcium phosphate - phosphoserine linkages between casein proteins have been extensively established as compared to the cases at pH 12 and 13. Consequently, the re-association of casein submicelles occurs at  $\text{pH} \geq 14$ . **Figure 5.12** describes the interactions between casein proteins which govern the dissociation and re-association processes.

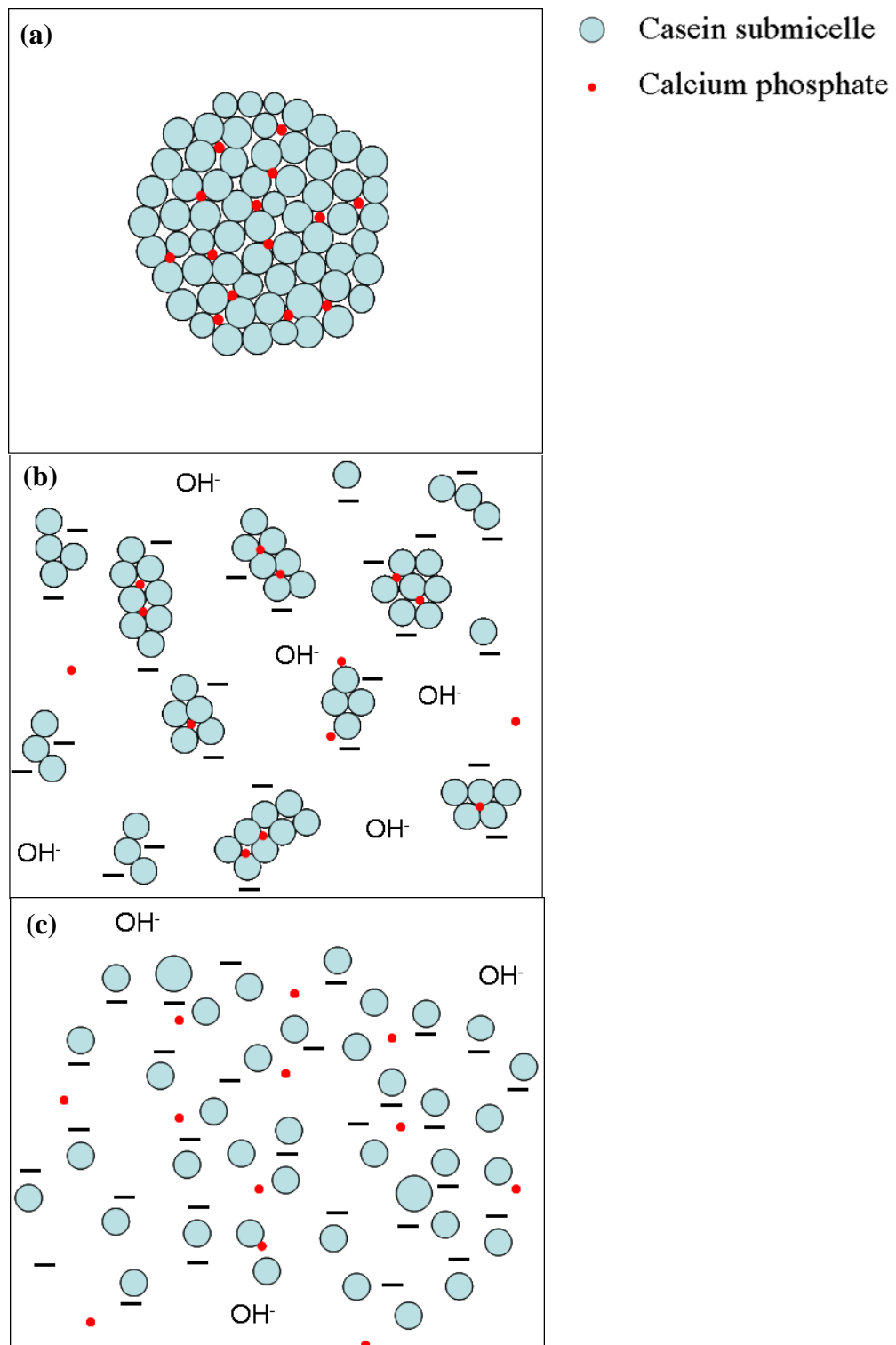


**Figure 5.10** Schematic diagram for the dissociation process of casein micelle in alkaline solution: (a) casein micelle; (b) a disruption occurs when  $\text{OH}^-$  diffuses into casein micelle; (c) negatively charged submicelles are dissociated from the casein micelle at pH 12 and 13.

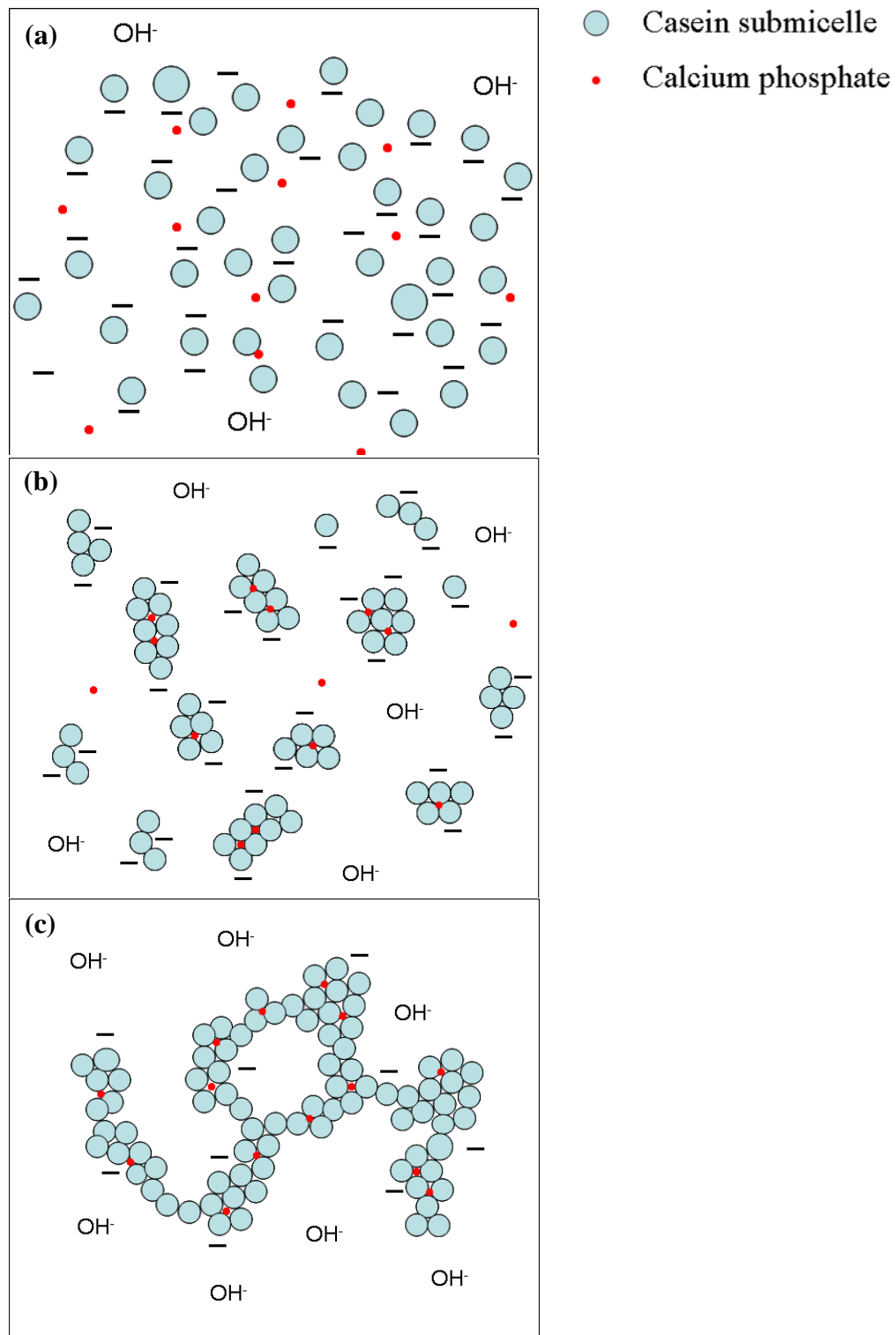


**Figure 5.11** Schematic diagram for the re-association process of casein submicelles at extremely alkaline pH: (a) individual casein submicelles existing at pH = 13; (b) slight re-association of submicelles occurs at pH 14; (c) a strong re-association occurs at pH > 14, allowing the formation of network aggregates.

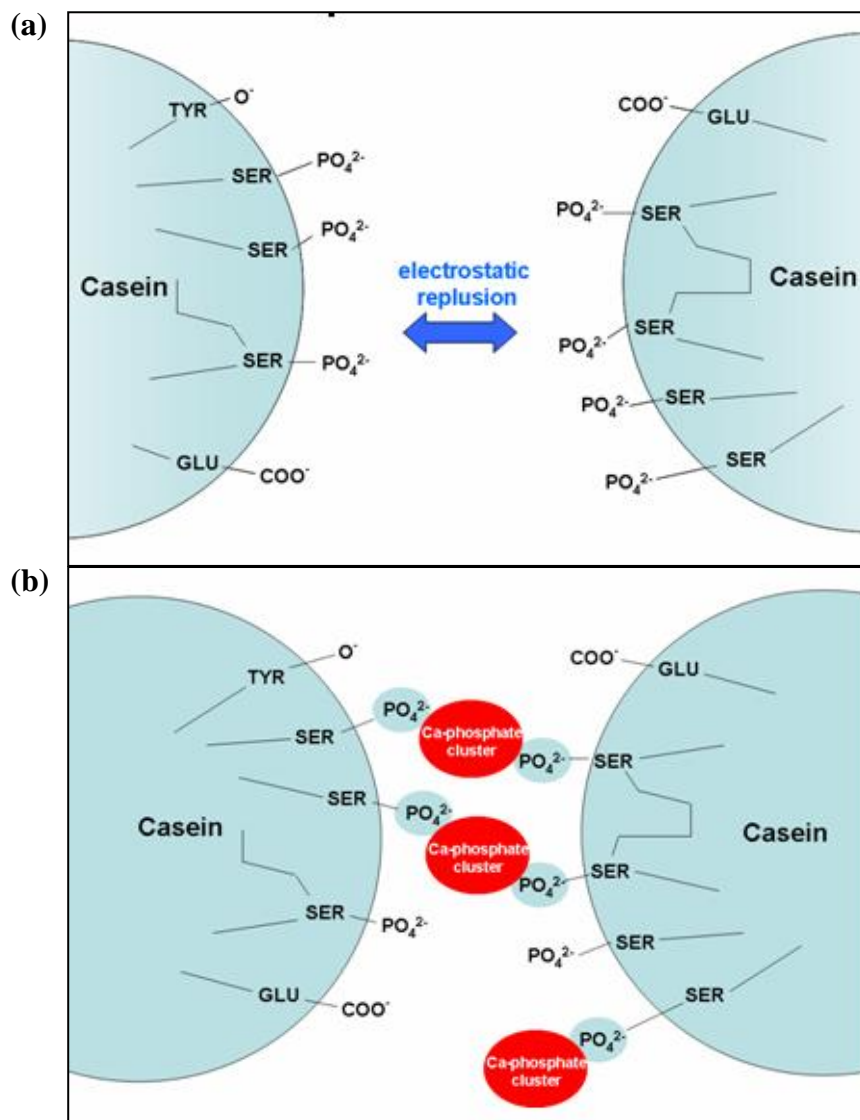


**Figure 5.12** Schematic illustration of the dominating interactions between casein proteins in the (a) dissociation and (b) re-association processes.

## 5.1.7 Morphology of casein submicelles and micelles

### 5.1.7.1 Morphology of casein submicelles

The atomic force microscopy (AFM) technique is capable of providing three dimensional visualization and both qualitative and quantitative information of the sample topology, thus revealing its morphology, particle size, etc [156, 157, 158, 159]. Using AFM measurements, some previous studies have reported on the

morphology of casein subunits, *e.g.* the pressure decomposed micellar structure of casein proteins [37]. But those AFM measurements were carried out in the liquid cells, in other words, in liquid surroundings. The resulting images severely suffer from the low scanning resolutions. To solve that problem, we investigated the morphology of casein proteins in dried state in this work. As described in section 4.2.7, a dried casein deposit was prepared from 1 g/L of casein solution at pH 12. During the drying procedure, the concentration of casein proteins as well as the solution pH was supposed to vary by regions. According to the observation, the drying of outer region of deposit occurred first, which was followed by the drying of middle and inner regions.

**Figure 5.13** depicts the drying direction of the casein droplet. There, the deposit is roughly divided into three regions. Specifically, a fast evaporation of water on the edge of deposit allows to “freeze” the original structure of casein proteins in solutions. Therefore, the observed morphology in the outer region (labeled as region 1) is supposed to resemble closely that in dilute casein solution.

According to the observation, the drying of the middle region on deposit is more time-consuming, which may be ascribed to a larger water volume on that area. The assembly of proteins, during this period of time, is very likely to occur as suggested by some earlier reports. This area is labeled as region 2 in the figure.

Furthermore, due to the good solubility of alkali in water, a NaOH-enriched zone is supposed to occur in the inner region of deposit, which has been labeled as region 3 in the figure. This inner region is covered by salt crystals from the observation, which is not suitable for AFM measurement due to the rough surface. The formation of a salt-enrich central zone on a dried deposit has been reported before by YAKHNO in an earlier study [160]. It is believed that the hydrodynamic centrifugal flow occurring in the droplet carried the micelles to the drop periphery, thus the inorganic salt was left in the center of deposit. In this section, the discussion on the morphology of inner

region is not taken into account, since it does not well represent casein proteins.

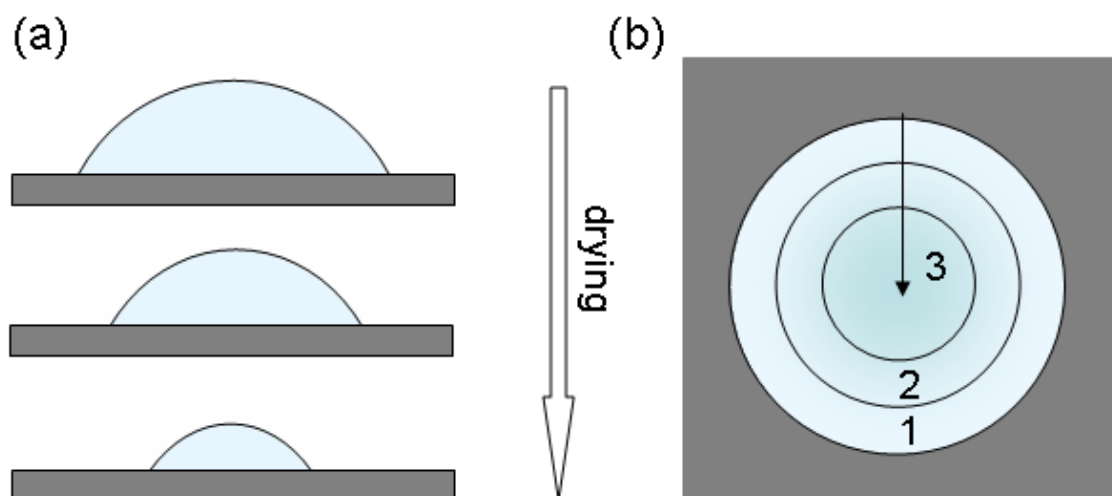


**Figure 5.13** Schematic illustration of (a) the drying process and (b) the drying direction of casein droplet ( $c_{\text{casein}}=1\text{g/L}$ ). 1, 2 and 3 denote the outer, middle and inner region of deposit, respectively.

In order to verify the above speculation, the morphology in the outer and middle region of a dried deposit was investigated by AFM. **Figure 5.14** depicts the images attained in the outer region of the casein deposit. Topographical analysis revealed a homogeneously distributed thin layer in that region, where roughly spherical particles with a mean diameter of  $\sim 20$  nm were observed. Section analysis revealed a uniform surface appearance where the height of particles was found to be  $\sim 11$  nm. **Figure 5.15** depicts the three dimensional height image of particles distributed in the outer region. Due to the comparable particle size and morphology, these observed structures were designated as casein submicelles. According to the discussion in section 5.1.2, casein submicelles are the dominant species existing in the alkaline solution of pH 12. Therefore, this finding confirms our earlier speculation. Namely, the morphology in the outer region of deposit represents the micellar structure of casein proteins in solution.

The submicelle profiles in the images are very clear. Compared to the previous report [37], the scanning resolution was greatly improved. To our knowledge, this work presents the best-quality AFM images of casein submicelles ever published.

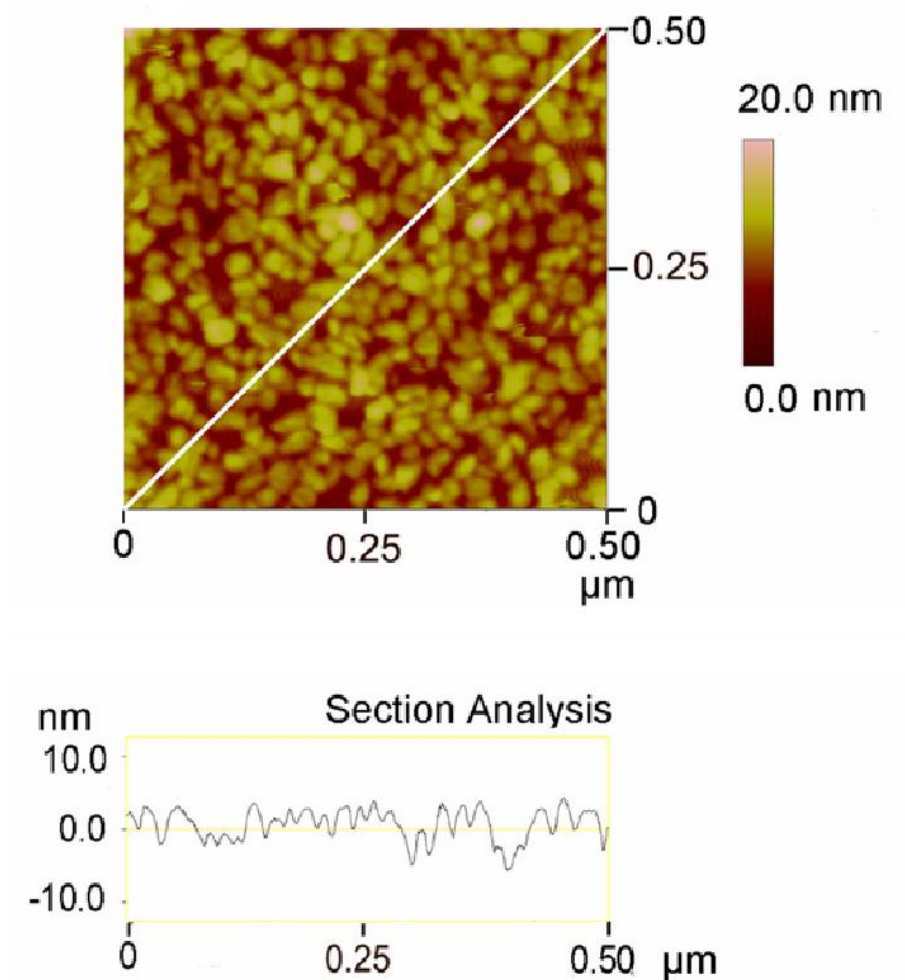


**Figure 5.14** Above: AFM topographical image of casein particles distributed in the outer region of a dried deposit; below: section analysis of the deposit surface along the indicated line.

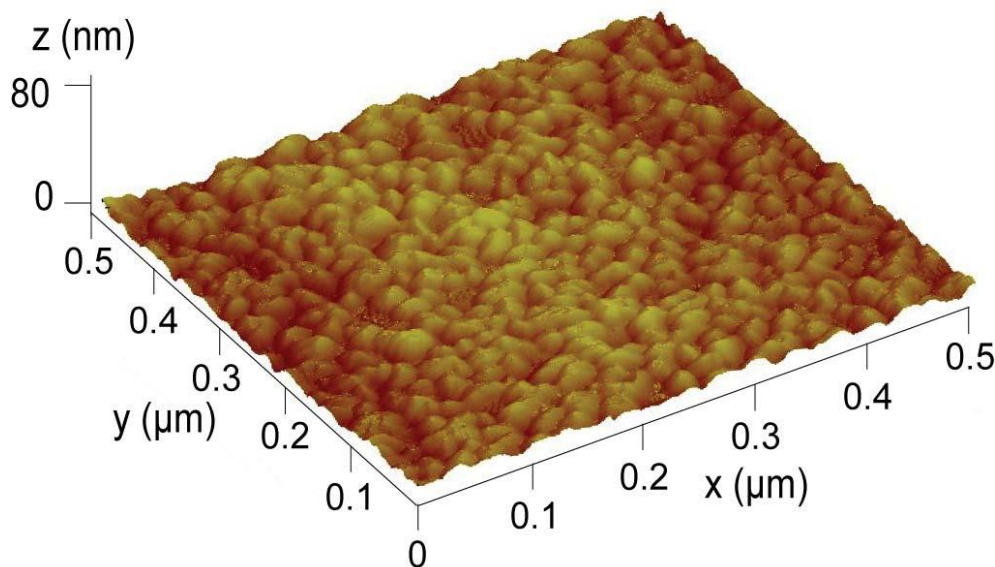


**Figure 5.15** AFM 3D height image of casein submicelles distributed in the outer region of dried casein deposit.

From above images, the diameters of casein submicelles in the outer region were found to be larger than the corresponding heights (20 nm vs. 11 nm). This implies that during the drying process, deformation of the spherical micelle may occur. Additionally, the particle size of the submicelles revealed by TEM ( $\sim 10$  nm) is slightly smaller than that deduced from this AFM analysis. This deviation might result from the broadening effect of the AFM tip. When tracing over a structure which is comparable in size to the radius of the tip ( $\sim 10$  nm), the lateral dimensions are extended and accordingly the particle size determined by AFM is overestimated.

#### 5.1.7.2 Assembly of casein in the droplet

Next, morphology of casein species occurring in the transitional zone between region 1 and 2 (see **Figure 5.13**) was studied using AFM. From **Figure 5.16**, gradual alignment of the globular aggregates along the radial direction was observed. The diameter of aggregates was found to range from  $\sim 240$  nm to  $\sim 60$  nm towards the outer edge.

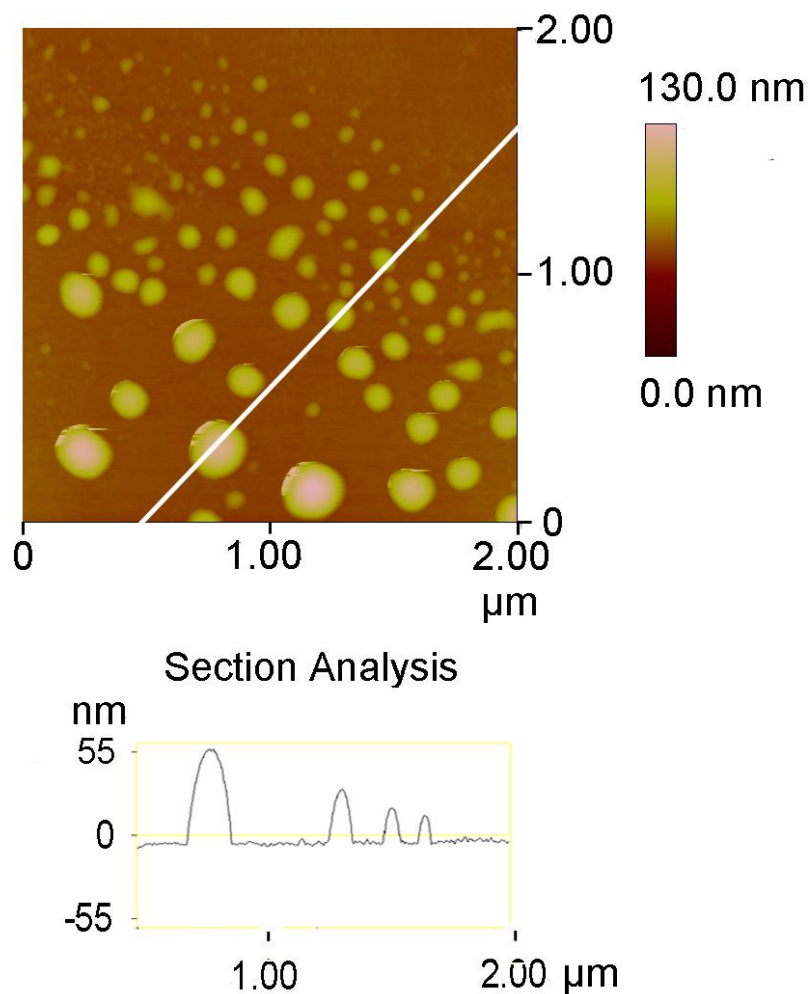


**Figure 5.16** Above: AFM topographical image of aggregates observed in the transitional zone between region 1 and 2; below: section analysis of the detected surface along the indicated line.

Furthermore, section analysis of the surface along the indicated line revealed a gradual decrease in height profile. The height of adjacent aggregates was found to be 62 nm, 36 nm, 26 nm and 18 nm, respectively. Similarly, some deformation of the spherical particles during evaporation of water is obvious. **Figure 5.17** depicts the three-dimensional height image of the aggregates distributed in the transitional region.

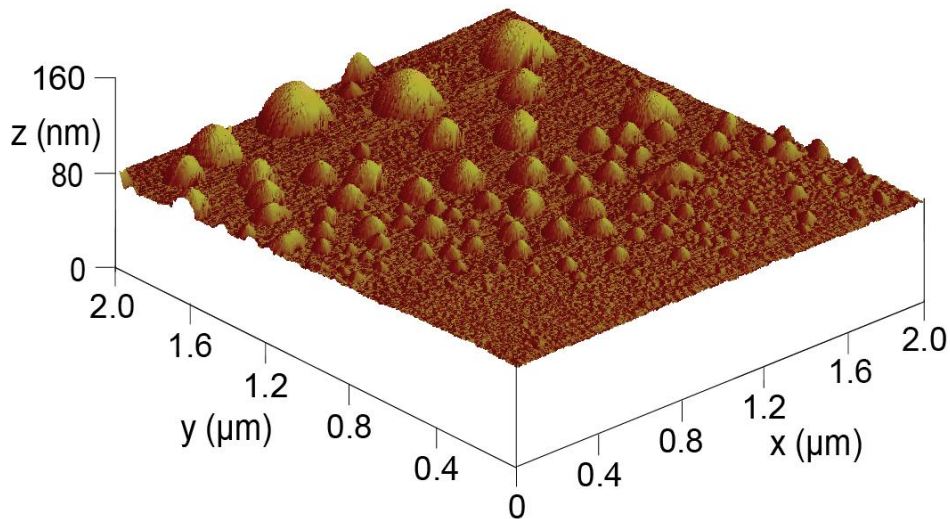


**Figure 5.17** AFM 3D height image of aggregates distributed in the transitional zone between region 1 and 2.

As proven by the observation, the drying of casein species present in the middle region consumed more time, thus making the assembly of casein proteins possibly occur in this region. Additionally, with the evaporation of water, the middle region became enriched in casein proteins due to their high solubility in alkaline solution. Therefore, the morphology of the middle region in the deposit is supposed to be different from that of the outer and the transitional region. To confirm this speculation, AFM experiments were carried out at several sites of middle region. The obtained images are shown in **Figure 5.18**, **Figure 5.19** and **Figure 5.20**.

According to these figures, the morphology of the middle region in dried casein deposits was found to vary significantly. The height image in **Figure 5.18** reveals an uneven surface in the detected domain, where the difference in the topographic height was found larger than 50 nm. Thus, it is difficult to distinguish the fine structure of casein in this domain. However, the AFM phase image generally gives better contrast between different materials. In this work, a clear assembled structure of casein proteins was demonstrated in AFM phase image. There, the short rods with an average width of 11 nm, along with clusters of different sizes were observed. The

latter was finely structured and composed of nanometer-scale small particles which are comparable to the submicelles observed in **Figure 5.14**.

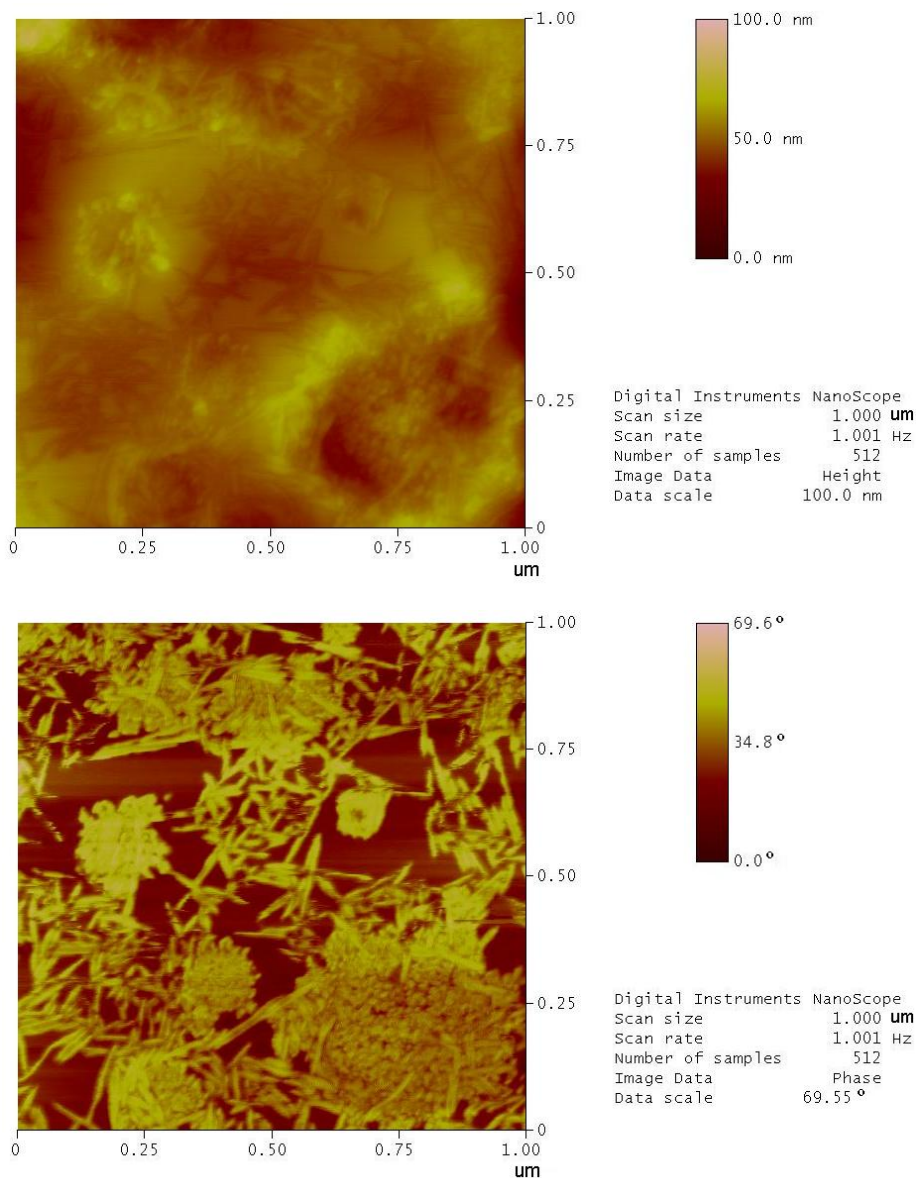


**Figure 5.18** AFM height image (top) and phase image (bottom) of the middle region in casein deposit – site 1.

The height image in **Figure 5.19** suggests a relatively smooth surface of the detected domain, where worm-like structures accompanied by spherical particles are observed. Additionally, the submicellar structure of casein proteins is clearly shown in the phase image. They are closely packed, forming the irregular shaped aggregates.

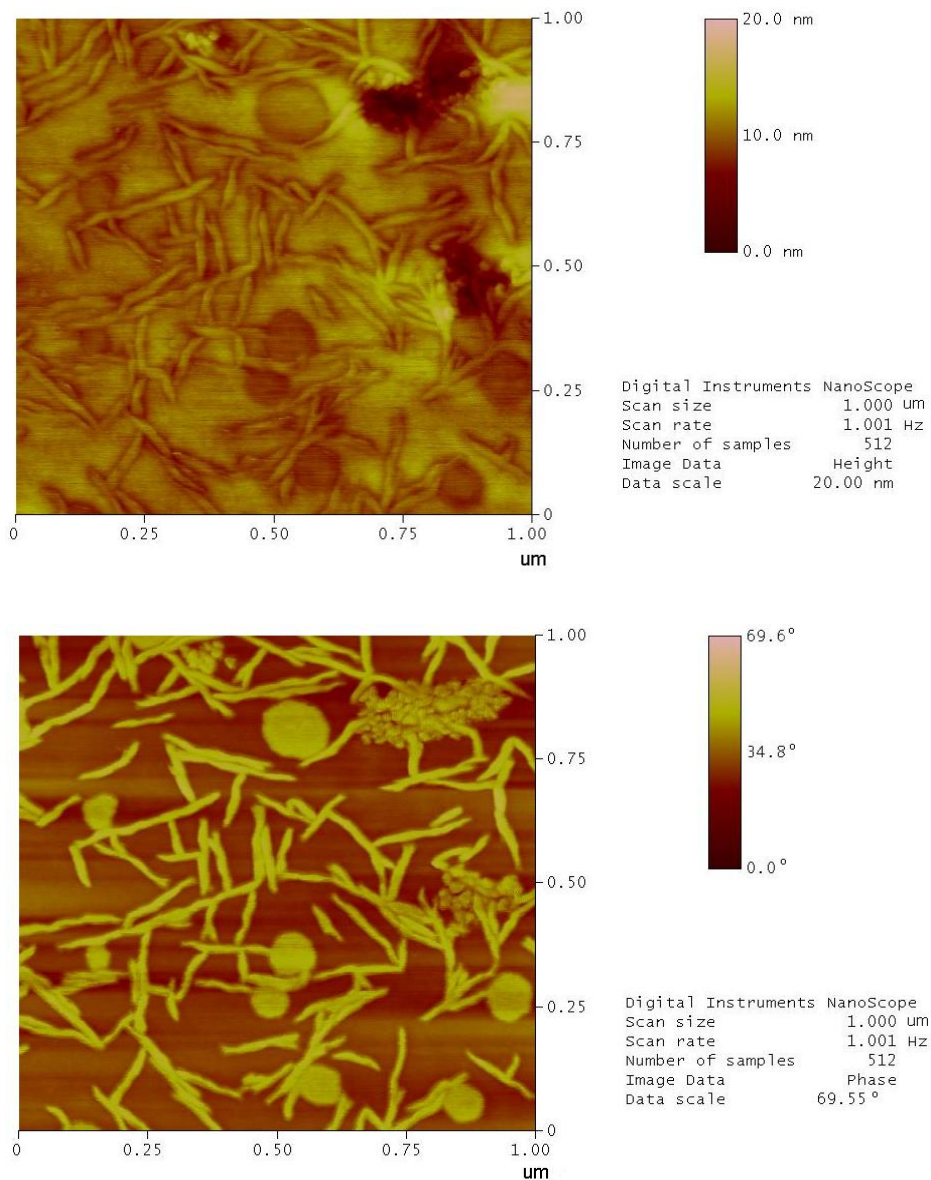


**Figure 5.19** AFM height image (top) and phase image (bottom) of the middle region in casein deposit – site 2.

The very rough surface is demonstrated in **Figure 5.20**, where the difference in topographic height exceeds 300 nm. The large agglomerates can be observed in the figure. They are tightly packed, forming an uncharacteristic morphology. The agglomerates were found to be soft and sticky during AFM visualization. They are composed of fine submicellar structure as was confirmed by phase image.

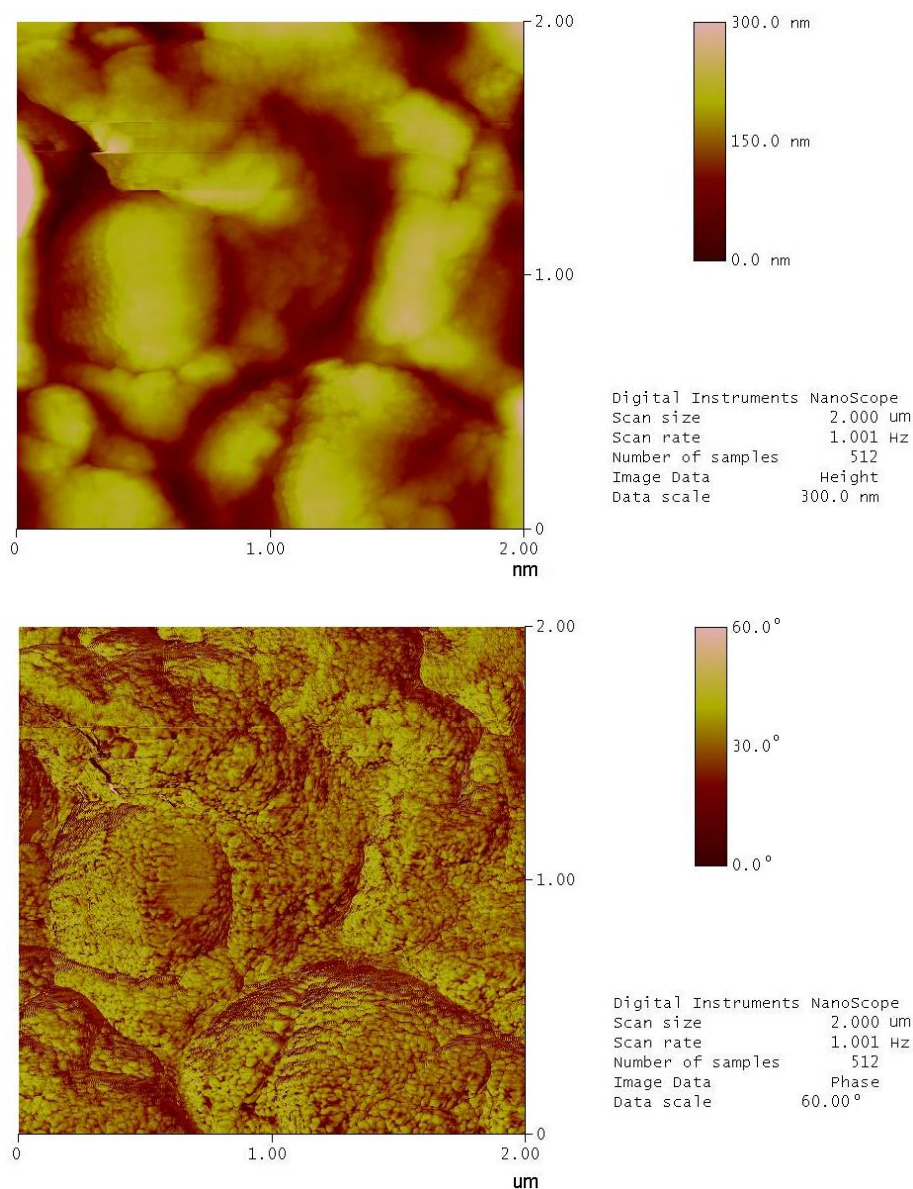


**Figure 5.20** AFM height image (top) and phase image (bottom) of the middle region in casein deposit – site 3.

For comparison, the topographic AFM images of blank sample, namely the dried deposit of pure NaOH solution, are shown in **Figure 5.21**. Several different sites of deposit were selected and detected, where the morphology of NaOH crystals was found to be similar. During the drying process, NaOH formed large branch-like crystals as revealed in the image. The difference in topographic height was found to be about 200 nm. The fine structure of crystals was characterized and the results are shown in **Figure 5.22**. There, the stripe-like morphology can be observed in images,

which possessed a width ranging from ~100 nm to ~250 nm. Different from the morphology observed for casein proteins, NaOH crystals are relatively larger in size. The surface of crystals is quite rough, unlike the smooth and clear profiles observed for the structure of casein proteins. From the above observations, we found that the assembly of casein proteins and pure NaOH crystals can differ considerably in morphology. The structures shown in **Figure 5.18 - Figure 5.20** indeed derive from casein proteins.

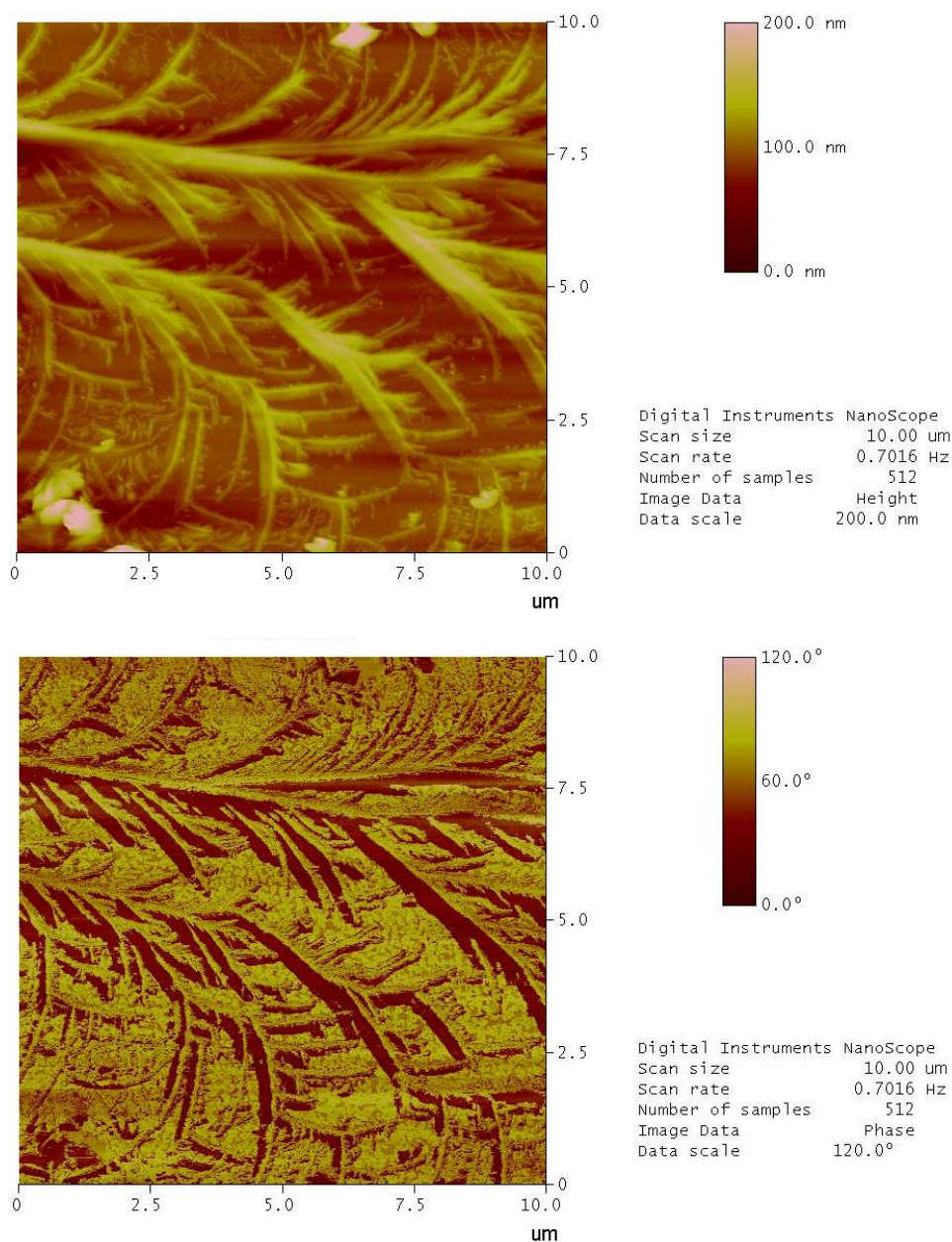


**Figure 5.21** AFM height image (top) and phase image (bottom) demonstrating the large NaOH crystals in blank sample.

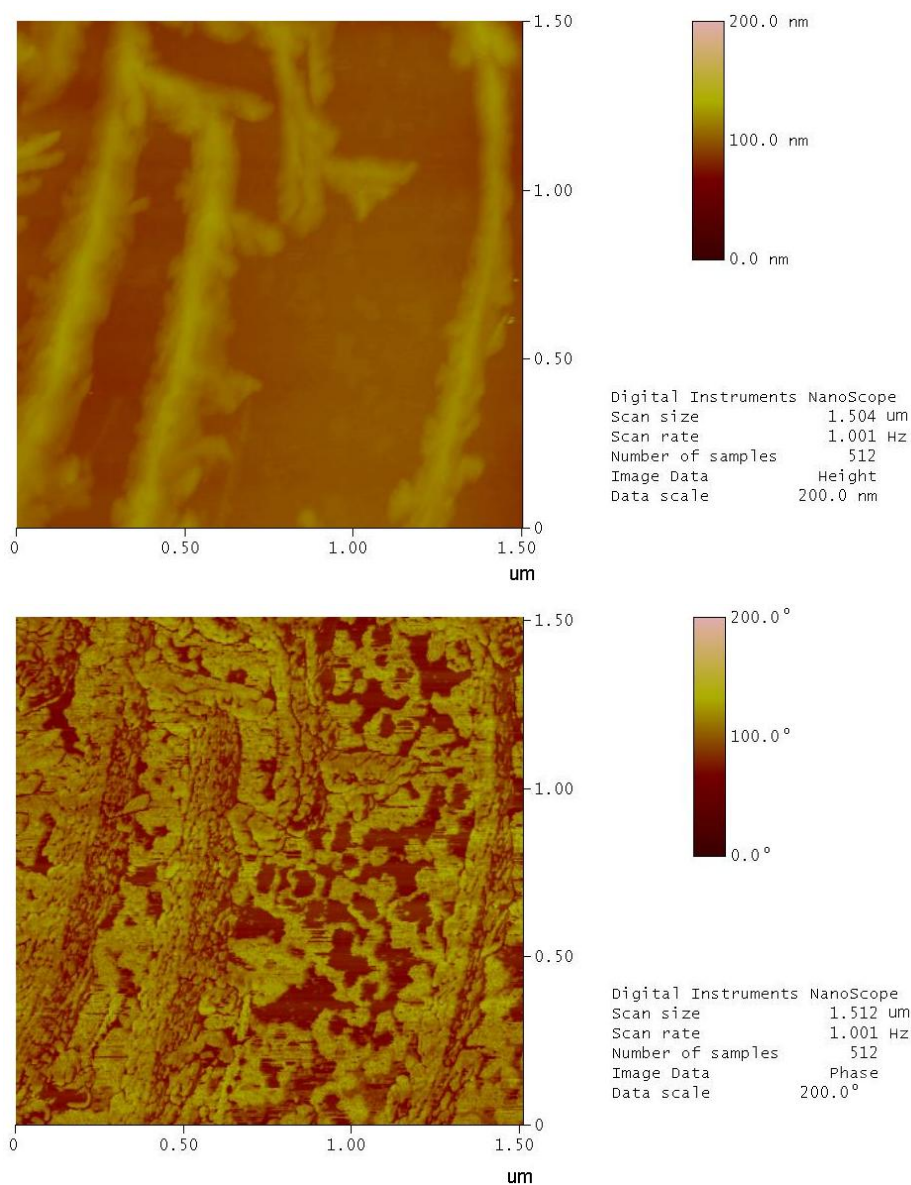


**Figure 5.22** AFM height image (top) and phase image (bottom) demonstrating the fine structure of NaOH crystals in blank sample.

According to those images, casein proteins were revealed to assemble during the drying of the droplet, thus resulting in the formation of different morphologies. In addition to the micelles/submicelles, rod and worm-like structures were observed in certain figures. During the drying process, the concentration of casein proteins and solution pH increased, which made the formation of different assembled structures possible. No clear correlation between the locations where the individual morphologies were detected was found.

The worm-like structure of casein proteins has been reported by ECROYD et al. in an earlier publication [161]. They proved that bovine milk  $\kappa$ -casein in general forms micelle-like species in equilibrium with dissociated forms. But when incubated under physiological pH and at 60 °C, the native  $\kappa$ -casein formed worm-like structures as shown in **Figure 5.23a**. They proposed dissociated forms of the protein as precursors for the assembly formation. Under incubation, reduced and carboxymethylated (RCM) bovine  $\kappa$ -casein underwent structural rearrangement within the protein, resulting in the formation of fibrillar assembly as revealed in **Figure 5.23b**. Additionally, THORN et al. reported that bovine  $\alpha_{s2}$ -casein readily formed fibrils *in vitro* [162]. When incubated at neutral pH, the spherical particles of casein were found to rapidly convert to twisted, ribbon-like fibrils (about 12 nm in diameter). **Figure 5.24** depicts the fibril-like morphology of  $\alpha_{s2}$ -casein (120  $\mu$ M) after one week of incubation at 50 °C. A further study indicated that the protein was less prone to fibril formation upon disulfide bond reduction with dithiothreitol. These results confirmed the inherent propensity of casein proteins to form assembled structures, which supports our observations.

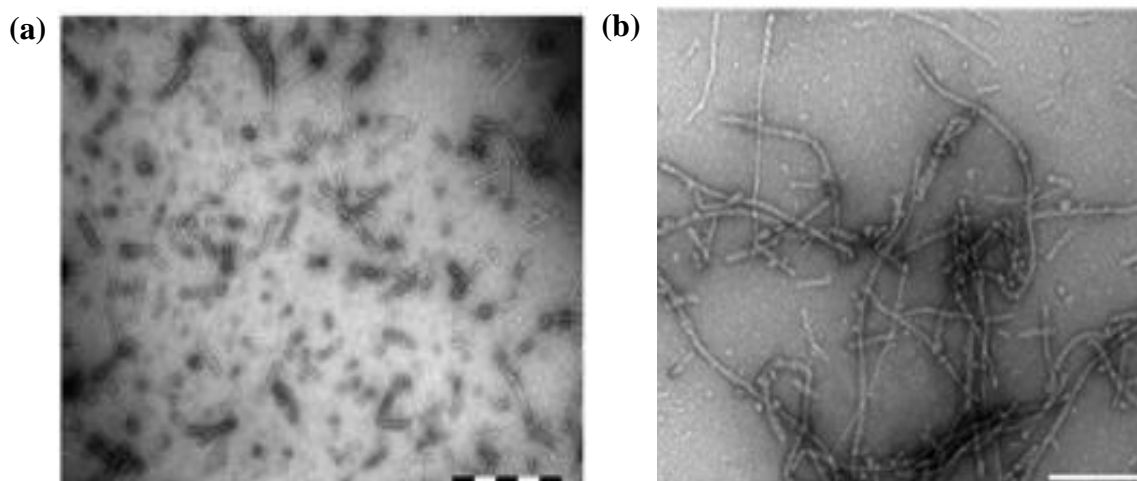


**Figure 5.23** Transmission electron micrographs of (A) worm-like structures formed from native  $\kappa$ -casein, following 2 days of incubation at 60 °C. Scale bar, 500 nm. (b) fibrils formed by RCM (reduced and carboxymethylated)  $\kappa$ -casein at concentrations above its CMC (critical micelle concentration). RCM  $\kappa$ -CN was incubated at 1.0

mg/ml. Scale bar, 200 nm [161].

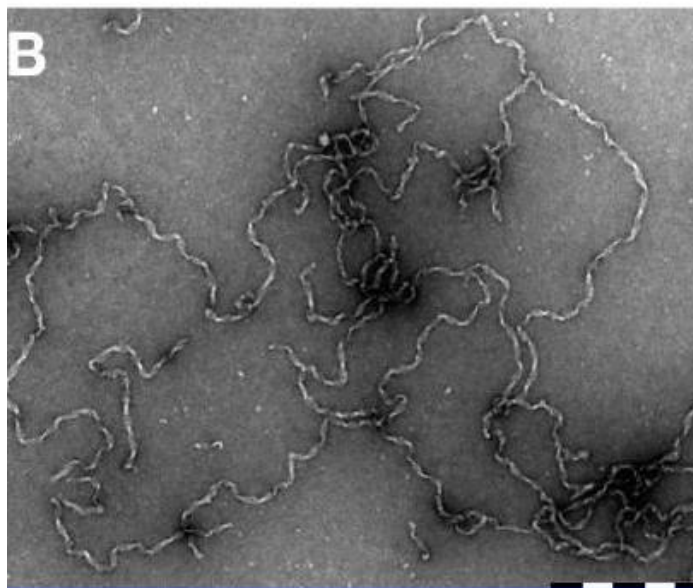


**Figure 5.24** Transmission electron micrograph showing  $\alpha_{s2}$ -casein (120  $\mu\text{M}$ ) after one week of incubation at 50  $^{\circ}\text{C}$ . The scale bar represents 500 nm [162].

Unfortunately, the reason for the different morphologies observed above is by far still unknown. The drying conditions of a droplet may be a significant factor determining the assembly of casein proteins. A further in-depth investigation is required for a better understanding of the assembly behavior of casein in the dried state.

### 5.1.8 Conclusion

The alteration of casein micellar behavior in alkaline solution (pH 12 - pH > 14) has been investigated. Turbidity experiments along with TEM and surface charge measurements revealed complete dissociation of casein micelles into submicellar structure in aqueous solutions of pH 12 and 13. As pH increased to  $\geq 14$ , an unexpected re-association of submicelles occurred, resulting in the formation of large aggregated structures. Calcium phosphate was found to be a dominant factor in governing this re-association process. It may moderate the interactions between proteins by neutralizing the negative charges of the casein molecules, and can also

contribute to the excessive establishment of phosphoserine – calcium phosphate – phosphoserine linkages in highly alkaline environments. Besides, the high ionic strength in casein solutions slightly promoted the re-association of casein submicelles.

A further study on Ca-depleted casein confirmed the importance of calcium content in the re-association of submicelles. The removal of calcium greatly reduced the aggregation tendency of casein proteins in highly alkaline solutions.

Based on above results, a schematic diagram was proposed to illustrate the alkaline-induced dissociation of casein micelle and re-association of casein submicelles in solutions. The overall micellar behavior is generally determined by the competition of electrostatic repulsive force and associative force derived from hydrophobic interaction and calcium phosphate linkage between casein proteins.

The morphology of casein species was investigated using AFM techniques. In the dried state, a roughly spherical submicellar structure with an average diameter of ~ 20 nm was observed in the outer region of the deposit. Due to a drying-induced deformation, submicelles were enlarged in the horizontal direction. These submicelles are believed to be the fundamental structural unit constructing casein micelles and aggregates in alkaline solution. Furthermore, self-assembly of the casein proteins occurred during the drying of the droplet. Different morphologies were observed in the middle region of the deposit. There, rod and worm-like structures formed after assembly were significantly different from the micellar structures found in aqueous solution.

## 5.2 Effect of protein composition on dispersing performance of casein superplasticizer

### 5.2.1 Dispersing performance of casein superplasticizer

The dispersing effectiveness of casein superplasticizer is mainly determined by the electrostatic repulsive forces it introduces to binder surfaces, which can be typically characterized by zeta potential measurement. **Figure 5.25** shows the zeta potential development of a cement paste upon titration with a concentrated casein solution. In the absence of casein, the zeta potential of cement particles was found to be -5 mV. With increased dosage of superplasticizer, the zeta potential gradually increased until a maximum value of -10.4 mV was reached at 0.24 wt.% of casein. After that, the increase in casein dosage did not lead to a further increase in the zeta potential values, and the curve leveled off.

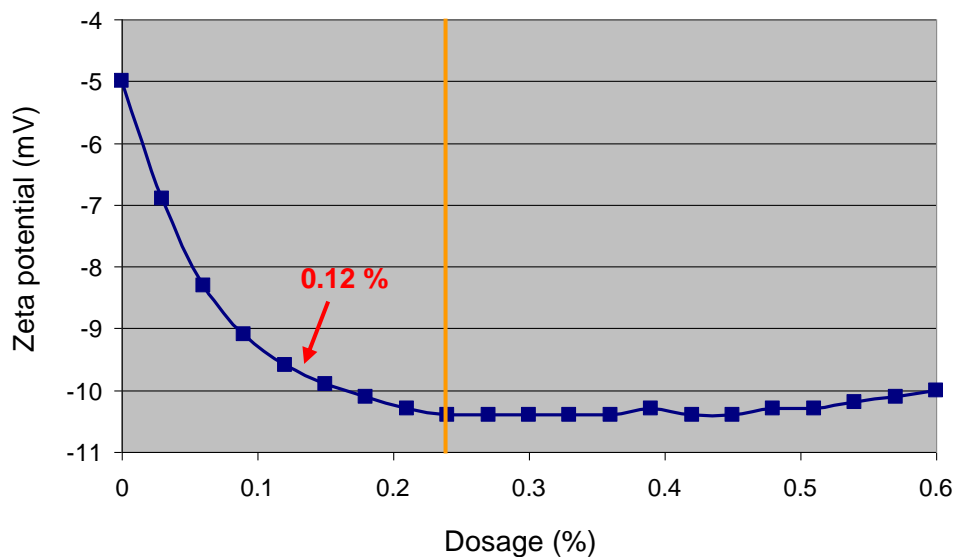


**Figure 5.25** Zeta potential of a cement paste as a function of casein dosage.

The development of zeta potential with increased casein dosage can be attributed to the adsorption of superplasticizer on cement particles. The adsorption of negatively charged casein changed the charge on the electrical double layer of cement surface, resulting in an increase in the absolute value of the zeta potential. This promoted

stronger strengthened electrostatic repulsion between cement particles. As a consequence, the stability of the dispersion was improved. The electrical double layer at the saturation adsorption state on binder surfaces is depicted in **Figure 5.26**.

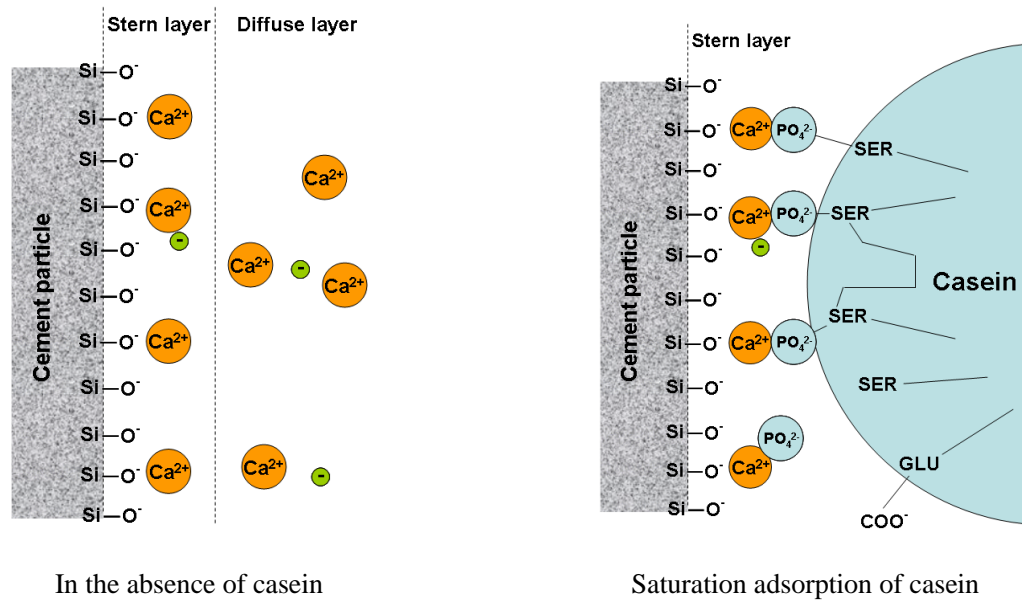


**Figure 5.26** Schematic illustration of electrical double layers existing in the absence of casein and at saturation adsorption of casein on the surfaces of cement particles.

Based on above zeta potential results, a dosage of 0.24 wt.% bwob of casein was optimal for the formulation of the SLU paste. The dispersing effectiveness of admixture was characterized by measuring the spread flow of the SLU paste according to EN 12706. The time-dependent paste flow was recorded and the result is shown in **Figure 5.27**. Over a time span of 60 min, the flow remained larger than 17 cm before it dropped as a result of accelerating cement hydration, suggesting an excellent plasticizing effect from casein. However, during the measurement strong segregation and bleeding occurred in the SLU paste, as is shown in **Figure 5.28**. The spread flow of the paste greatly fluctuated, which is unacceptable in actual application.

To eliminate the bleeding problem of the cement grout, the dosage of casein

superplasticizer was adjusted to 0.20 wt.%, 0.15 wt.%, 0.12 wt.% and 0.10 wt.%, respectively. The flowability of these SLU pastes and the bleeding phenomena were characterized and the results are shown in **Figure 5.27** and **Figure 5.28**. According to them, decreased dosage of casein superplasticizer effectively reduced the bleeding of cement paste. Until a dosage of 0.12 wt.% was reached, the SLU paste was coherent and homogenous, suggesting that the segregation problem has been solved. At this dosage, a spread flow of > 15 cm over a time span of 30 min was obtained, which indicates sufficient dispersing performance of casein at that dosage. Based on those results, a casein dosage of 0.12 wt.% will be employed in the following formulation of SLUs in this thesis.

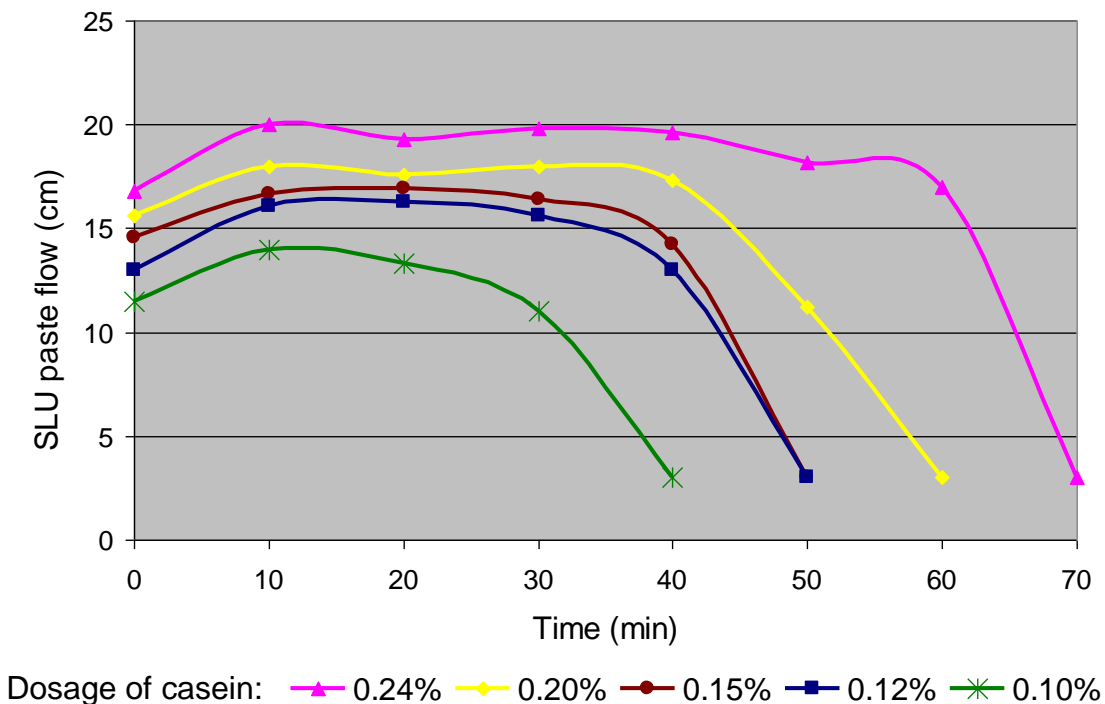


**Figure 5.27** Flowability versus time for self-levelling grout containing different dosages of casein superplasticizer.

Furthermore, the adsorption amount of casein on the binder surface was measured using total organic carbon (TOC) and ionic chromatography (IC) methods. First, the total amount of retarder and of casein superplasticizer left unadsorbed in the SLU

pore solution was measured by TOC analysis. Next, the retarder amount was quantified using IC measurement. As a result, the casein concentration remained in the pore solution can be obtained by subtraction. Based on the above method, adsorption of casein on the binder was found to be 90.7%. This result indicates that casein superplasticizer exhibits a strong tendency to adsorb on cement.

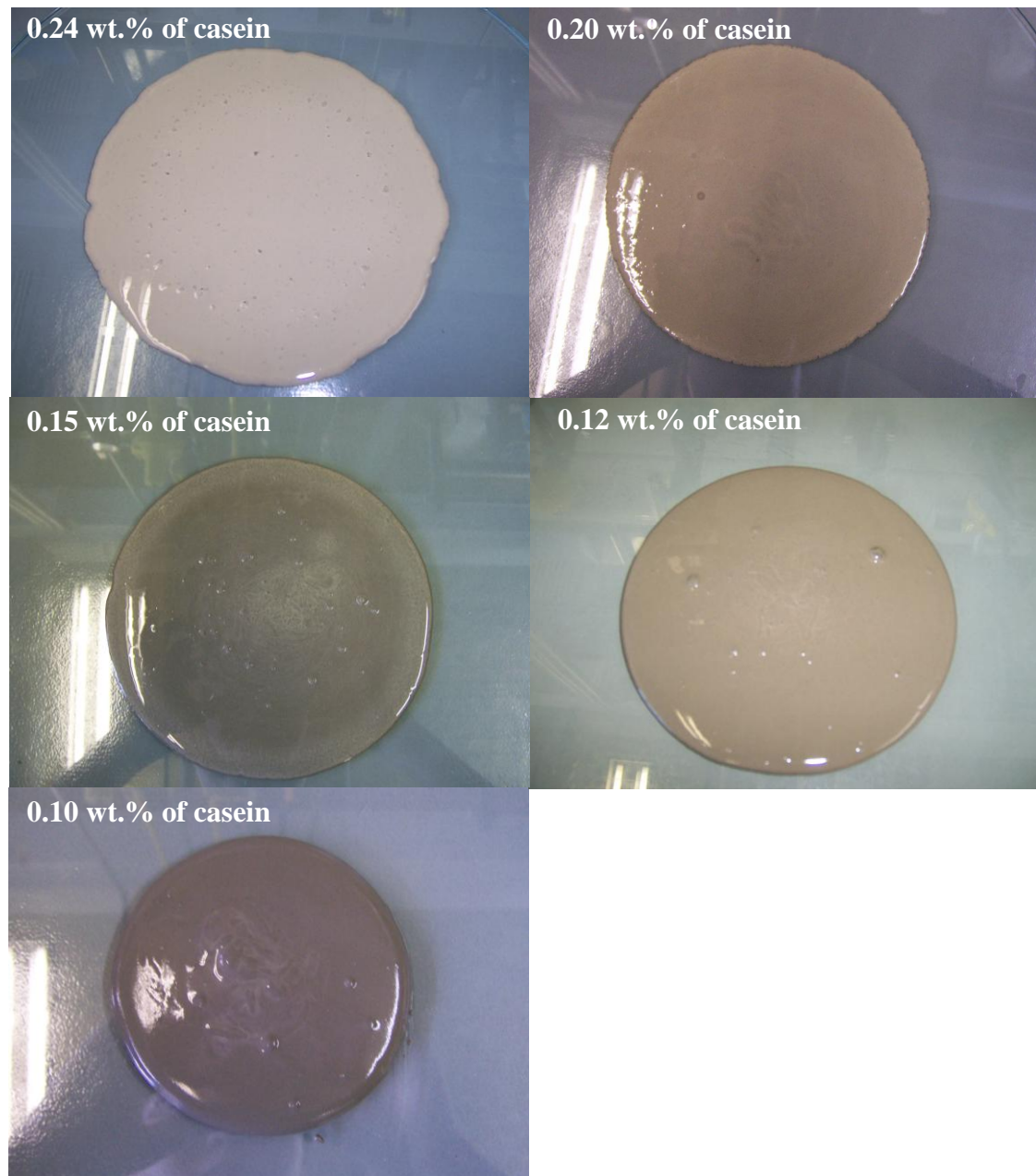


**Figure 5.28** Photographs of self-levelling grouts containing increased dosages (0.1 – 0.24 wt.%) of casein superplasticizer taken 20 min after preparation of the grout.

## 5.2.2 Quality criteria for dispersion effectiveness of casein

### 5.2.2.1 Fluctuation in quality of commercial casein samples

As a natural biopolymer, the quality of casein varies significantly, depending on the species of cattle, dietary conditions, environmental factors, manufacturing process, etc [163]. Accordingly, widely fluctuant dispersing effectiveness has been reported for caseins superplasticizers from different batches. Here, five-randomly selected industrial casein samples provided by Ardex GmbH (Witten/Germany) were tested as superplasticizers in SLUs. The samples were designated as casein #1, casein #2, and so forth. The dispersing power of these caseins was characterized using the time-dependent mini slump test. The results obtained are displayed in **Figure 5.29**.

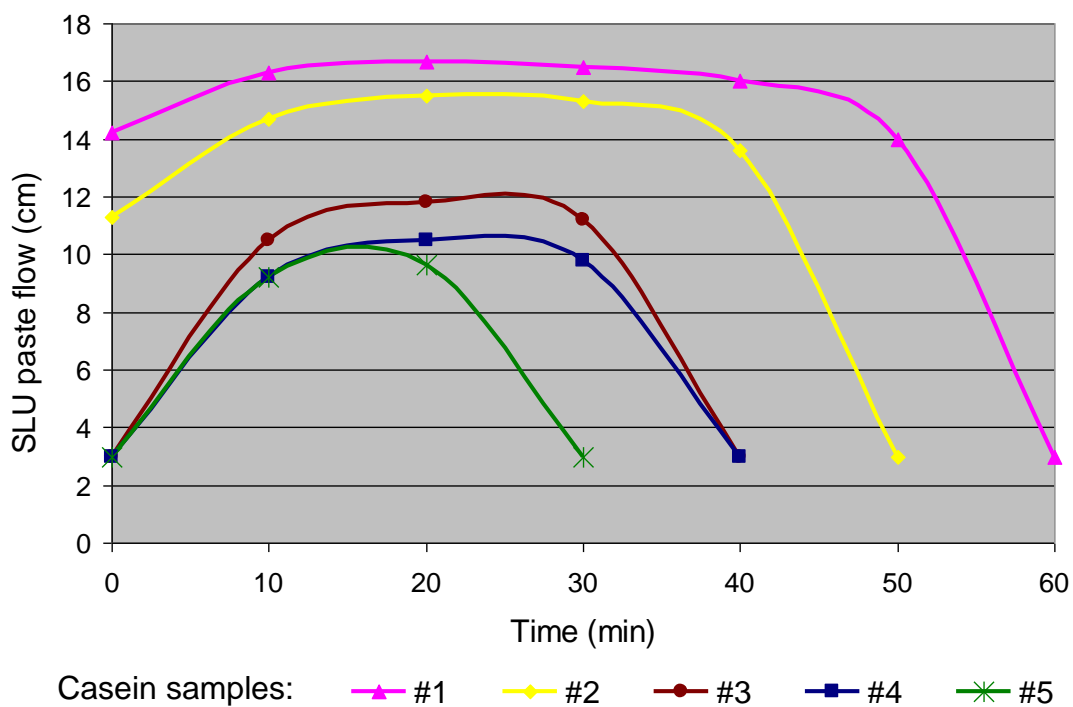


**Figure 5.29** Flowability versus time for self-levelling grout containing casein superplasticizers of different batches.

Among these samples, casein #1 and #2 exhibited strong and long lasting dispersing effectiveness in SLUs, where the spread flow of paste remained larger than 14 cm for

at least 30 min. Casein #3 and #4 exhibited inadequate dispersing power. There, the largest spread flow was found at less than 12 cm. The worst performance was observed for casein sample #5 which hardly gave any dispersion in SLU paste. This result confirms the huge fluctuation in the quality of commercial casein superplasticizers, which generally poses a serious problem for the formulators using this product.

#### **5.2.2.2 Method to assess the quality of casein superplasticizer**

Because of the quality fluctuations, the industry has to routinely test the casein samples to estimate their performance before application. Unfortunately, this testing process is very time consuming and a significant amount of mortar specimens have to be prepared which is a considerable time and cost factor. To solve that problem, we investigated and explored the reason for the huge quality variation of casein samples, aiming to develop a fast and inexpensive quality assessment method.

First, the physical property of casein samples, specifically the particle size distribution of each casein powder was determined by sieving. The result obtained is shown in **Figure 5.30**. It is seen that the larger particles ( $> 200 \mu\text{m}$ ) in casein #5 accounted for 12.5 wt.% of the total weight, which indicates the grinding applied to this casein sample is not sufficient. This might be responsible for the poor dispersing effectiveness of casein #5. With respect to casein #4, 0.6 wt.% of particles were found larger than  $200 \mu\text{m}$ , 54.5 wt.% between  $200$  and  $125 \mu\text{m}$ , and 44.9 wt.% smaller than  $125 \mu\text{m}$ . Apparently, this casein sample was ground sufficiently. However, the mini slump test displayed in **Figure 5.29** indicates a rather poor dispersing effectiveness of this casein #4. It suggests that the particle size of casein powder is not the critical factor to determine the quality of casein superplasticizer.

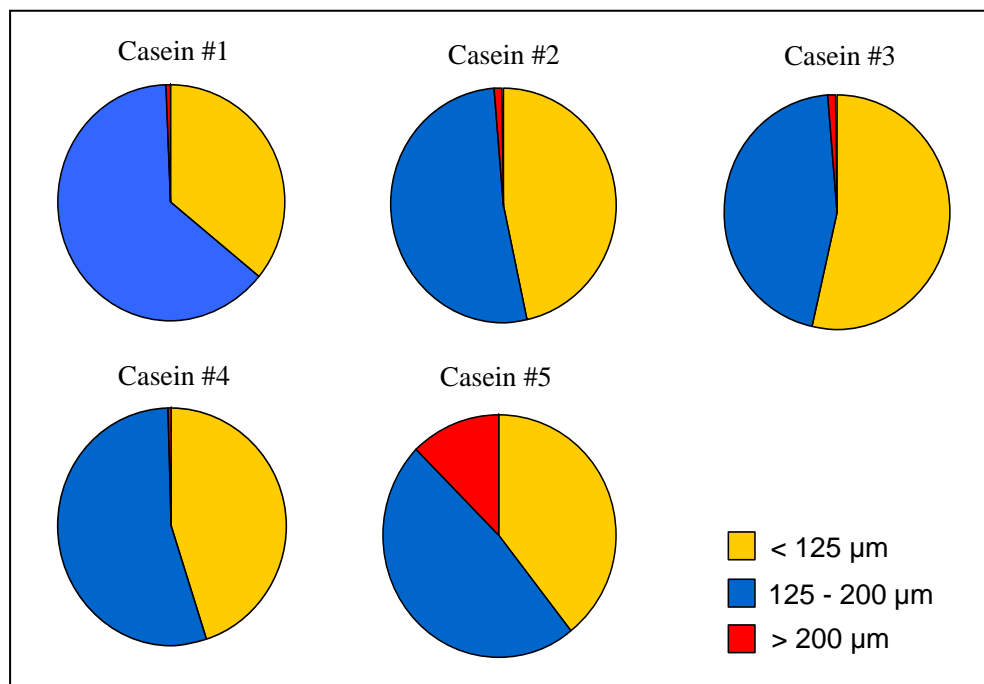


**Figure 5.30** Particle size distribution of the powdered casein samples tested.

It is well known that the chemical composition is closely related to the properties and functions of materials. In this work, to determine the impact of biochemical composition of casein on its plasticizing effect, the five casein samples were fractionated and characterized by anion exchange FPLC. The elution profiles thus obtained are shown in **Figure 5.31**.

From the figure it becomes apparent that  $\alpha$ - and  $\beta$ -casein are the primary components in casein. Whereas,  $\kappa$ -casein only accounts for minor peaks on the elution profile. From casein #1 to casein #5, the intensity of the  $\kappa$ -casein peaks decreased significantly. Through integration of the chromatograms, the peak area percentage of each protein fraction was calculated and the results are listed in **Table 5.1**. Note that the different absorbance coefficients of the casein proteins were not taken into account in the calculation. Hence, the results do not represent the real content of the proteins in the casein samples.

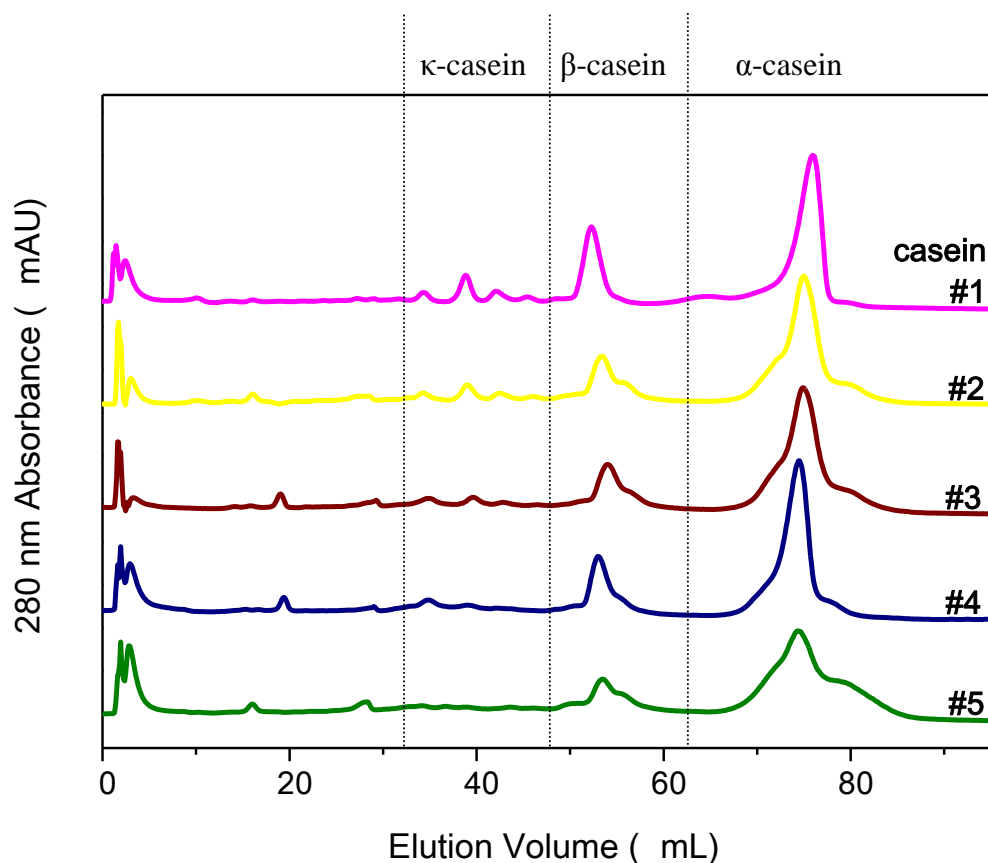


**Figure 5.31** Ion-exchange FPLC profiles of five commercial casein samples, fractionated on Resource Q column.

**Table 5.1** Relative percentages of  $\alpha$ -,  $\beta$ - and  $\kappa$ -casein contained in the commercial casein samples, calculated from peak areas

	Casein #1	Casein #2	Casein #3	Casein #4	Casein #5
$\alpha$ -casein %	68.9	73.6	75.0	72.4	80.0
$\beta$ -casein %	22.9	20.3	20.3	23.4	18.3
$\kappa$ -casein %	8.2	6.2	4.7	4.2	1.6

From **Table 5.1**, there is no clear trend existing for the  $\alpha$ - and  $\beta$ -casein contents in the different casein samples. However, the peak area percentage of  $\kappa$ -casein was found to decrease steadily from casein #1 to casein #5. This is exactly in line with the plasticizing effect of the casein samples found in the mini slump test (**Figure 5.29**). Thus, it can be concluded that the content of  $\kappa$ -casein is critical for the performance of

casein superplasticizer. The more  $\kappa$ -casein is contained in a casein sample, the stronger its dispersing power.

Furthermore, the relative contents of  $\alpha$ -,  $\beta$ - and  $\kappa$ -casein, specifically the ratios between the peak areas of  $\alpha$ - and  $\kappa$ -casein ( $\alpha/\kappa$ ) and  $\beta$ - and  $\kappa$ -casein ( $\beta/\kappa$ ) were calculated by integration of the chromatograms. The result obtained is displayed in **Figure 5.32**. There, a clear trend became evident in terms of peak area ratios. From casein sample #1 to casein sample #5,  $\alpha/\kappa$ - and  $\beta/\kappa$ -casein ratios increase steadily. Specifically, for the  $\alpha/\kappa$ -casein ratio, values of 8.39 for casein #1, 11.93 for casein #2, 16.01 for casein #3, 17.20 for casein #4 and 49.50 for casein #5 were found, which indicates a remarkably different composition of the casein samples. From this result it is concluded that not only the absolute content of  $\kappa$ -casein, but also the relative amount of  $\alpha$ - to  $\kappa$ - and of  $\beta$ - to  $\kappa$ -casein can be applied as a quality criterion for the dispersing power of casein. The lower the  $\alpha/\kappa$ - and  $\beta/\kappa$ -casein ratios, the better is the dispersing effectiveness of a casein sample.

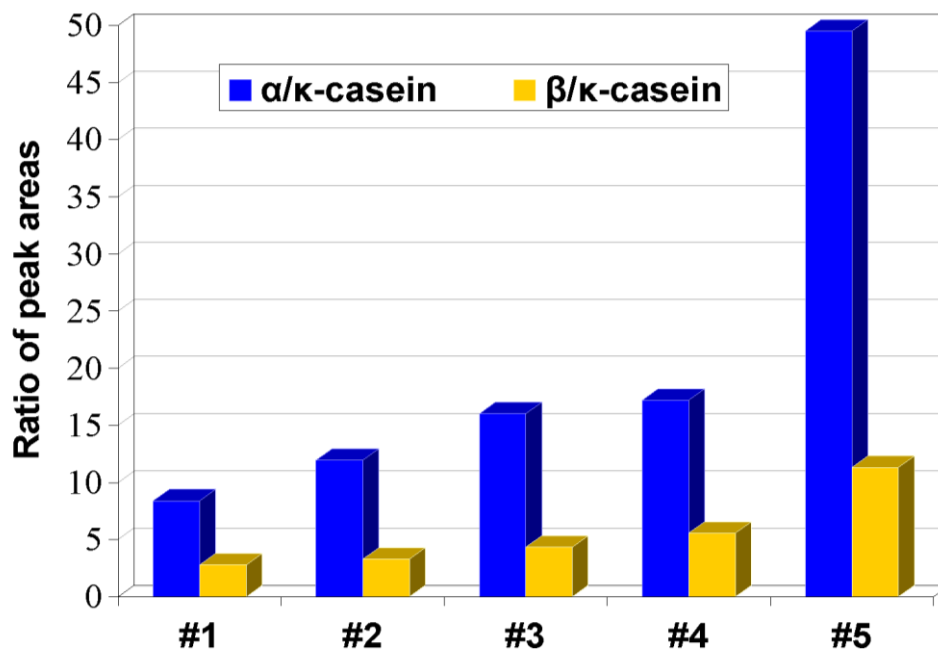


**Figure 5.32** Ratios of peak areas for  $\alpha/\kappa$ - and  $\beta/\kappa$ -casein proteins in five commercial casein samples, determined by FPLC.

Additionally, the difference between products as expressed by the  $\alpha/\kappa$ - and  $\beta/\kappa$ -casein ratios is more significant than the  $\kappa$ -casein content only. Therefore, it allows a more detailed classification and assessment of the quality of casein samples. Based on our method, a  $\kappa$ -casein content of  $>6\%$  and an  $\alpha/\kappa$ -casein ratio of  $<12$  appear to be the reference levels for high quality casein. When a casein sample shows a  $\kappa$ -casein content of below  $6\%$  or an  $\alpha/\kappa$ -casein ratio of more than  $12$ , it can be expected to perform poorly as superplasticizer or even fail entirely.

From the above discussion it is evident that  $\kappa$ -casein plays a critical role in the performance of casein superplasticizer. This seems to contradict the findings in our earlier study where  $\alpha$ -casein was revealed to show the major plasticizing effect in comparison to  $\beta$ - and  $\kappa$ -casein [109]. To understand this phenomenon, the behavior of different casein samples in a simplified cement pore solution was investigated. In the previous chapter, casein micelles were found to be unstable in alkaline solution, where they dissociate into submicelles at pH 12 and 13 (section 5.1.2). In SLUs, casein is exposed to the pore solution with a pH value of  $\sim 12$ . Thus, one can expect that when casein is dosed to a SLU paste, significant disintegration of the casein micelles will occur, and much smaller submicelles will be present in the pore solution. In this work, the alkaline solution of pH 12 was used as a simple model for the SLU pore solution. Particle size distributions of casein samples in these model solutions were characterized using dynamic light scattering (DLS) measurement. The results obtained are shown in **Figure 5.33**.

There, the casein micelles were found to dissociate into small submicelles which possess mean diameters of  $\sim 10 - 20$  nm. The size of the submicelles shows a clear tendency to decrease with increased amount of  $\kappa$ -casein. Specifically, the more  $\kappa$  protein fraction a casein sample contains, the smaller are the submicelles it forms in alkaline solution.

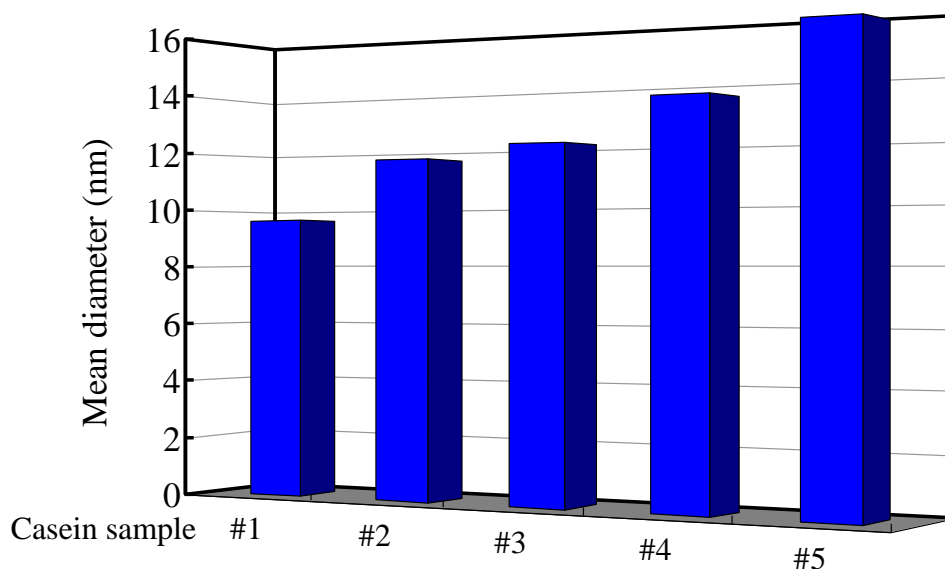


**Figure 5.33** Average diameter of submicelles of different casein samples in alkaline solution, measured by dynamic light scattering ( $\text{pH} = 12$ ,  $c_{\text{casein}} = 1 \text{ g/L}$ ).

It is now clear that in a SLU formulation, casein dissociates into submicelles due to the alkaline pH. Furthermore, the size of casein submicelles is closely related to the content of  $\kappa$ -casein. This correlation is in good agreement with some earlier reports [164]. Due to the pronounced hydrophilic domains,  $\kappa$ -casein is revealed to locate preferentially on the surface of micelles. With respect to submicelles,  $\kappa$ -casein forms an outer layer which covers the core of  $\alpha$ - and  $\beta$ -caseins as illustrated in **Figure 5.34**, thus inhibiting the further growth of the submicelle. Through this mechanism, the amount of  $\kappa$ -casein present in a casein sample governs the final size of the submicelles [165]. In alkaline solution, the casein sample containing a high proportion of  $\kappa$ -casein tends to form submicelles possessing smaller particle size. Concerning the five casein samples studied here, the relative amount of  $\kappa$ -casein decreased in the order from casein #1 to casein #5. Accordingly, their particle sizes in alkaline solution are supposed to increase by the same order, which well explains the DLS results mentioned in **Figure 5.33**.

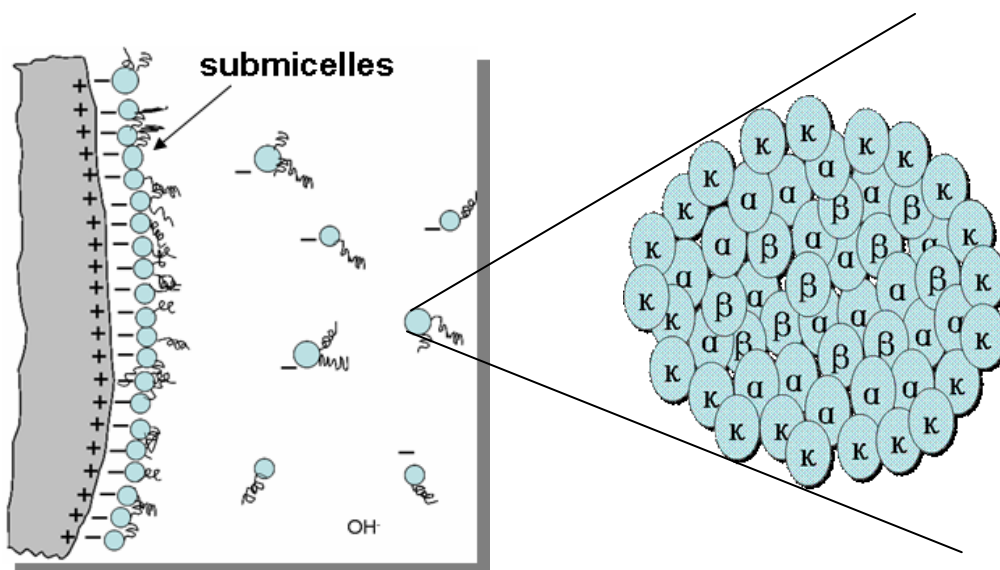


**Figure 5.34** Schematic drawing of the adsorption of casein submicelles on cement particles. Zoomed image: structure of casein submicelles.

To sum up, we have evidenced that in SLUs not the large casein micelles, but very small submicelles adsorb onto the surface of the binder and provide dispersing effectiveness. In this work, casein samples of different batches dissociate into submicelles of different sizes due to the variations in their biochemical composition. Smaller submicelles can adsorb in larger number onto the cement surface and thus will provide a more densely packed polymer layer. Through this mechanism, stronger electrostatic repulsion between the cement particles is instigated and higher flowability of the SLU paste is achieved. The proposed working mechanism of casein in cement is illustrated in **Figure 5.34**.

### 5.2.3 Conclusion

The adsorption of negatively charged casein on the surface of binders can increase the absolute value of zeta potential and strengthen the electrostatic stability of cement particles. However, the high dosage of casein superplasticizer can cause unwanted segregation of the cement paste. Considering sufficient fluidity and homogeneity of the grout, a casein dosage of 0.24 wt.% bwob is believed to be appropriate and will be

used in future formulation of SLUs in this thesis.

The quality of commercial casein superplasticizers, namely their dispersing effectiveness, was found to show huge variations in SLU pastes. Ion exchange FPLC was used to examine the biochemical composition of different casein samples. The results suggest that  $\kappa$ -casein plays the key role in governing the dispersing effectiveness of casein in SLUs. Specifically, the proportion of  $\kappa$ -casein in whole casein, as well as the relative ratio of  $\alpha$ - to  $\kappa$ -casein can be applied as criteria for assessing the quality of caseins. A  $\kappa$ -casein content of  $>6\%$  and an  $\alpha/\kappa$ -casein ratio of  $<12$  appear to be the reference levels for high quality casein. This chromatographic method allows a facile and inexpensive assessment of the quality of commercial casein superplasticizers.

The working mechanism of casein superplasticizer in cement paste was analyzed using DLS measurement. The results suggest that casein micelles dissociate into small submicelles ( $\sim 10$  nm) in SLUs. These submicelles supposedly adsorb onto the surface of the binder and perform the plasticizing effect. Additionally, it was found that the particle size of casein submicelles is closely related to its  $\kappa$ -casein fraction. A casein superplasticizer containing a larger proportion of  $\kappa$ -fraction is supposed to dissociate into smaller submicelles in the pore solution, and consequently adsorb in a larger number on the binder surface. More explicitly, the dispersing effectiveness of casein superplasticizer is mainly governed by the biochemical composition of its proteins.

## 5.3 Fractionation and modification of casein superplasticizer

### 5.3.1 Casein fractions

Casein superplasticizer was separated into  $\alpha$ -,  $\beta$ -, and  $\kappa$ -casein proteins using the chromatographic method mentioned in section 4.2.5. The dispersing effectiveness of individual casein proteins in SLU pastes was characterized by mini slump test. In this measurement, a slump cone with an internal diameter of 14 mm and a height of 25 mm was used to reduce the consumption of casein fractions. Additionally, the water to binder ratio was adjusted to 0.35 to achieve paste flow. The results obtained are shown in **Figure 5.35**.

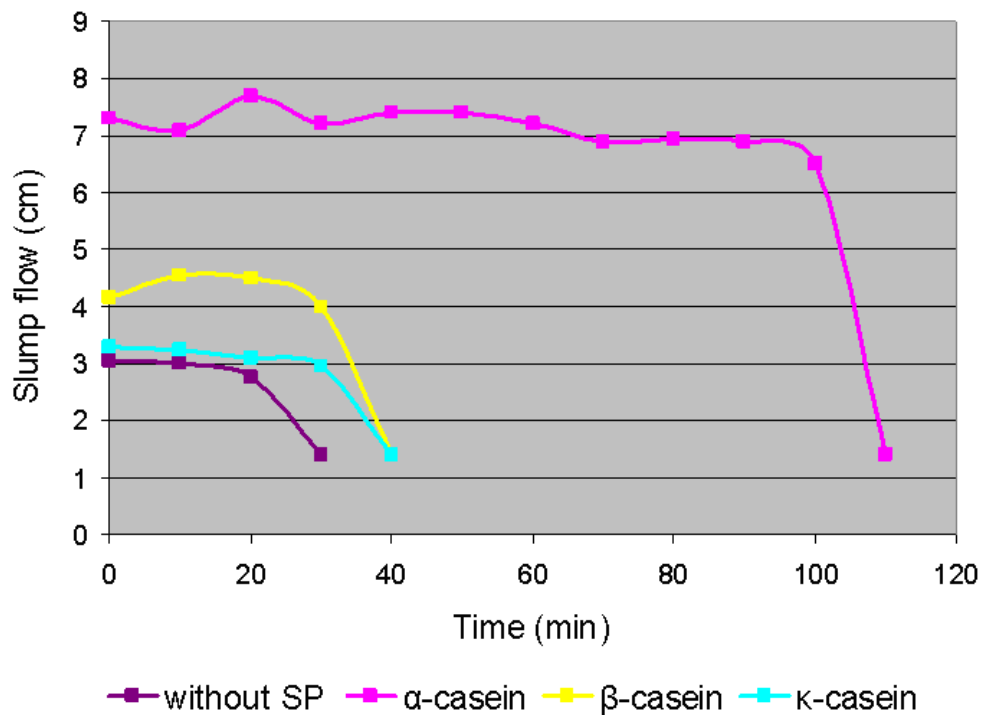


**Figure 5.35** Dispersing effectiveness of individual casein fractions in self-levelling grout.

From **Figure 5.35**, it is very clear that  $\alpha$ -casein exhibits the best dispersing effectiveness in SLU paste. The spread remained at a high level over 100 min of flow time. Whereas,  $\beta$ - and  $\kappa$ -casein only poorly disperse cement. Especially  $\kappa$ -casein

hardly showed any dispersing effectiveness in SLU paste.

Furthermore, the self healing property of the individual casein fractions was determined using the cutting test. Knife-cuts were conducted every few minutes, and then the recovery of the disturbed surface was evaluated. As shown in **Figure 5.36**, the cuts on the grout surface healed completely in the first 10 min. Then, at  $t = 20$  min, the cut healed, but left an indistinct scar on the cut edge. Furthermore, at  $t = 35$  min, the grout surface failed to correct itself to a smooth plane, and the cut no longer healed. The same experiments were carried out on  $\beta$ - and  $\kappa$ -casein dispersed SLU pastes. Unfortunately, no self healing effect at all was observed there. In other words,  $\beta$ - and  $\kappa$ -casein fractions do not provide self healing properties to SLUs.



**Figure 5.36** Self healing property of a model SLU paste containing  $\alpha$ -casein as superplasticizer.

### 5.3.2 Reconstituted casein superplasticizer

In section **5.3.1**, the individual casein proteins were fractionated from the whole casein and characterized with respect to their performance in SLU paste. Here, these fractionated casein proteins were recombined in the same composition as found in the original casein sample, aiming to find out any difference in performance between

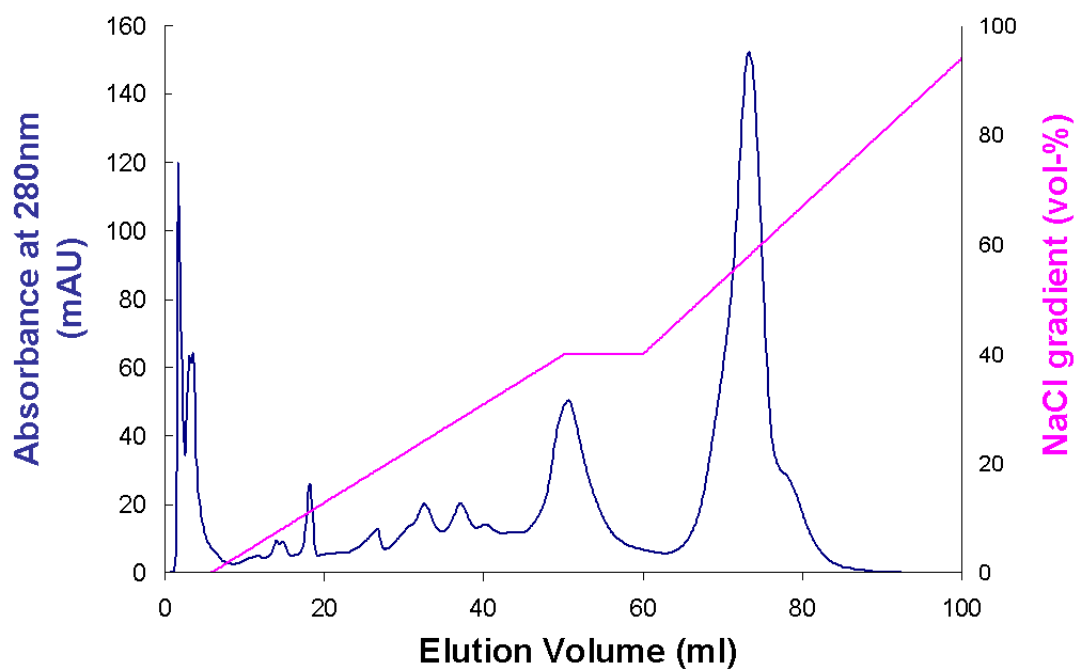
original and reproduced casein.

First, casein was characterized using FPLC as mentioned in 4.2.5. The elution profile obtained is shown in **Figure 5.37**. In order to calculate the biochemical composition of this original casein sample, the Beer-Lambert Law was applied. As is shown in **Equation 5.1**, Beer-Lambert Law describes a linear relationship between absorbance and concentration of an absorbing substance.

$$A_{\lambda} = \varepsilon \cdot c \cdot L$$

**Equation 5.1** Beer-Lambert Law

There,  $A_{\lambda}$  is the measured absorbance at a specified wavelength ( $\lambda$ ),  $\varepsilon$  is molar absorption coefficient or molar extinction coefficient of the substance,  $c$  is the concentration of substance, and  $L$  is the path length. The reported absorbance coefficients of each casein protein at 280 nm is shown in **Table 5.2** [166]. According to Beer-Lambert Law, the percentage contents of  $\alpha$ -,  $\beta$ -, and  $\kappa$ -casein were obtained and the results are shown in the table as well.

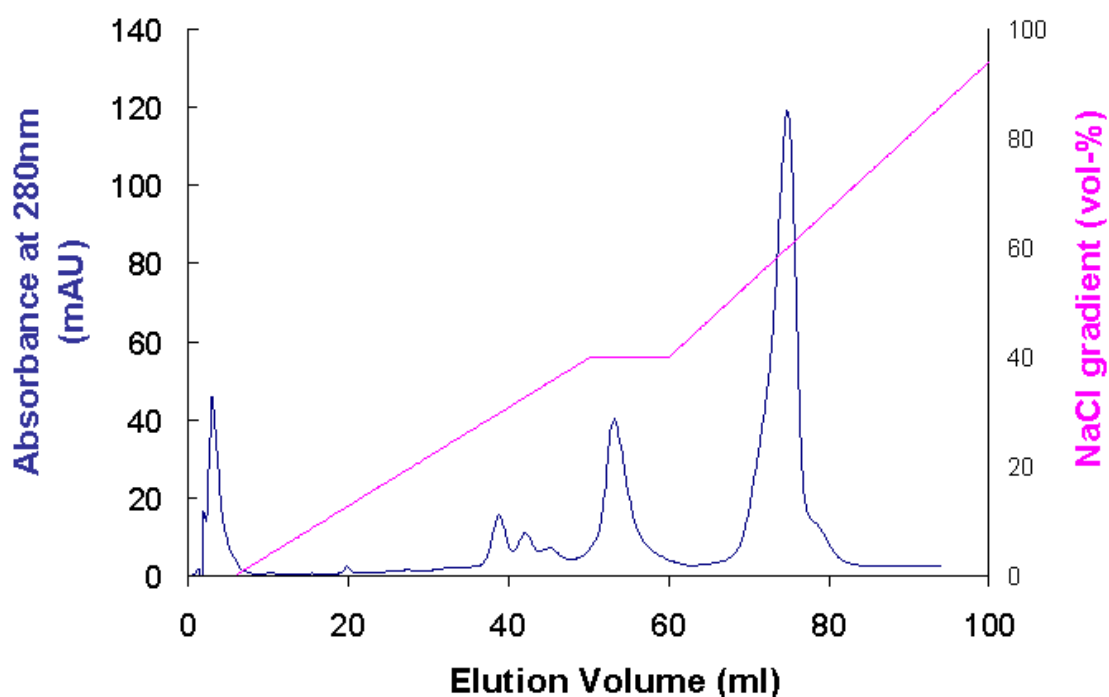


**Figure 5.37** Ion-exchange FPLC profile of the original casein sample.

**Table 5.2** Protein composition of the original casein sample.

Fraction	Absorbance coefficient at 280 nm ( $A_{1\text{cm}}^{1\%}$ ) [166]	Calculated content (wt.%)
$\alpha$ -casein	10	49.6
$\beta$ -casein	4.6	37.2
$\kappa$ -casein	9.6	10.5

Next, a reconstituted casein sample was prepared by blending the individual casein proteins in the proportion shown in **Table 5.2**. The reproduced casein was subjected to FPLC measurement. As shown in **Figure 5.38**, FPLC chromatography confirmed the identical composition of recombined casein to that of the original casein. Furthermore, **Figure 5.39** visualizes the appearance of the recombined and original casein samples.

**Figure 5.38** Ion-exchange FPLC profile of casein reconstituted from its individual proteins.

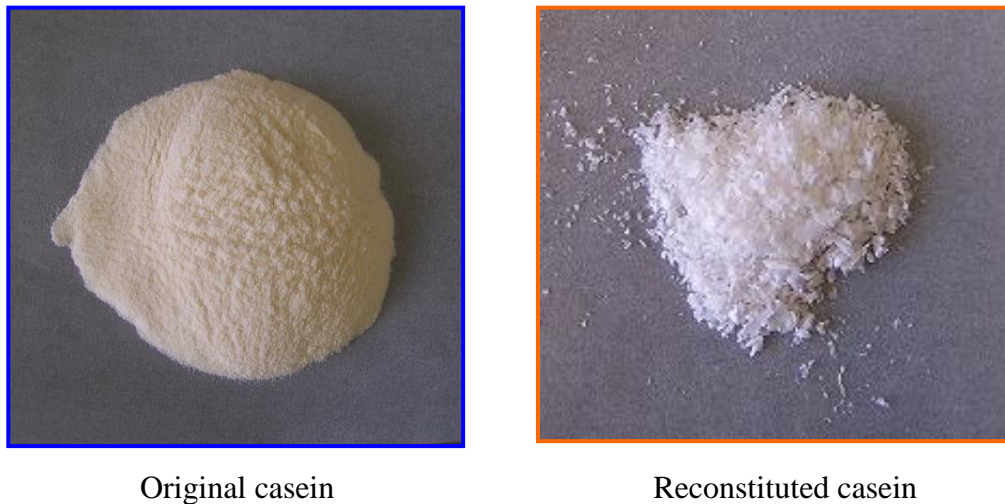


**Figure 5.39** Appearances of original and reconstituted casein samples.

The dispersing effectiveness of the reconstituted casein in SLU paste was characterized using the mini slump test. The results obtained are shown in **Figure 5.40**. For comparison, performance of the original casein sample is also displayed in the figure.

As can be seen there, the initial flow of the SLU paste containing reconstituted casein was slightly higher (14.6 cm vs. 13.0 cm for the original casein). With increased flow time, the difference in the spreads of both pastes became less and less. Until after 20 min, the spreads became identical. The slightly better performance of reconstituted casein may be attributed to the dissociated form of proteins present in this sample. It is known that casein possesses a micellar structure. In cement pore solution, casein micelles have to disintegrate under the attack of alkali before they can adsorb on cement. This dissociation process may be time consuming, which accordingly results in reduced initial dispersing effectiveness of casein. However, the reconstituted casein is a mixture of individual proteins, where the micellar structure does not exist anymore. These dissociated forms of casein proteins can adsorb quickly on the binder surface, thus promoting a good dispersing effect from the very beginning.

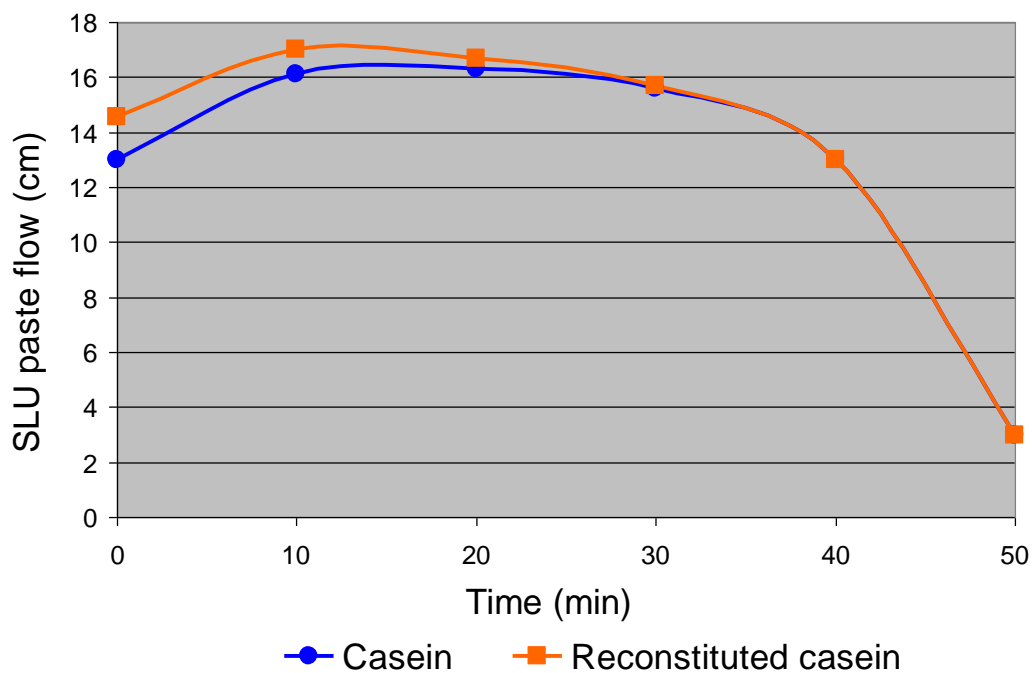


**Figure 5.40** Comparison of dispersing effectiveness of original and reconstituted casein samples in SLU paste.

### 5.3.3 Modified casein samples

A casein precipitate enriched in  $\alpha$ - and  $\beta$ -proteins was produced using the method mentioned in section 4.1.5. The resultant precipitate was further treated by chemicals as described in **Figure 5.41** [167]. As a consequence,  $\alpha_{s2}$ -casein was removed from the precipitate and a  $\alpha_{s1}$ - and  $\beta$ -casein enriched fraction was obtained. **Figure 5.42** shows the visual appearances of the original casein and the chemically treated casein samples.

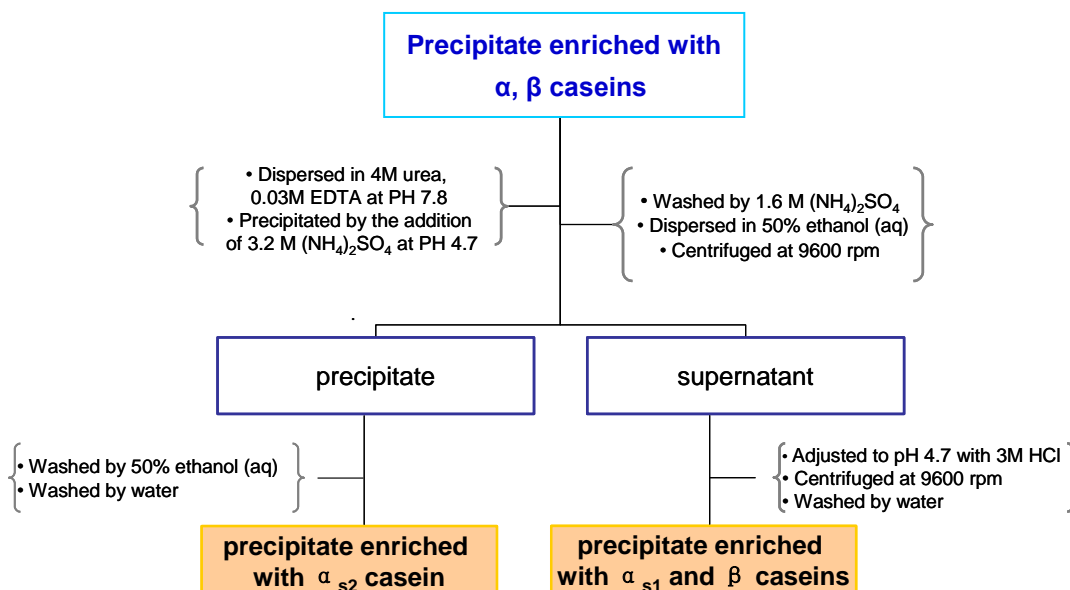


**Figure 5.41** Steps taken to obtain casein samples enriched in  $\alpha_{s2}$ - and  $\alpha_{s1}$ -/ $\beta$ -casein [167].



**Figure 5.42** Appearances of original and processed (modified) casein superplasticizer.

FPLC was used to determine the composition of the processed casein. In order to better monitor the elution profile of  $\alpha_{s2}$ -casein, the amount of dithiothreitol was increased to 12 mg in the process of sample preparation (see section 4.1.7). **Figure 5.43** compares the FPLC chromatograms of the treated and the original casein samples. According to this, the minor components commonly present in casein, namely  $\gamma$ -,  $\kappa$ - and  $\alpha_{s2}$ -proteins, were mostly removed from the processed casein.

Instead, this sample mainly consisted of  $\alpha_{s1}$ - and  $\beta$ -casein, the primary proteins present in original casein.

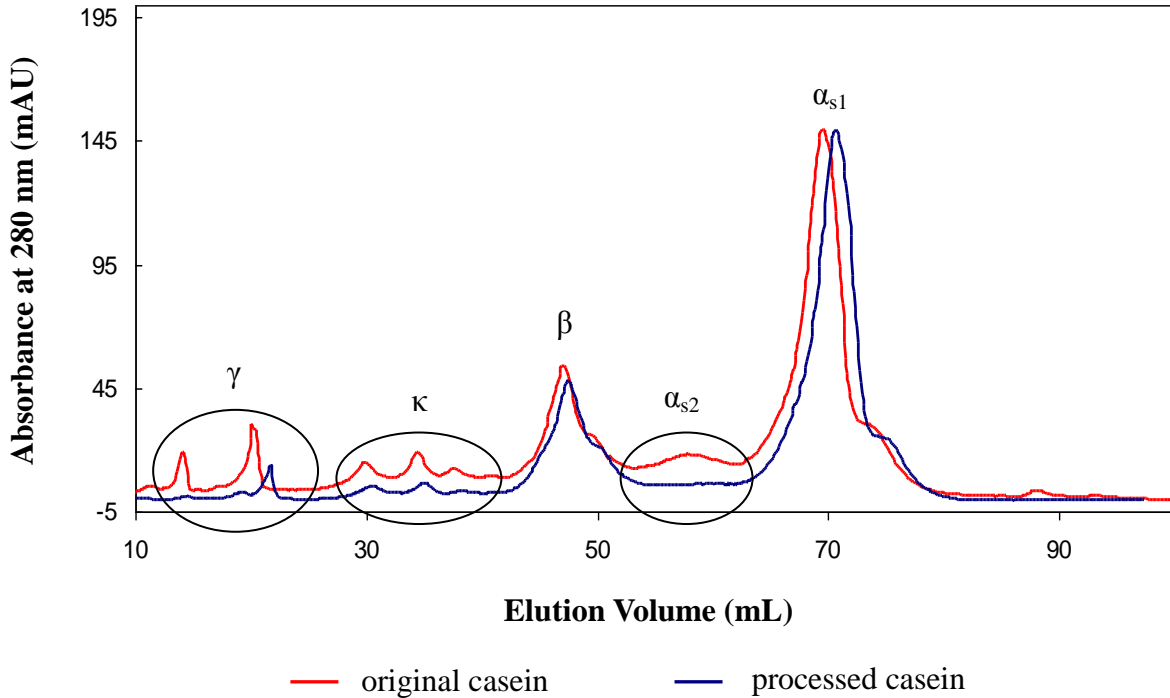


**Figure 5.43** Ion-exchange FPLC profiles of original and processed casein.

Furthermore, the dispersing power of the processed casein sample was characterized using mini slump test. The result is shown in **Figure 5.44**. Over a time span of 70 min, the spread of the SLU paste containing processed casein remained larger than 15 cm, indicating good dispersing power of this sample. Maximum spread value of the paste was 15.3 cm, which was slightly lower than that from original casein. Additionally, the processed casein was found to provide a longer lasting dispersing effect, i.e. increased workability period for the mortar. Hence, it is superior over original casein.

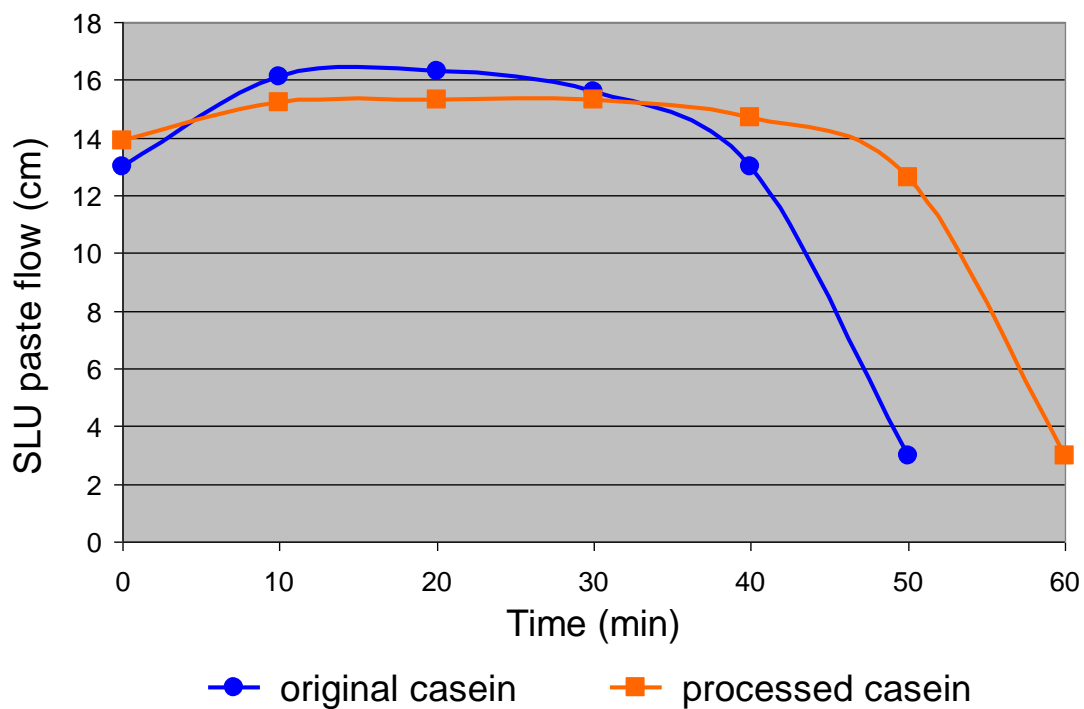
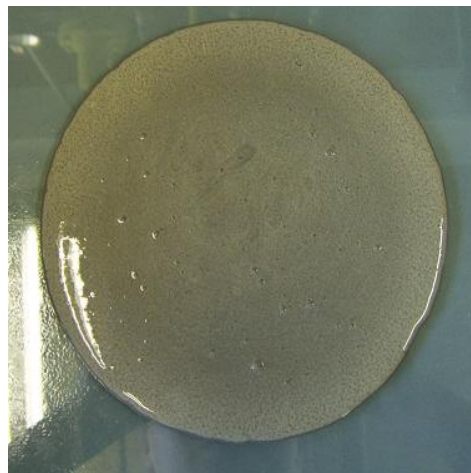


**Figure 5.44** Comparison of the dispersing effectiveness of original casein and processed casein samples.



SLU paste dispersed by original casein



SLU paste dispersed by processed casein

**Figure 5.45** Photographs of self-levelling grouts containing original and processed casein samples at 0.24 wt.% dosage. Photos were taken 20 min after mixing of the pastes.

More important, processed casein showed improved compatibility with inorganic binders. **Figure 5.45** presents the photographs of self-levelling grouts containing 0.24 wt.% of original and processed casein superplasticizer. It can be seen that segregation and bleeding of the SLU paste containing processed casein is considerably less than for original casein. It suggests that after chemical treatment, casein exhibits better compatibility with the materials present in SLUs. Unfortunately, the reason for the above improvement could not be investigated. It may be related to the micellar structure of casein in the absence of minor proteins, such as  $\kappa$ - and  $\alpha_{s2}$ -casein. Determination of this mechanism needs further investigations.

### 5.3.4 Conclusion

The individual casein protein families, *i.e.*  $\alpha$ -,  $\beta$ -, and  $\kappa$ -casein fractions, were separated from whole casein by FPLC method and their performance in SLU paste was investigated. It was found that  $\alpha$ -casein provides the best dispersing effectiveness in cement paste. In contrast,  $\beta$ - and  $\kappa$ -casein hardly provide any plasticizing effect. Additionally, the unique self healing property of casein was revealed to derive from  $\alpha$ -casein.

A reconstituted casein sample was prepared by blending the individual proteins in a composition identical to that of original casein. The dispersing effectiveness of recombined casein in SLU paste was found to be comparable to that of casein. Interestingly, reconstituted casein initially (0 – 20 min.) showed higher paste flow than original casein.

Additionally, casein superplasticizer was chemically treated with a series of reagents, resulting in the formation of a precipitate enriched in  $\alpha_{s1}$ - and  $\beta$ -casein. Mini slump tests revealed a long lasting dispersing effect of the processed casein sample. More importantly, the modified casein produced a more coherent SLU paste with less bleeding and segregation.

## 5.4 Effect of heat treatment on casein quality

The manufacture of casein superplasticizer involves extensive heat treatment, *e.g.* in the processes of curd cooking, dewheying, washing, drying, etc. Particularly in the drying procedure, a treatment temperature of  $> 100\text{ }^{\circ}\text{C}$  is generally applied to evaporate the moisture contained in the casein curd. As is well known, many of the amino acid residues in proteins are temperature sensitive, such as lysine (Lys), arginine (Arg), methionine (Met) and tryptophan (Try), which according to the literature are contained in the amino acid sequence of casein molecules (see **Figure 2.2 - Figure 2.5**). Therefore, it is reasonable to envision the casein proteins may undergo some structural/chemical changes during the drying process, which probably influences the dispersing power of casein superplasticizer in cement mortar. Although the thermal stability of casein proteins in milk and in buffers has been extensively studied, and heat induced aggregation behavior of casein micelles are fairly well characterized [168, 169, 170, 171], no work has been done on the effects of heat induced change in the dispersing quality of casein superplasticizer. To fill this gap, we studied the influence of temperature and exposure time on the composition and dispersing power of casein. **Table 5.3** shows the heating temperature and durations which have been applied to casein samples in this work.

**Table 5.3** Heating temperature and durations applied to casein superplasticizer.

Heating temperature	Heating duration					
50 °C	1 h	–	–	5 h	24 h	48 h
80 °C	1 h	–	–	5 h	24 h	48 h
110 °C	1 h	2 h	3 h	5 h	24 h	48 h

### 5.4.1 Moisture content of heat treated casein

As is shown in **Figure 5.46**, the non-treated casein powder had an initial moisture content of 11.5 wt.%. After being cured in the oven, water adsorbed on casein powder was removed, and the moisture content of samples decreased accordingly. Specifically, casein treated at 50 °C and 80 °C showed a gradual decrease in the moisture content over the entire heating period. However, when treated at 110 °C, the moisture content of casein decreased very quickly in the first hour of curing before it leveled off and approached the equilibrium moisture content of 4.0 %. The result suggests that casein powder has a high affinity to water vapor. It is not possible to remove the entire adsorbed moisture even after 48 h of heating duration. Based on the above, it is clear that the active content in casein powder became more “concentrated” after the heat treatment. This way, the dispersing effectiveness of heat treated casein is supposed to be enhanced.

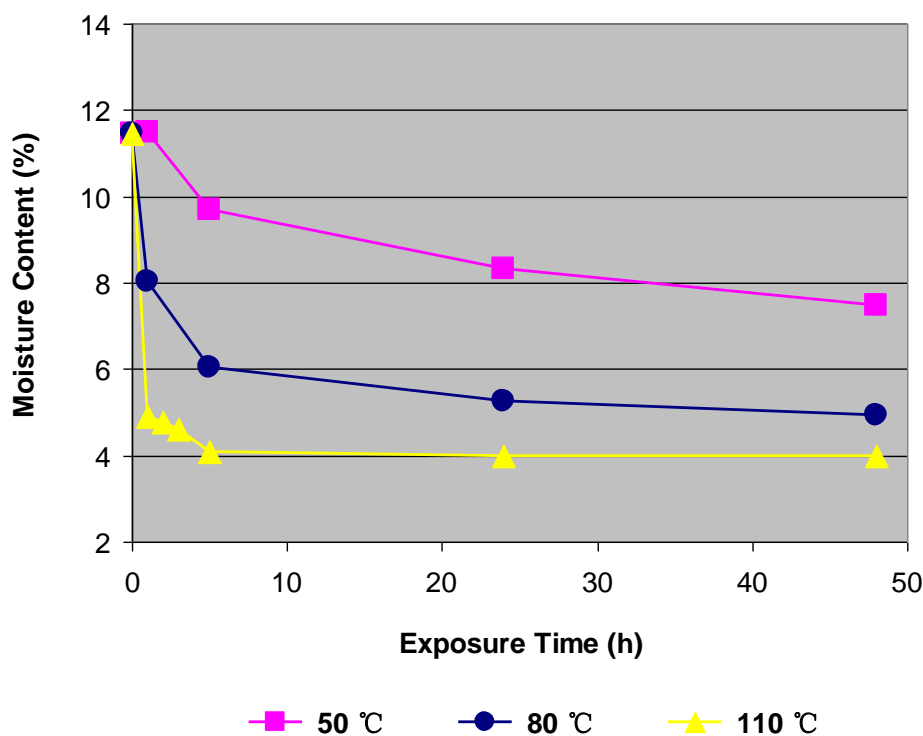


**Figure 5.46** Influence of the heating temperature and period on the moisture content of casein.

### 5.4.2 Dispersion power of heat treated casein

Original and heat treated casein powders were used as superplasticizers in SLUs. The dispersing power of the samples was determined by mini slump test and the results obtained are shown in **Figure 5.47**.

The casein powders treated at 50 °C performed comparable or slightly stronger than original casein. Tested over a time span of 60 min, the flow remained > 13 cm for 40 min before it dropped as a result of commencing cement hydration.

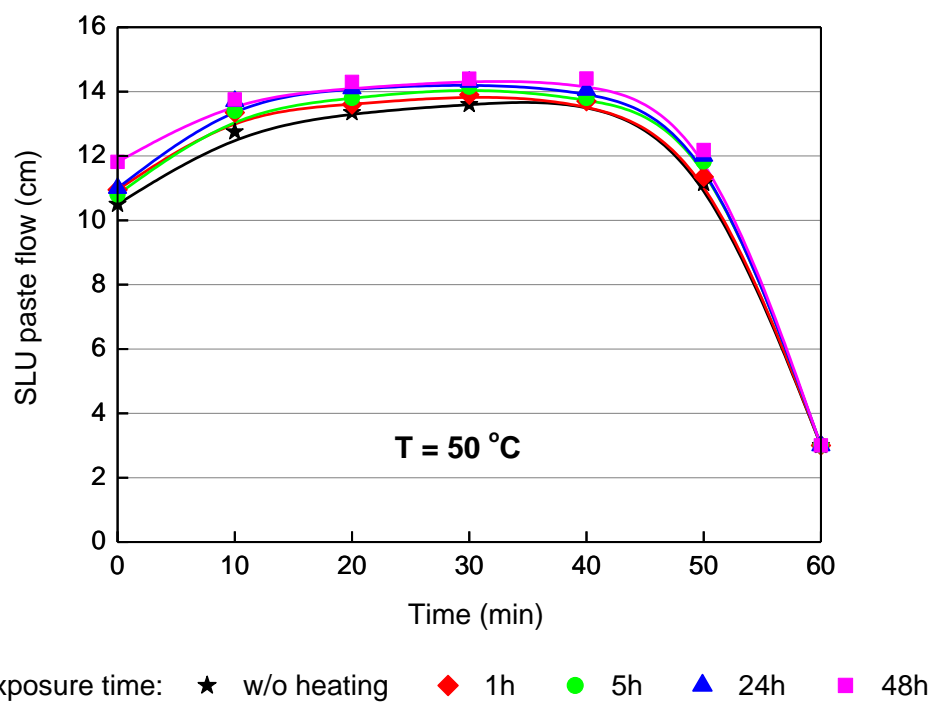
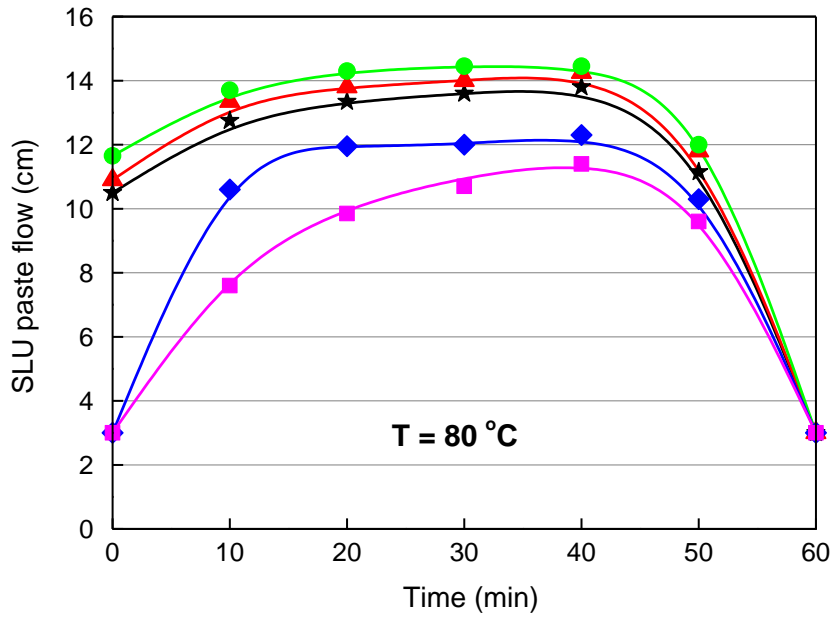


**Figure 5.47** Dispersing effectiveness of a casein sample heated at 50 °C for various time periods, applied in a self-levelling grout.

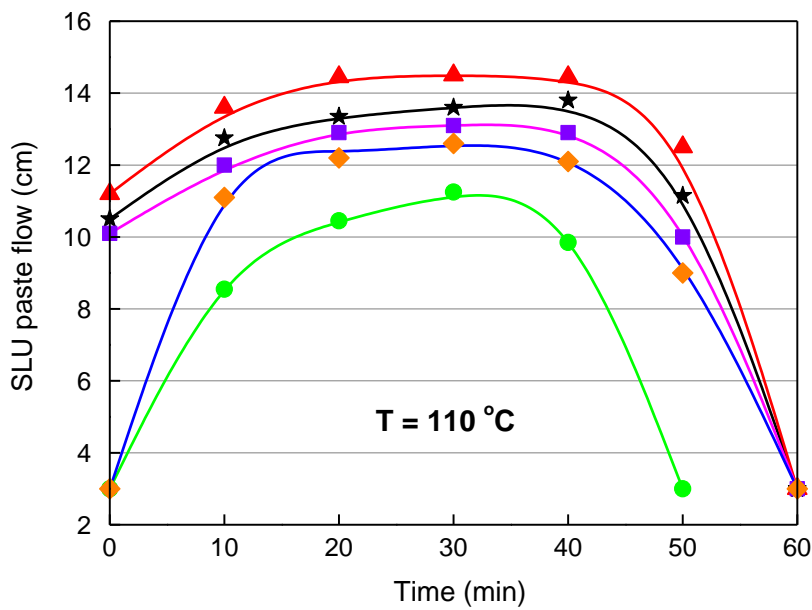
As the heating temperature rose to 80 °C, for short durations (1 h and 5 h), dispersing power of the sample increased slightly and a maximum paste flow of 14.5 cm was attained. However, when the exposure time increased to 24 h or 48 h, then flowability of the SLU pastes was significantly decreased. Although a flow time of 60 min still was maintained, the spread value of the cement paste was much lower, compared to

that of original casein (**Figure 5.48**).



exposure time: ★ w/o heating ▲ 1 h ● 5 h ◆ 24 h ■ 48 h

**Figure 5.48** Dispersing effectiveness of a casein sample heated at 80 °C for various time periods, applied in a self-levelling grout.



exposure time: ★ w/o heating ▲ 1 h ■ 2 h ◆ 3 h ● 5 h

**Figure 5.49** Dispersing effectiveness of a casein sample heated at 110 °C for various time periods, applied in a self-levelling grout.

At further increased heating temperature of 110 °C, the dispersing power of the treated casein was found to be dramatically different, depending on exposure times (**Figure 5.49**). After being treated for 1 h, the casein sample even showed a slightly improved dispersing effect compared to the original casein. When heat treatment was extended to 2 h, a very minor, yet for the application acceptable decrease in dispersing power was observed while after 3 h of exposure, the quality of this casein sample now became affected seriously. Moreover, after 5 h, the dispersing power of the casein had declined substantially, and a maximum spread diameter of 11 cm only was achieved. Furthermore, as the heating durations reached 24 h and 48 h, the treated casein failed entirely to disperse cement, indicating that substantial decomposition (denaturation) of the biopolymer had taken place.

#### **5.4.3 Anionic charge of heat treated casein**

In this part of the work, the anionic charge density of heat treated casein samples was investigated to better understand the different dispersing power they performed. The titration measurement was carried out in an alkaline solution of pH 12 as a model for the SLU pore solution.

According to **Figure 5.50**, original casein showed an anionic charge density of 1,887 µeq/g in alkaline solution. After heat treatment at 50 °C, the charge densities of casein increased slightly with exposure time, and a maximum value of 2,050 µeq/g was achieved after heating for 48h. This result may be attributed to the decreased moisture content, in other words the increased active content of the casein samples after heat treatment. This finding also explains the slight increase in the dispersing power of 50 °C treated casein superplasticizer (**Figure 5.47**).

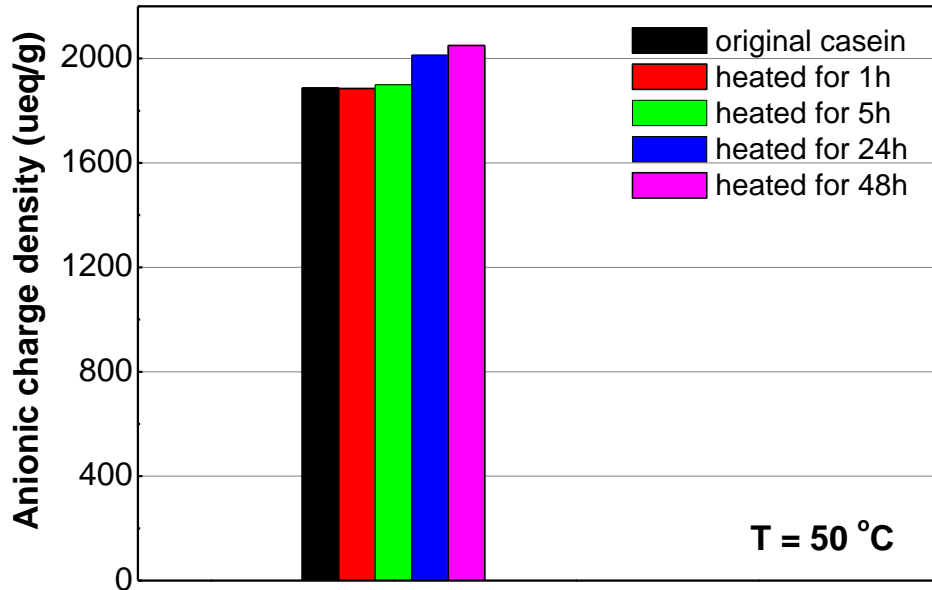


**Figure 5.50** Anionic charge density of casein samples treated at 50 °C, measured in alkaline solution (pH 12,  $c_{\text{casein}} = 1 \text{ g/L}$ ).

When subjected to heating temperatures of 80 °C and 110 °C, the charge densities of the caseins did not show a uniform trend, as revealed in **Figure 5.51** and **Figure 5.52**. Especially at 110 °C, the anionic charge densities of the casein samples decreased after being treated for 24 h and 48 h, reaching 1,799  $\mu\text{eq/g}$  and 1,707  $\mu\text{eq/g}$ , respectively. It suggests that under those harsh conditions, some chemical changes may occur in the casein molecules. Most likely, partial decomposition of the proteins occurred during heat treatment and accordingly the charge density of casein was reduced due to alterations in the molecular structure.

Additionally, it is noted that the charge densities of the casein samples did not always correlate well with their dispersing power in SLU paste. For example, when treated at 80 °C for 24 h and 48 h or at 110 °C for 5 h, the casein samples performed rather poor even though they attained high anionic charge density in alkaline solutions.

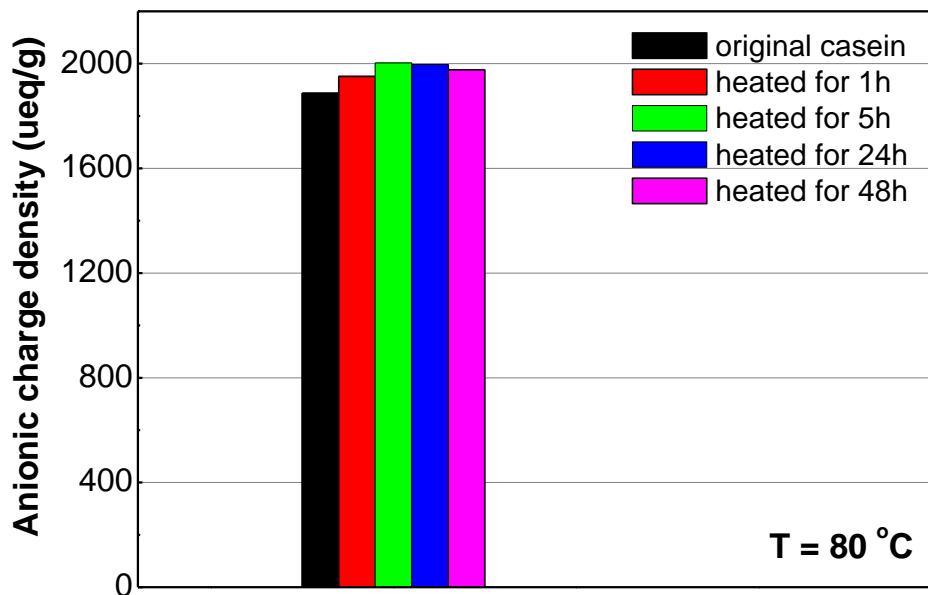


**Figure 5.51** Anionic charge density of casein samples treated at 80 °C, measured in alkaline solution (pH 12,  $c_{casein} = 1$  g/L).

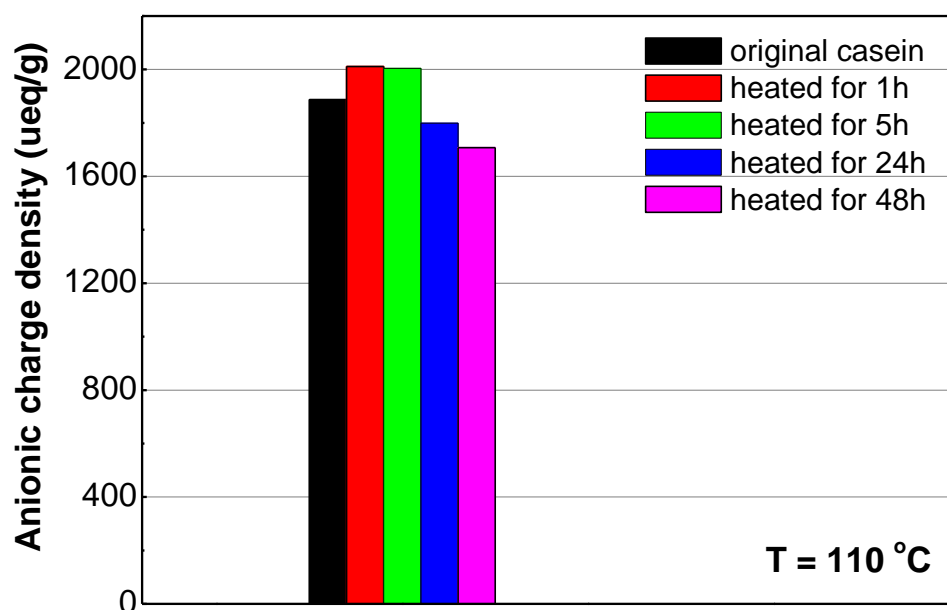


**Figure 5.52** Anionic charge density of casein samples treated at 110 °C, measured in alkaline solution (pH 12,  $c_{casein} = 1$  g/L).

#### 5.4.4 GPC analysis of heat treated casein

Based on the results from above, we postulate that a chemical change occurs in the casein proteins during heat treatment. To verify that, GPC measurements were carried out on the treated casein samples and the results are shown in **Figure 5.53** - **Figure 5.55**.

According to **Figure 5.53**, the GPC elution profiles of casein samples treated at 50 °C were identical with that of original casein. Their molecular weight ( $M_w$ ) was around 39,000 Da which is consistent with the values reported previously. This result suggests heat treatment at 50 °C hardly influences the molecular structure of casein proteins.

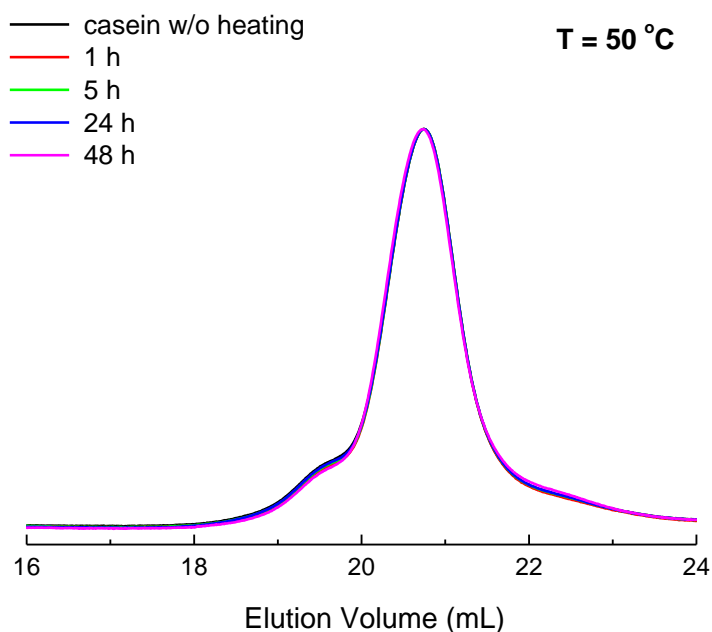


**Figure 5.53** GPC elution profiles of casein samples treated at 50 °C.

In **Figure 5.54**, the elution profiles of caseins exposed to 80 °C show heat induced alterations. Specifically, a growth of the higher molecular weight components (eluted at ~ 17 to ~ 20 mL) which correspond to a  $M_w$  of 102,000 Da occurred after prolonged exposure time. This indicates that a polymerized structure of casein proteins was formed during heat treatment. According to literature, it most likely

derives from the crosslinking between the  $\epsilon$ -amino group of the lysine residue and the carboxyl group in casein molecules [172, 173]. Additionally, also some lower molecular weight components (eluted at 21.5 – 22.9 mL) increased slightly after heating durations of 24 h and 48 h.

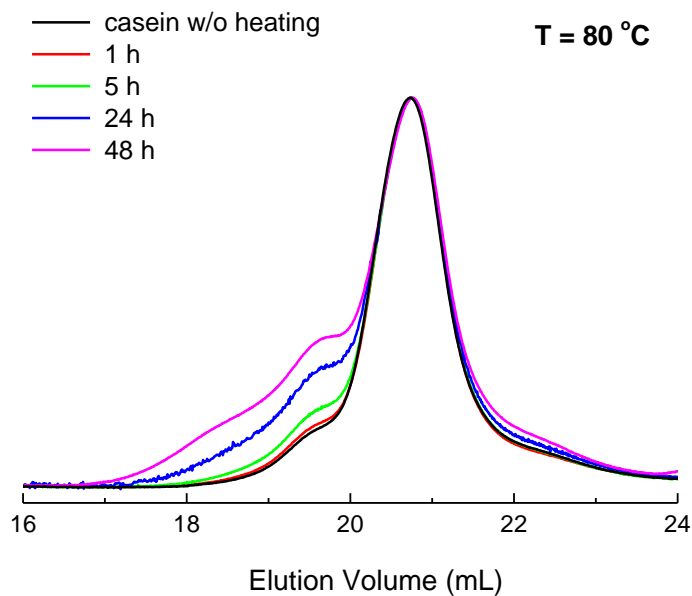


**Figure 5.54** GPC elution profiles of casein samples heated to 80 °C.

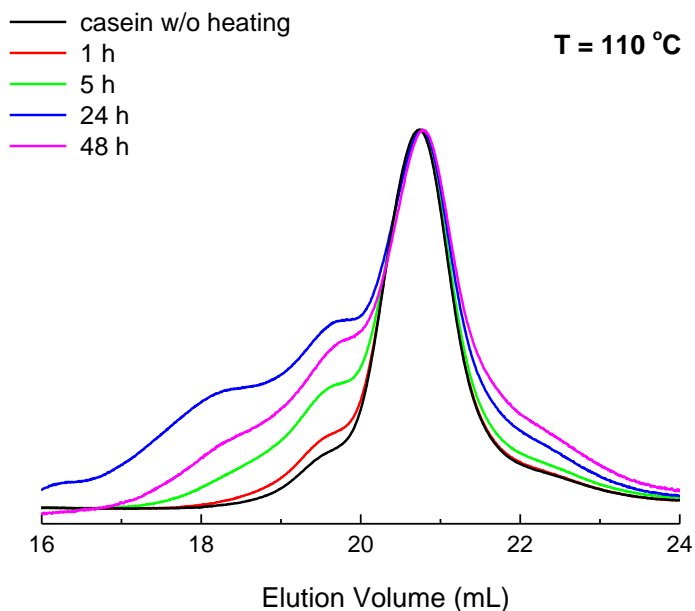


**Figure 5.55** GPC elution profiles of casein samples heated to 110 °C.

The lower molecular weight components significantly increased as the heating temperature rose to 110 °C. They were found to possess a  $M_w$  of 16,000 Da which can be assigned to be small peptides formed in the heat induced decomposition of the casein molecules. According to previous studies, these small peptides may be subjected to further dephosphorylation [174, 175]. Therefore, phosphate groups, the source of negative charge in casein molecules, may be eliminated to some extent, which supposedly explains the slight decrease in anionic charge density of caseins treated at 110 °C (see **Figure 5.52**). The mechanism for the formation of these low molecular weight components is still unknown. However, some previous studies reported that non enzymic cleavage of the peptide linkage in the protein liberated small fragments when heated to 100 °C [172, 176].

To summarize, a heat induced denaturation of casein proteins was disclosed, whereby crosslinking and decomposition reactions co-occurred in the casein molecules, resulting in the formation of polymerized casein proteins as well as small casein peptides.

#### **5.4.5 FPLC analysis of heat treated casein**

Towards a better understanding of the structural changes occurring in the proteins during heating, anion exchange FPLC measurements were carried out on the heat-exposed caseins. The chromatograms obtained are shown in **Figure 5.56 - Figure 5.58**.

From **Figure 5.56**, it is apparent that the absorbance peaks of caseins treated at 50 °C were highly identical to those of original casein, indicating that no chemical change had occurred in the protein fractions at that temperature.

However, the chromatograms of caseins exposed to 80 °C showed a strong dependence on the heating durations, as revealed in **Figure 5.57**. Specifically, the absorbance peaks of samples treated for long periods were found to be different from

that of original casein, whereby the shoulder peak of  $\alpha$ -casein (occurring at 80 - 90 mL) increased. This change was accompanied by a decrease in the main peak of  $\alpha$ - and of  $\beta$ -casein.

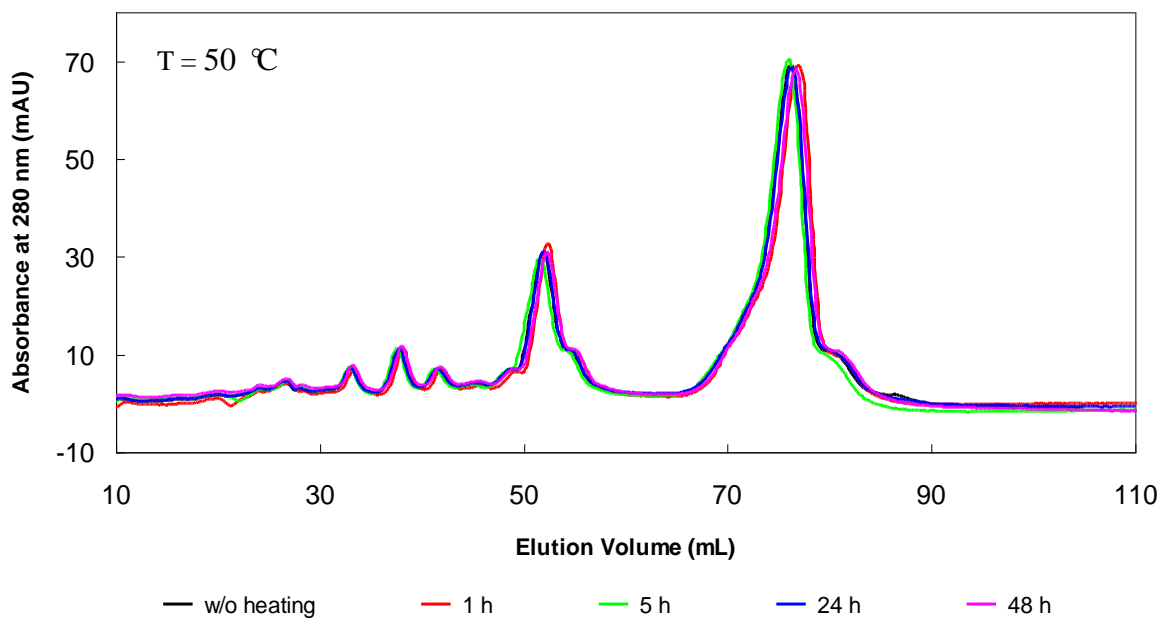


**Figure 5.56** Anion exchange FPLC elution profiles of casein samples treated at 50 °C.

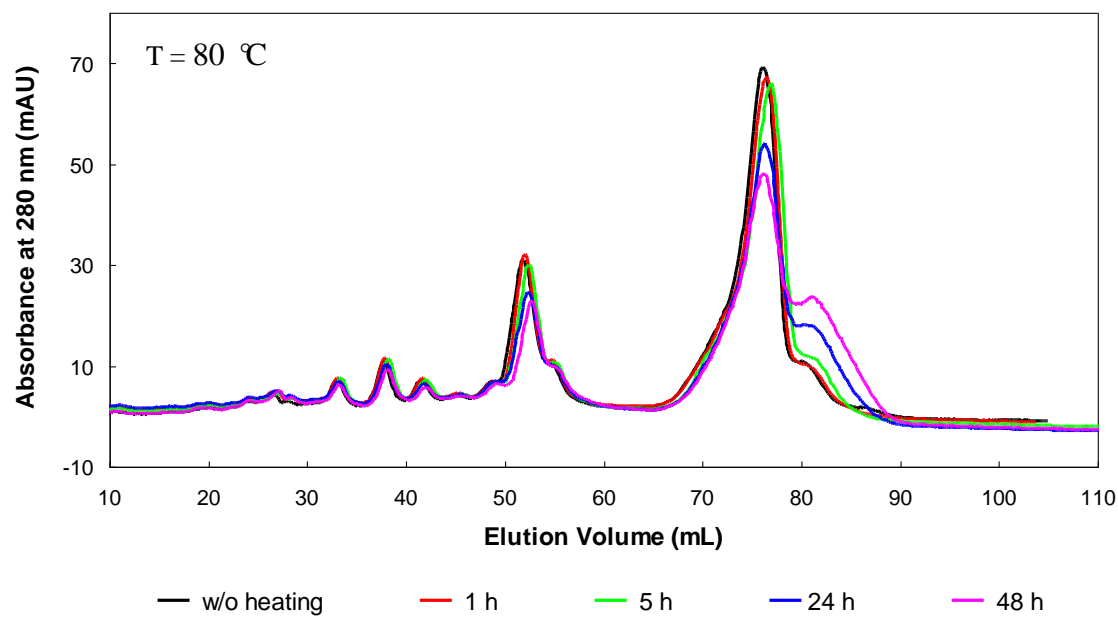


**Figure 5.57** Anion exchange FPLC elution profiles of casein samples treated at 80 °C.

Very significant changes were detected for casein samples treated at 110 °C, as is shown in **Figure 5.58**. After 24 h at 110 °C, the biochemical composition of casein had changed greatly. Specifically, the intensity of the shoulder peak of  $\alpha$ -casein at 81.5 mL increased by 112 %, as compared to that of original casein, achieving an absorbance of 22 mAU at 280 nm. This result confirms that a significant chemical change had occurred in the proteins during the heat treatment. It should be noted the chromatogram of casein treated for 48 h could not be attained due to the very high viscosity of the casein/urea buffer solution. It possibly derives from extensive formation of crosslinked and decomposed casein proteins.

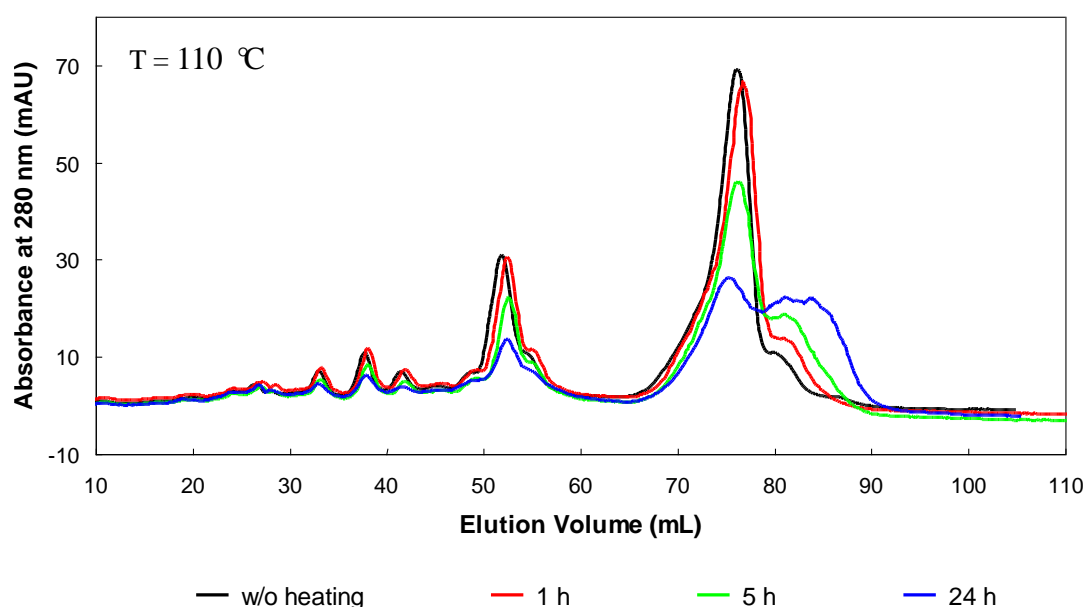


**Figure 5.58** Anion exchange FPLC elution profiles of casein samples treated at 110 °C.

According to previous studies, an increase in the tailing edge, *i.e.* the shoulder peak of  $\alpha$ -casein, may be caused by a loss of positive charges in the casein molecules, which is probably due to the crosslinking between the  $\epsilon$ -amino group of lysine and carboxyl groups present in the proteins [177]. The decreases in  $\alpha$ - and  $\beta$ -casein major peak area further confirmed decomposition of the casein proteins as revealed before by GPC analysis. Uncharged dephosphorylated casein peptides were produced during the heat

induced decomposition, which were not able to absorb on the anion exchange FPLC column and accordingly did not contribute to the UV absorbance at 280 nm. Thus, the FPLC results are consistent with the GPC analysis from above (see section 5.4.4).

#### **5.4.6 Thermal stability of casein superplasticizer**

Based on the results above, we conclude that the influence of heat treatment on the chemical structure of casein molecules is both temperature- and exposure time-dependent. The correlation between these parameters is summarized in **Table 5.4**. A heating temperature of 50 °C does not cause any chemical change in the casein proteins, regardless of exposure time. As temperature rose to 80 °C and 110 °C, crosslinking and decomposition reactions occurred in the protein molecules. The effect became stronger at longer exposure times. At 110 °C, a substantial chemical change in the molecules was observed after a heating duration of 5 h only. The denaturation reactions of casein proteins allow the formation of large polymerized casein as well as the uncharged casein peptides, which most likely reduce the adsorption capacity of casein on cement. Consequently, such heat exposure decreases the dispersing effect of casein on cement.

It was found that a heating temperature of 110 °C in combination with an exposure time of up to 2 h can be regarded as optimal condition for processing and drying casein powder. It does not induce chemical changes to casein and allows the moisture entrapped in casein powder to evaporate to a large extent.

**Table 5.4** Influence of temperature and exposure time on the chemical structure and dispersion quality of casein.

Exposure time Temperature	1 h	5 h	24 h	48 h
50 °C	unchanged	unchanged	unchanged	unchanged
80 °C	unchanged	unchanged	crosslinked decomposed	crosslinked decomposed
110 °C	unchanged	crosslinked decomposed	crosslinked decomposed	crosslinked decomposed

#### 5.4.7 Conclusion

The influence of heat treatment on the quality of casein superplasticizer was investigated. Heat exposure induced moisture evaporation from the casein powder which allowed the formation of a more active casein. The dispersing power of “concentrated” casein, however, did not increase linearly with decreased moisture content. Instead, it was greatly reduced after heat exposure at 110 °C over prolonged time periods. Anionic charge density measurements suggested that a chemical change may have occurred in the casein molecules, which was proven by GPC and FPLC experiments. During heat treatment, crosslinking accompanied by decomposition of the casein proteins had occurred which allowed the formation of large polymerized casein molecules and small dephosphorylated casein peptides, respectively. This denaturation supposedly impaired the adsorption ability of casein on cement and, as a consequence, reduced its plasticizing effect. High temperature and short exposure time, specifically 110 °C and up to 2 h, are proposed as optimal heating conditions for drying casein product. It facilitates fast water evaporation without harming the dispersing power of the superplasticizer in SLUs.

## 6 Summary

In this thesis, the biopolymer casein was investigated with respect to its colloidal properties as well as its application as superplasticizer in cementitious materials. In the pH range of 12 to > 14, first dissociation of casein micelles in dilute solution followed by re-association of casein submicelles were demonstrated employing different characterization techniques. Turbidity as well as zeta potential measurements of aqueous casein dispersions suggested that dissociation of casein micelles occurs in solutions of pH 12 – 13. TEM images revealed that the submicelles found were ~ 10 nm in diameter. At pH  $\geq$  14, re-association of the submicelles occurred, resulting in the formation of crosslinked network aggregates.

The colloidal behavior of casein in alkaline solution can be understood by analyzing the interactions between the casein proteins. It became apparent that calcium phosphate bindings play a critical role in maintaining the integrity of casein micelles and promoting the formation of aggregates. The binding of  $\text{Ca}^{2+}$  to phosphoserine present in the casein proteins significantly reduced electrostatic repulsion between the casein particles, meanwhile promoting an excessive establishment of phosphoserine – calcium phosphate – phosphoserine linkages in highly alkaline environment. This finding was confirmed by a study of the colloidal properties of Ca-depleted casein. The results suggest that removal of calcium from the casein micelles greatly reduces the aggregation tendency of the proteins in highly alkaline solution.

In addition to the micellar behavior in aqueous solutions, the assembly of casein proteins in the dried state was characterized using AFM technique. The morphology of a dried deposit of casein solution was investigated. There, the roughly spherical submicellar structure as well as the assembly of casein proteins was observed in different regions of the deposit. The particle size of submicelles as determined by AFM (~ 20 nm) was found to be slightly larger than those from TEM (~ 10 nm). This difference was attributed to the drying-induced deformation of submicelles and the

broadening effect of the AFM tip during measurement. In addition to submicelle/micelle formation, the casein proteins were found to assemble into rod and worm-like structures on the dried deposit. These results demonstrated a significantly different behavior of casein in solution and in the dried state.

In the second part of this thesis, the technical application of casein as superplasticizer in building materials was studied. In self-levelling underlayments (SLUs), a casein dosage of 0.12 wt.% bwob was found to be sufficient to provide excellent cement dispersion. Furthermore, casein was found to possess a highly negative charge in the pore solution of SLU paste, thus enabling adsorption on the surface of the binder.

The huge quality fluctuation known from commercial casein samples has been confirmed in this work. Five different casein samples were systematically characterized with respect to their physical properties and biochemical compositions. It was found that ion-exchange fast protein liquid chromatography (FPLC) method is sensitive to recognize the differences in the casein samples. Through chromatographic analysis, the proportion of  $\alpha$ -,  $\beta$ -, and  $\kappa$ -casein fractions present in whole casein was determined.  $\kappa$ -casein was found to be critical in governing the dispersing effectiveness of casein in SLUs. A  $\kappa$ -casein content of  $>6\%$  and an  $\alpha/\kappa$ -casein ratio of  $<12$  were revealed to be reliable reference levels for high quality casein. This FPLC method is facile and efficient, *e.g.* it consumes milligram-scale quantity of casein sample for each measurement, and the running time is less than 1 hour.

A working mechanism for casein in cement was proposed based on dynamic light scattering (DLS) measurements of casein solutions at pH 12, which was a model solution for SLU pore solution. It was revealed that casein submicelles are the species which adsorb onto the binder surface, thus facilitating the dispersing effect of casein. Furthermore, particle size of the submicelles was found to be closely related to the content of  $\kappa$ -casein. The more  $\kappa$ -casein is contained in a sample, the smaller are the submicelles which dissociate. The smaller submicelles can adsorb in larger number

onto the surface of cement, thus instigating a higher flowability of the paste. This finding suggests that the biochemical composition of casein determines its dispersing performance in SLUs.

In addition to commercial casein products, also fractionated and modified casein samples were studied in this thesis. The results revealed that there was a considerable variability in the performance of individual casein fractions ( $\alpha$ -,  $\beta$ - and  $\kappa$ -casein).  $\alpha$ -casein stood out over other fractions because it provided the best flow properties as well as an unique self-healing effect on the surface of the grout. Furthermore, a reconstituted casein was prepared from individual pure proteins. Its dispersing performance was characterized using the mini slump test. Compared to original casein, the recombined casein showed improved plastification over the first 20 min after mixing the SLU. Additionally, a chemically treated casein was prepared which showed longer lasting dispersing effectiveness, and good compatibility with other components present in SLUs.

It is known that the quality of casein is influenced by many factors. Here, the effect of heat treatment on the performance of casein was investigated. Specifically, heat induced alteration of casein relative to its moisture content, dispersing power, charge property as well as chromatographic profiles were discussed. Mini slump measurements suggested that at harsh conditions characterized by high temperature and long exposure time, performance of treated casein in SLU paste was reduced significantly. It is believed that crosslinking along with decomposition of the casein proteins occurs during heat treatment, which results in the formation of large polymerized casein molecules and small dephosphorylated casein peptides, respectively. These denatured casein proteins can not adsorb on the binder surfaces, and are responsible for the poor dispersing power of treated casein. However, casein can also benefit from heating for short time periods. In this study, a heat treatment at 110 °C for up to 2 h was found to present optimal drying conditions for casein powder.

To summarize, this thesis attempted a systematic investigation on casein proteins from the aspects of scientific research, industrial application as well as technology development. The results appear to be useful for dry mortar formulators and others who consider natural biopolymers as admixtures in building materials.

## 7 Zusammenfassung

In der vorliegenden Arbeit wurde das Biopolymer Casein im Hinblick auf dessen kolloidale Eigenschaften sowie die Anwendung als Fließmittel in zementären Systemen untersucht. Im pH-Bereich von 12 bis  $> 14$  wurde die Dissoziation von Casein-Mizellen in verdünnten Lösungen, sowie die Reassoziaton von Casein-Submizellen gezeigt. Sowohl Trübungsmessungen als auch die Partikelladung von Casein-Dispersionen lassen auf eine ausgeprägte Dissoziation der Mizellen bei pH-Werten von 12 – 13 schließen. TEM-Aufnahmen zeigten, dass Submizellen in einem Größenbereich von 10 nm die vorherrschende Spezies in diesen Lösungen sind. Bei einer Erhöhung des pH-Werts auf  $\geq 14$  trat Reassoziaton der Submizellen ein, aus welcher die Bildung von quervernetzten Aggregaten folgte.

Das kolloidale Verhalten von Casein in basischen Lösungen wurde an Hand der Wechselwirkungen von Casein-Proteinen untersucht. Es wird angenommen, dass Calcium-Phosphat-Bindungen eine entscheidende Rolle für die Stabilität der Casein-Mizellen spielen und die Bildung von Aggregaten begünstigen. Die Bindung von  $\text{Ca}^{2+}$  und Phosphoserin in Casein-Proteinen verringert die elektrostatische Abstoßung zwischen den Casein-Partikeln deutlich, während sie die vermehrte Bildung von Phosphoserin-Calciumphosphat-Phosphoserin-Bindungen in stark basischen Umgebungen fördert. Dieser Befund wurde durch Untersuchungen der kolloidalen Eigenschaften von Calcium-verarmtem Casein bestätigt. Die Ergebnisse lassen den Schluss zu, dass die Entfernung von Calcium aus Casein-Mizellen eine signifikante Verringerung der Aggregationsneigung der Proteine in stark alkalischer Lösung zur Folge hat.

Zusätzlich zum mizellaren Verhalten in wässriger Lösung wurde der Aufbau der Casein-Proteine im getrockneten Zustand mittels AFM betrachtet. Die Morphologie von Casein in Form einer eingetrockneten Lösung wurde untersucht. Dabei wurde sowohl die angenähert sphärische submizellare Struktur als auch der Aufbau der

Casein-Proteine in verschiedenen Bereichen der Proben beobachtet. Die Partikelgröße der Submizellen gemessen mittels AFM (~ 20 nm) lag etwas höher als der über TEM bestimmte Wert (~ 10 nm), was auf eine durch Trocknung bedingte Deformation der Submizellen sowie den Verbreiterungseffekt der AFM-Spitze während der Messung zurückzuführen ist. Des Weiteren wurde herausgefunden, dass Casein-Proteine im getrockneten Rückstand verschiedene Strukturen ausbilden, wobei die Streifenform die vorherrschende war. Diese Ergebnisse zeigten, dass das Verhalten von Casein in wässriger Lösung und in eingetrocknetem Zustand unterschiedlich ist.

Im zweiten Teil der Arbeit wurde die technische Anwendung von Casein als Fließmittel in der Bauindustrie diskutiert. In Selbstverlaufsmassen wurde eine Casein-Dosierung von 0,12 Gew.-% (bwob) als ausreichend gefunden und dabei das Zetapotential untersucht sowie das Ausbreitmaß mittels 'mini slump' Test bestimmt. Bei dieser Dosierung konnte ein Bluten der Suspension vollständig unterbunden werden, während die Fließfähigkeit hoch blieb. Anhand von Messungen des organischen Kohlenstoffgehalts wurde herausgefunden, dass Casein in der Porenlösung der Selbstverlaufsmasse eine hohe negative Ladung besitzt, womit es leicht an der Oberfläche des Bindemittels adsorbieren kann.

Über Jahrzehnte wurde in der Anwendung immer wieder von großen Unterschieden im verflüssigenden Effekt von Casein berichtet. In der Industrie werden Caseinproben umfangreich auf ihre Leistung in zementären Systemen getestet, was einen signifikanten Kostenfaktor darstellt. Um dieses Problem zu lösen, wurde in dieser Arbeit eine schnelle und günstige Chromatographiemethode zur Prüfung der Qualität von Casein entwickelt. Fünf kommerzielle Caseinproben unterschiedlicher Qualität wurden auf ihre physikalischen Eigenschaften und biochemische Zusammensetzung untersucht. Die Ergebnisse ließen darauf schließen, dass die Methode der Ionenaustausch-FPLC (Fast Protein Liquid Chromatography) dazu geeignet ist, Unterschiede verschiedener Caseinproben herauszufinden. Durch die chromatographische Analyse wurden die Gehalte an  $\alpha$ -,  $\beta$ - und  $\kappa$ -Casein bestimmt. Es

wurde gefunden, dass  $\kappa$ -Casein eine entscheidende Rolle für die Dispergierwirkung von Casein in Selbstverlaufsmassen spielt. Ein  $\kappa$ -Casein-Gehalt von  $> 6\%$  und ein  $\alpha/\kappa$ -Casein-Verhältnis von  $> 12$  wurden als Richtwert für qualitativ hochwertiges Casein ermittelt. Für die FPLC-Messung wird Casein nur im mg-Bereich benötigt, die Messdauer beträgt unter einer Stunde.

Der Wirkmechanismus von Casein-Fließmittel wurde anhand von DLS-Messungen (dynamische Lichtstreuung) von Caseinlösungen bei pH 12, welche als Modelllösungen für Porenlösungen von Selbstverlaufsmassen dienen, ermittelt. Demzufolge bilden Casein-Submizellen die Spezies, die an der Bindemitteloberfläche adsorbiert und damit für die Dispergierwirkung des Fließmittels verantwortlich sind. Außerdem wurde gefunden, dass die Submizellen unterschiedliche Größen aufweisen. Insbesondere zeigten Proben mit einem höheren Anteil von  $\kappa$ -Casein kleinere Partikelgrößen der Submizellen. Dieses Ergebnis erklärt den Zusammenhang zwischen der biochemischen Zusammensetzung und der Dispergierwirkung der Casein-Fließmittel.

Zusätzlich zu den kommerziellen Casein-Fließmitteln wurden in dieser Arbeit auch fraktioniertes und modifiziertes Casein untersucht. Die Ergebnisse zeigten, dass es große Unterschiede in der Wirkung der einzelnen Caseinfraktionen ( $\alpha$ -,  $\beta$ - and  $\kappa$ -Casein) gibt.  $\alpha$ -Casein besitzt exzellente Fließeigenschaften und verleiht dem Mörtel einzigartige Selbstheilungseigenschaften an der Oberfläche. Des Weiteren wurde Casein durch Vermischen der entsprechenden Mengen der reinen Casein-Proteine hergestellt und mittels 'Mini slump' Test charakterisiert. Es zeigte sich, dass das wiedervereinigte Casein eine ähnliche Dispergierwirkung wie natives Casein aufweist, jedoch ein höheres initiales Fließmaß im Bereich  $t = 0 - 20$  min besitzt. Des weiteren wurde ein chemisch behandeltes Casein hergestellt und untersucht. Dieses zeigte nicht nur eine lang anhaltende Dispergierwirkung, sondern auch eine hervorragende Kompatibilität zu anderen Komponenten in Selbstverlaufsmassen.

Es ist bekannt, dass die Qualität von Casein von vielen Faktoren beeinflusst wird, wie beispielsweise den Herstellungsbedingungen. Deshalb wurde der Einfluss einer Hitzebehandlung auf die Eigenschaften von Casein untersucht. Vor allem die durch die Hitze induzierte Veränderung von Feuchtigkeitsgehalt, Dispergierwirkung und Ladungseigenschaften, sowie auch die chromatographischen Eigenschaften wurden betrachtet. Fließmaßbestimmungen zeigten, dass durch eine drastische Hitzebehandlung, spezifiziert durch hohe Temperatur und lange Einwirkungszeit, die Wirkung von Casein in Selbstverlaufsmassen erheblich reduziert werden kann. Es wird davon ausgegangen, dass während einer solchen Hitzebehandlung Quervernetzungsreaktionen zusammen mit einem Abbau von Casein stattfinden, wobei große polymerisierte Caseinmoleküle und dephosphorylierte Caseinpeptide gebildet werden. Diese denaturierten Proteine sind vermutlich für die schlechte Wirkung von stark hitzebehandeltem Casein verantwortlich. In Rahmen dieser Arbeit wurden Trocknungsbedingungen von 110 °C und eine Belastungszeit von max. 2 Std. als optimal herausgefunden.

Somit wurde in dieser Arbeit eine systematische Untersuchung von Casein-Proteinen unter den Aspekten der akademischen Forschung, industriellen Anwendung wie auch der technologischen Weiterentwicklung durchgeführt. Die Ergebnisse erscheinen interessant für die Formulierer von Trockenmörteln sowie für jeden, der natürliche Biopolymere als Zusatzmittel für Baumaterialien in Betracht zieht.

## 8 Reference

---

- [1] H.D. Belitz, W. Grosch, P. Schieberle, Milk and dairy products, in: Food chemistry, Springer, Leipzig, 2009, pp.498-544.
- [2] P.F. Fox, A.L. Kelly, Developments in the chemistry and technology of milk proteins 3. product-related aspects of milk proteins, Food Australia 55 (2003) 337-340.
- [3] J. Plank, Applications of biopolymers and other biotechnological products in building materials, Appl Microbiol Biotechnol 66 (2004) 1-9.
- [4] H.D. Belitz, W. Grosch, P. Schieberle, Amino acids, peptides, proteins, in: Food chemistry, Springer, Leipzig, 2009, pp.8-89.
- [5] P.H. Agarkar, V.L. Maheshwari, Y.A. Kulkarni, Chemistry of amino acids and proteins, in: Biochemistry for nursing, Nirali Prakashan, Abhyudaya Pragati, 2008, pp.3.1-3.20.
- [6] J. G. Salway, Amino acids and the primary structure of proteins, in: Medical biochemistry at a glance, Wiley-Blackwell, New Jersey, 2006, pp.22-23.
- [7] P.F. Fox, Milk proteins: general and historical aspects, in: P.F. Fox, P.L.H. McSweeney (Eds.), Advanced dairy chemistry volume 1: proteins, Kluwer Academic / Plenum Publishers, New York, 2003, pp.1-41.
- [8] H.E. Swaisgood, Chemistry of the caseins, in: P.F. Fox, P.L.H. McSweeney (Eds.), Advanced dairy chemistry volume 1: proteins, Kluwer Academic / Plenum Publishers, New York, 2003, pp.139-187.
- [9] H. Singh, R.J. Bennett, Milk and milk processing, in: R.K. Robinson (Ed), Dairy microbiology handbook third edition, John Wiley and Sons. Inc., New York, 2002, pp.6-7.
- [10] V.A. Vaclavik, E.W. Christian, Milk and milk products, in: Essentials of food science, Springer, New York, 2007, pp. 239.
- [11] D. Rose, J.R. Brunner, E.B. Kalan, B.L. Larson, P. Melnychyn, H.E. Swaisgood, D.F. Waugh, Nomenclature of the proteins of cow's milk: third revision, J Dairy Sci 53 (1970) 1-17.
- [12] B. Vaia, M.A. Smiddy, A.L. Kelly, T. Huppertz, Solvent-mediated disruption of bovine casein micelles at alkaline pH, J Agric Food Chem 54 (2006) 8288-8293.
- [13] P.F. Fox, P.L.H. McSweeney, Milk proteins, in: Dairy chemistry and biochemistry, Kluwer Academic/Plenum Publisher, New York, 1998, pp. 181.

---

[14] N.P. Wong, *Fundamental of dairy chemistry*, Van Nostrand Reinhold, 1988, New York, pp.481-492.

[15] H.S. Rollema, Casein association and micelle formation, In: P.F. Fox (Ed), *Advanced dairy chemistry*, Vol.1: proteins, Elsevier Science Publisher, 1992, Essex, pp.111-140.

[16] J.R. Brunner, Milk proteins, in: J.R. Whitaker, S.R. Tannenbaum, *Food proteins*, AVI Publishing Company, 1977, Connecticut, pp.175-208.

[17] C. Phadungath, Casein micelle structure: a concise review, *Songklanakarin J Sci Technol* 27 (2005) 201-212.

[18] C. Holt, Structure and stability of bovine casein micelles, *Adv Protein Chem* 43 (1992) 63-151.

[19] C.G. De Kruif, C. Holt, Casein micelle structure, functions and interactions, in P.F. Fox, P.L.H. McSweeney (Eds.), *Advanced dairy chemistry volume 1: proteins*, Kluwer Academic / Plenum Publishers, New York, 2003, pp. 252.

[20] P. Walstra, Casein sub-micelles: do they exist?, *Int Dairy J* 9 (1999) 189-192.

[21] H.M. Farrell Jr, Physical equilibria: proteins, in: R. Jenness, N.P. Wong, E.H. Marth, M. Keeney (Eds), *Fundamentals of dairy chemistry third edition*, Aspen Publisher, New York, 1999, pp. 470-471.

[22] R.J. Hill, R.G. Wake, Amphiphile nature of  $\kappa$ -casein as the basis for its micelle stabilizing property, *Nature* 221 (1969) 635-639.

[23] D.J. McMahon, D.J. Brown, Composition, structure, and integrity of casein micelles: a review, *J Dairy Sci* 67 (1984) 499-512.

[24] D.S. Horne, Casein micelle structure and stability, in: A. Thompson, M. Boland, H. Singh (Eds), *Milk proteins from expression to food*, Academic Press, 2008, New York, pp.138-139.

[25] C. Holt, D.T. Davies, A.J.R. Law, The effects of colloidal calcium phosphate content and milk serum free calcium ion concentration on the dissociation of bovine casein micelles, *J Dairy Res* 53 (1986) 557-572.

[26] C.V. Morr, R.V. Josephson, R. Jenness, P.B. Manning, Composition and properties of submicellar casein complexes in colloidal phosphate-free skim milk, *J Dairy Sci* 54 (1971) 1555-1563.

[27] A. Madadlou, M.E. Mousavi, Z. Emam-Djomeh, D. Sheehan, M. Ehsani, Alkaline pH does not disrupt re-assembled casein micelles, *Food Chem* 116 (2009) 929-932.

- 
- [28] R.P.W. Williams, L. D'Ath, B. Zisu, Role of protein aggregation in heat-induced heat stability during milk powder manufacture, *Dairy Sci Technol* 88 (2008) 121-147.
- [29] V. Raikos, Effect of heat treatment on milk protein functionality at emulsion interfaces. A review, *Food Hydrocolloids* 24 (2010) 259-265.
- [30] S.D. Rozycki, M.P. Buera, M.S. Pauletti, Heat-induced changes in dairy products containing sucrose, *Food Chem* 118 (2010) 67-73.
- [31] T. Huppertz, A.L. Kelly, Properties and constituents of cow's milk, in: A.Y. Tamime (Ed), *Milk processing and quality management*, John Wiley & Sons Publisher, 2009, Oxford, pp. 35.
- [32] T.T. Le, P. Saveyn, H.D. Hoa, P. Van der Meeren, Determination of heat-induced effects on the particle size distribution of casein micelles by dynamic light scattering and nanoparticle tracking analysis, *Int Dairy J* 18 (2008) 1090-1096.
- [33] M. Panouille, D. Durand, T. Nicolai, E. Larquet, N. Boisset, Aggregation and gelation of micellar casein particles, *J Colloid Interface Sci* 287 (2005) 85-93.
- [34] J.E. O'Connell, A.L. Kelly, M.A.E. Auty, P.F. Fox, K.G. De Kruif, Ethanol-dependent heat-induced dissociation of casein micelles, *J Agric Food Chem* 49 (2001) 4420-4423.
- [35] T.C.A. McGann, P.F. Fox, Physico-chemical properties of casein micelles reformed from urea-treated milk, *J Dairy Res* 41 (1974) 45-53.
- [36] C. Holt, Casein micelle substructure and calcium phosphate interactions studied by sephacryl column chromatography, *J Dairy Sci* 81 (1998) 2994-3003.
- [37] R. Gebhardt, W. Doster, J. Friedrich, U. Kulozik, Size distribution of pressure-decomposed casein micelles studied by dynamic light scattering and AFM, *Eur Biophys J* 35 (2006) 503-509.
- [38] F.M. Harte, S.R. Gurram, L.O. Luedecke, B.G. Swanson, G.V. Barbosa-Canovas, Effect of high hydrostatic pressure and whey proteins on the disruption of casein micelle isolates, *J Dairy Res* 74 (2007) 452-458.
- [39] A.J.R. Law, J. Leaver, X. Felipe, V. Ferragut, R. Pla, B. Guamis, Comparison of the effects of high pressure and thermal treatments on the casein micelles in goat milk, *J Agric Food Chem* 46 (1998) 2523-2530.
- [40] T. Huppertz, B. Vaia, M.A. Smiddy, Reformation of casein particles from alkaline-disrupted casein micelles, *J Dairy Res* 75 (2008) 44-47.
- [41] J.E. O'Connell, P.F. Fox, The two-stage coagulation of milk proteins in the minimum of the heat coagulation time-pH profile of milk: effect of casein micelle size,

---

J Dairy Sci 83 (2000) 378-386.

[42] S. Ahmad, M. Piot, F. Rousseau, J.F. Grongnet, F. Gaucheron, Physico-chemical changes in casein micelles of buffalo and cow milks as a function of alkalisation, Dairy Sci Technol 89 (2009) 387-403.

[43] A. Madadlou, M.E. Mousavi, Z. Emam-Djomeh, D. Sheehan, M. Ehsani, Alkaline pH does not disrupt re-assembled casein micelles, Food Chem 116 (2009) 929-932.

[44] Y. Liu, R. Guo, pH-dependent structures and properties of casein micelles, Biophys Chem 136 (2008) 67-73.

[45] S.H.C. Lin, S.L. Leong, R.K. Dewan, V.A. Bloomfield, C.V. Morr, Effect of calcium ion on the structure of native bovine casein micelles, Biochemistry 11 (1972) 1818-1821.

[46] A. Pitkowski, T. Nicolai, D. Durand, Stability of caseinate solutions in the presence of calcium, Food Hydrocolloids 23 (2009) 1164-1168.

[47] E. Dickinson, M.G. Semenova, L.E. Belyakova, A.S. Antipova, M.M. Il'in, E.N. Tsapkina, C. Ritzoulis, Analysis of light scattering data on the calcium ion sensitivity of caseinate solution thermodynamics: relationship to emulsion flocculation, J Colloid Interface Sci 239 (2001) 87-97.

[48] C. Holt, Casein micelle substructure and calcium phosphate interactions studied by sephacryl column chromatography, J Dairy Sci 81 (1998) 2994-3003.

[49] C. Holt, Inorganic constituents of milk. III. The colloidal calcium phosphate of cow's milk, J Dairy Res 49 (1982) 29-38.

[50] A. Pitkowski, T. Nicolai, D. Durand, Scattering and turbidity study of the dissociation of casein by calcium chelation, Biomacromolecules 9 (2008) 369-375.

[51] C.R. Southward, Casein products, Consumer and applications science section, New Zealand dairy research institute.

[52] L.A. De Graaf, P. Kolster, Industrial proteins as a green alternative for 'petro' polymers: Potentials and limitations, Macromol Sy 127 (1998) 51-58.

[53] W. Mansfield Clark, H.F. Zoller, A.O. Dahlberg, A.C. Weimar, Studies on technical casein. II--grain-curd casein, Ind Eng Chem 12 (1920) 1163-1167.

[54] P. Kolster, L.A. De Graaf, J.M. Vereijken, Application of cereal proteins in technical applications, in: G.M. Campbell, C. Webb, S.L. Mckee (Eds), Cereals: novel uses and processes, Springer, 1997, New York, pp.107-110.

- 
- [55] J.L. Audic, B. Chaufer, G. Daufin, Non-food applications of milk components and dairy co-products : a review, *Lait* 83 (2003) 417-438.
- [56] C. Winter, J. Plank, The European dry-mix mortar industry (Part 1), *Zement Kalk Gips*, 2007, 62-69.
- [57] D.E. Kuehner, H.W. Blanch, J.M. Prausnitz, Salt-induced protein precipitation: phase equilibria from an equation of state, *Fluid Phase Equilibria* 116 (1996) 140-147.
- [58] K. Cai, J.L.C. Miller, C.J. Stenland, K.J. Gilligan, R.C. Hartwell, J.C. Terry, R.B. Evans-Storms, R. Rubenstein, S.R. Petteway, D.C. Lee, Solvent-dependent precipitation of prion protein, *BBA- Protein Struct M* 1597 (2002) 20-35.
- [59] J.J. Bustamante, M. Aguilar, A.O. Martinez, L.S. Haro, Facilitation of protein purification by the precipitation of proteins in buffers containing solvents, high salts, chelating agents, cheotropic agents and detergents using pyrogallol red-molybdate, *FASEB J* 11 (1997) A1361-A1361.
- [60] J. Szamos, E. Kiss, 3-phase partitioning of crude protein extracts, *J Colloid Interface Sci* 170 (1995) 290-292.
- [61] C. Nakahori, S. Nakai, Fractionation of caseins directly from skim milk by gel chromatography. 1. Elution with sodium dodecylsulfate, *J Dairy Sci* 55 (1971), 25-29.
- [62] T. Sanogo, D. Paquet, F. Aubert, G. Linden, Purification of  $\alpha$ 1-casein by fast protein liquid chromatography, *J Dairy Sci* 72 (1989) 2242-2246.
- [63] T.M. Wei, R. McL. Whitney, Batch fractionation of bovine caseins with diethylaminoethyl cellulose, *J Dairy Sci* 68 (1985) 1630-1636.
- [64] E. Bramanti, F. Ferri, G. Raspi, L. Lampugnani, M.C. Spinetti, K.E. Miller, R.E. Synovec, New method for separation and determination of denatured caseins by hydrophobic interaction chromatography, *Talanta* 54 (2001) 343-349.
- [65] P.J. Kennelly, V.W. Rodwell, Proteins: determination of primary structure, in: M. Weitz, K.J. Davis (Eds), *Harper's illustrated biochemistry*, McGraw-Hill, China, 2009, pp.21-30.
- [66] P. Zakaria, J.P. Hutchinson, N. Avdalovic, Y. Liu, P.R. Haddad, Latex-coated polymeric monolithic ion-exchange stationary phases. 2. micro-ion chromatography, *Anal Chem* 77 (2005) 417-423.
- [67] C. Horvath, W. Melander, I. Molnar, Liquid chromatography of ionogenic substances with nonpolar stationary phases, *Anal Chem* 49 (1977) 142-154.
- [68] C. Horvath, W. Melander, I. Molnar, P. Molnar, Enhancement of retention by ion-pair formation in liquid chromatography with nonpolar stationary phases, *Anal*

---

Chem 49 (1977) 2295-2305.

[69] L.R. Snyder, J.J. Kirkland, J.W. Dolan, The column, in: Introduction to modern liquid chromatography, John Wiley & Sons, 2010, New Jersey, pp.199-223.

[70] W. Kopaciewicz, M.A. Rounds, J. Fausnaugh, F.E. Regnier, Retention model for high-performance ion-exchange chromatography, J Chromatogr A 266 (1983) 3-21.

[71] Ion Exchange chromatography & chromatofocusing principles and methods, Handbooks from GE Healthcare, Data File 11-0004-21 AB, GE Healthcare, Uppsala, 2010.

[72] O. Mikes, Fundamentals of ion-exchange chromatography, in: Z. Deyl, K. Macek, J. Janak (Eds.), Liquid column chromatography: a survey of modern techniques and applications, Elsevier, Amsterdam, 1975, pp.69-85.

[73] B. Védie, I. Myara, M.A. Pech, J.C. Maziere, C. Maziere, A. Caprani, N. Moatti, Fractionation of charge-modified low density lipoproteins by fast protein liquid chromatography, J Lipid Res 32 (1991) 1359-1369.

[74] C.M. Hollar, A.J.R. Law, D.G. Dalgleish, R.J. Brown, Separation of Major Casein Fractions Using Cation-Exchange Fast Protein Liquid Chromatography, J Dairy Sci 74 (1991) 2403-2409.

[75] D.T. Davies, A.J.R. Law, Quantitative fractionation of casein mixtures by fast protein liquid chromatography, J Dairy Sci 54 (1987) 369-376.

[76] C. Kunz, B. Lonnerdal, Human milk proteins: separation of whey proteins and their analysis by polyacrylamide gel electrophoresis, fast protein liquid chromatography (FPLC) gel filtration, and anion-exchange chromatography, Am J Clin Nutr 49 (1989) 464-470.

[77] D. Sheehan, S. O'Sullivan, Fast protein liquid chromatography, in: P. Cutler (Ed), Protein purification protocols, Humana Press, New Jersey, 2004, pp.253-258.

[78] B.G. Kim, S. Jiang, C. Jolicoeur, P.C. Aitcin, The adsorption behavior of PNS superplasticizer and its relation to fluidity of cement paste, Cem Concr Res 30 (2000) 887-893.

[79] J. Golaszewski, J. Szwabowski, Influence of superplasticizer on rheological behavior of fresh cement mortars, Cem Concr Res 34 (2004) 235-248.

[80] P.J. Andersen, D.M. Roy, J.M. Gaidis, W.R. Grace&Co., The effects of adsorption of superplasticizer on the surface of cement, Cem Concr Res 17 (1987) 805-813.

[81] N.B. Singh, R. Sarvahi, N.P. Singh, Effect of superplasticizer on the hydration of

---

cement, *Cem Concr Res* 22 (1992) 725-735.

[82] R. Krstulovic, A. Zmikić, P. Dabić, Examination of reaction between the NSF superplasticizer and cement, *Cem Concr Res* 24 (1994) 948-958.

[83] V.S. Ramachandran, Superplasticizers, in: *Progress in Cement and Concrete*, 1, Part II, ABI Books, New Delhi, 1992, pp. 345-375.

[84] K. Yamada, T. Takahashi, S. Hanehara, M. Matsuhisa, Effects of the chemical structure on the properties of polycarboxylate-type superplasticizer, *Cem Concr Res* 30 (2000), 197-207.

[85] J. Plank, C. Hirsch, Impact of zeta potential of early cement hydration phases on superplasticizer adsorption, *Cem Concr Res* 37 (2007) 537-542.

[86] J. Plank, K. Poellmann, N. Zouaoui, P.R. Andres, C. Schaefer, Synthesis and performance of methacrylic ester based polycarboxylate superplasticizers possessing hydroxy terminated poly(ethylene glycol) side chains, *Cem Concr Res* 38 (2008) 1210-1216.

[87] Nippon Shokubai Co., Ltd., Cement Dispersant, JP Sho (1981) 59-18338.

[ 88 ] M. Mosquet, Y. Chevalier, S. Brunel, J.P. Guicquero, P. Leperchec, Polyoxyethylene di-phosphonates as efficient dispersing polymers for aqueous suspensions, *J Appl Polym Sci* 65 (1997) 2545-2555.

[ 89 ] C. Jolicoeur, M.A. Simard, Chemical admixture-cement interactions: Phenomenology and physico-chemical concepts, *Cem Concr Compos* 20 (1998) 87-101.

[90] S. Hanehara, K. Yamada, Interaction between cement and chemical admixture from the point of cement hydration, absorption behaviour of admixture, and paste rheology, *Cem Concr Res* 29 (1999) 1159-1165.

[91] K. Yamada, S. Hanehara, Interaction mechanism of cement and superplasticizers - The roles of polymer adsorption and ionic conditions of aqueous phase, *Concr Sci Eng* 3 (2001) 135-145.

[92] W. Prince, M. Edwards-Lajnef, P.C. Aitcin, Interaction between ettringite and a polynaphthalene sulfonate superplasticizer in a cementitious paste, *Cem Concr Res* 32 (2002) 79-85.

[93] S. Collepardi, L. Coppola, R. Troli, M. Collepardi, Mechanism of actions of different superplasticizers for high-performance concrete, *Proceedings of the second CANMET/ACI conference on "High-performance concrete. Performance and quality of concrete structures"*, 1999, Gramado (Brazil), pp. 503-523.

---

[ 94 ] C. Jolicoeur, M.A. Simard, Chemical admixture-cement interactions: phenomenology and physico-chemical concepts, *Cem Concr Compos* 20 (1998) 87-101.

[95] S. Kuckova, R. Hynek, M. Kodicek, MALDI-MS applied to the analysis of protein paint binders, in M.P. Colombini, F. Modugno (Eds), *Organic mass spectrometry in art and archaeology*, John Wiley&Sons, Ltd, West Sussex, 2009, pp. 169-170.

[96] J.F. Georgin, J. Ambroise, J. Pera, J.M. Reynouard, Development of self-leveling screed based on calcium sulfoaluminate cement: Modelling of curling due to drying, *Cem Concr Compos* 30 (2008) 769-778.

[97] G. Barluenga, F. Hernandez-Olivares, Self-levelling cement mortar containing grounded slate from quarrying waste, *Constr Build Mater* 24 (2010) 1601-1607.

[98] K. Onishi, T.A. Bier, Investigation into relations among technological properties, hydration kinetics and early age hydration of self-leveling underlayments, *Cem Concr Res* 40 (2010) 1034-1040.

[99] A. Anderberg, L. Wadsoe, Drying and hydration of cement based self-leveling flooring compounds, *Dry Technol* 25 (2007) 1995-2003.

[100] J. Plank, Recent developments in dry mortar technology in Europe, South East Asia Drymix Mortar Association, Technical Bulletin 1, 6-23.

[101] C. Binggeli, P. Greichen, Floor design considerations, in: *Interior graphic standards*, John Wiley and Sons, 2010, New Jersey, pp.345-353.

[102] [http://www.whlxly.com/nt/case\\_detail.asp\\_150\\_26.html](http://www.whlxly.com/nt/case_detail.asp_150_26.html)

[103] D. Urban, K. Takamura, Applications of redispersible powders, in: *Polymer dispersions and their industrial applications*, Wiley-VCH Verlag GmbH Publisher, 2002, Weinheim, pp.345-346.

[104] L.L. Xu, P.M. Wang, G.F. Zhang, Calorimetric study on the influence of calcium sulfate on the hydration of Portland cement–calcium aluminate cement mixtures, *J Therm Anal Calorim* (2011) 1-7.

[105] D.N. Huntzinger, T.D. Eatmon, A life-cycle assessment of Portland cement manufacturing: comparing the traditional process with alternative technologies, *J Clean Prod* 17 (2009) 668-675.

[106] S.N. Ghosh, Portland cement: introduction, composition and properties, in: G.C. Bye (Ed), *Advances in cement technology: chemistry, manufacture and testing*, Taylor&Francis, 2002, New Delhi, pp.1-30.

- 
- [107] H.G. van Oss, A.C. Padovani, Cement manufacture and the environment, part II: environmental challenges and opportunities, *J Ind Ecol* 7 (2003) 93-126.
- [108] M.L. Gambhir, Concrete making materials – I: cement, in: *Concrete technology*, Tata McGraw-Hill Education, 2004, Uttar Pradesh, pp.14-16.
- [109] Ch. Winter, J. Plank, R. Sieber, The efficiencies of  $\alpha$ -,  $\beta$ - and  $\kappa$ -casein fractions for plasticizing cement-based self leveling grouts, *Calcium Aluminate Cements: Proceedings of the Centenary Conference*, Avignon, France, 31 June - 2 July 2008, HIS BRE Press, 2008.
- [110] I. Jawed, J. Skalny, J.F. Young, Hydration of Portland cement, In: P. Barnes (Ed), *Structure and performance of cements*, Applied Science Publishers, 1983, Essex, pp. 237-318
- [111] H. Poellman, Composition of cement phases, in: J. Bensted, P. Barnes (Eds), *Structure and performance of cement*, Spon Press, 2002, London, pp.38-39.
- [112] W.H. Gitzen, L.D. Hart, G. MacZura, Properties of some calcium aluminate cement compositions, *J Am Ceram Soc* 40 (1957) 158-167.
- [113] K. Scrivener, Calcium aluminate cements, in: J. Newman, B.S. Choo (Eds), *Advanced concrete technology: constituent materials*, Butterworth-Heinemann, 2003, Oxford, pp.2/1-2/9.
- [114] J. Bensted, Calcium aluminate cements, in: J. Bensted, P. Barnes (Eds), *Structure and performance of cement*, Spon Press, 2002, London, pp.114-122.
- [115] K.M Parker, J.H. Sharp, Refractory calcium aluminate cements, *Trans J Br Ceram Soc* 81 (1982) 35-42.
- [116] X.D Cong, R.J. Kirkpatrick, Hydration of calcium aluminate cements: a solid-state  $^{27}\text{Al}$  NMR study, *J Am Ceram Soc* 76 (1993) 409-416.
- [117] M. Heikal, M.S. Morsy, M.M. Radwan, Electrical conductivity and phase composition of calcium aluminate cement containing air-cooled and water-cooled slag at 20, 40 and 60 °C, *Cem Concr Res* 35 (2005) 1438-1446.
- [118] M. Singh, M. Garg, Study on anhydrite plaster from waste phosphogypsum for use in polymerised flooring composition, *Constr Build Mater* 19 (2005) 25-29.
- [119] J. Plank, D. Vlad, Studies on the effect of polycarboxylate superplasticizers in sulphatically activated anhydrite self-levelling floor screed, *ZKG International* 59 (2006) 28-39.
- [120] W. Gutt, P.J. Nixon, Use of waste materials in the construction industry analysis of the RILEM symposium by correspondence, *Materials and Structures*, 12 (1979)

---

255-306.

[121] H. Yoshinobu, M. Koji, K. Ryuichi, I. Ko, Dimensional change of self-leveling materials based on aluminous cement-Portland cement-Anhydrite, JCA Proceedings of Cement & Concrete, 58 (2005) 81-86.

[122] J. Plank, Ch. Winter, Competitive adsorption between superplasticizer and retarder molecules on mineral binder surface, Cem Concr Res 38 (2008) 599-605.

[123] A. De Gasparo, M. Herwegh, R. Zurbriggen, K. Scrivener, Quantitative distribution patterns of additives in self-leveling flooring compounds (underlayments) as function of application, formulation and climate conditions, Cem Concr Res 39 (2009) 313-323.

[124] S. Karlsson, E. Banhidi, Z.G. Banhidi, A.C. Albertsson, Accumulation of malodorous amines and polyamines due to clostridial putrefaction indoors. Proceeding of the 3rd International Conference on Indoor Air Quality and Climate, vol.3. The Swedish Council for Building Research, Stockholm, Sweden, pp. 287-293.

[125] S. Karlsson, Z.G. Banhidi, A.C. Albertsson, Identification and characterization of alkali-tolerant clostridia isolated from biodeteriorated casein-containing building materials, Appl Microbiol Biotechnol 28 (1988) 305-310.

[126] J. Plank, P.R. Andres, I. Krause, Ch. Winter, Gram scale separation of casein proteins from whole casein on a Source 30Q anion-exchange resin column utilizing fast protein liquid chromatography (FPLC), Protein Express Purif 60 (2008) 176-181

[127] M. Gretz, Synthese und kolloidchemische Eigenschaften hybrider core-shell Partikel und ihre mögliche Anwendung in der Bauchemie, Dissertation, Lehrstuhl für Bauchemie, Technische Universität München, Garching, 2009.

[128] F. Dugonjić-Bilić, Chemical admixtures for oil well and CO<sub>2</sub>-tolerant cements: synthesis, characterization, effectiveness and working mechanism, Dissertation, Lehrstuhl für Bauchemie, Technische Universität München, Garching, 2010.

[129] J. Plank, B. Sachsenhauser, Experimental determination of the effective anion charge density of polycarboxylate superplasticizers in cement pore solution, Cem Concr Res 39 (2009) 1-5.

[130] Source 15Q, Source 15S, Source 15Q 4.6/100 PE (Tricorn), Source 15S 4.6/100 PE (Tricorn), Resource Q, Resource S, High performance ion exchange chromatography, Data File 18-1123-65 AE, GE Healthcare, Uppsala, 2005.

[131] Source 30Q Source 30S, High performance ion exchange chromatography, Data file 18-1107-12 AB, GE Healthcare, Uppsala, 2007.

- 
- [132] R.V. Levy, M.W. Jornitz, Types of filtration, in: T. Scheper, M.W. Jornitz (Eds), Sterile filtration, Springer, New York, 2006, pp.1-25.
- [133] J.C. Cuevas, E. Scheer, Fabrication of metallic atomic-size contacts, in: Molecular electronics: an introduction to theory and experiment, World Scientific Publishing, London, 2010, pp.19-23.
- [134] G. Kaupp, Atomic force microscopy, in: Atomic force microscopy, scanning nearfield optical microscopy and nanoscratching: application to rough and natural surfaces, Springer, Edewecht, 2006, pp.1-9.
- [135] J. W. Niemantsverdriet, Microscopy and imaging, in: Spectroscopy in catalysis: an introduction, John Wiley & Sons, Weinheim, 2007, pp.200-204.
- [136] J. Plank, K. Poellmann, N. Zouaoui, P.R. Andres, C. Schaefer, Synthesis and performance of methacrylic ester based polycarboxylate superplasticizers possessing hydroxy terminated poly(ethylene glycol) side chains, Cem Concr Res 38 (2008) 1210-1216.
- [137] H.M. Shang, G.Z. Cao, Template-based synthesis of nanorod or nanowire arrays, in: Springer handbook of nano-technology, B. Bhushan (Ed), Springer, New York, 2006, pp.161-175.
- [138] J. Plank, B. Sachsenhauser, Impact of molecular structure on zeta potential and adsorbed conformation of  $\alpha$ -allyl- $\omega$ -methoxypolyethylene glycol – maleic anhydride superplasticizers, J Adv Concr Tech 4 (2006) 233-239.
- [139] Zetasizer nano user manual, Malvern Instruments Ltd., 2007, pp.14-6.
- [140] P. Dreizen, R.W. Noble, D.F. Waugh, Light scattering studies of  $\alpha_{s1,2}$ -caseins, J Am Chem Soc 84 (1962) 4938-4943.
- [141] IonPac® AS11 and AS11-HC anion-exchange columns, Dionex GmbH.
- [142] V.K. Sharma, D.S. Kalonia, Experimental detection and characterization of protein aggregates, in: W. Wang, C.J. Roberts (Eds), Aggregation of Therapeutic Proteins, John Wiley&Sons, 2010, New Jersey, pp.205-256.
- [143] G.J.O. Martin, R.P.W. Williams, D.E. Dunstan, Comparison of casein micelles in raw and reconstituted skim milk, J Dairy Sci 90 (2007) 4543-4551.
- [144] Y. Liu, R. Guo, Interaction between casein and the oppositely charged surfactant, Biomolecules 8 (2007) 2902-2908.
- [145] D. Takahashi, Y. Kubota, K. Kokai, T. Izumi, M. Hirata, E. Kokufuta, Effects of surface charge distribution of proteins in their complexation with polyelectrolytes in an aqueous salt-free system, Langmuir 16 (2000) 3133-3140.

---

[146] P.L. Dubin, S.S. The, D.W. McQuigg, C.H. Chew, L.M. Gan, Binding of polyelectrolytes to oppositely charged ionic micelles at critical micelle surface charge densities, *Langmuir* 5 (1989) 89-95.

[ 147 ] S.K. Kam, J. Gregory, Charge determination of synthetic cationic polyelectrolytes by colloid titration, *Colloid Surface A* 159 (1999) 165-179.

[148] N. Taniguchi, Amino acids and proteins, in: J. Baynes, M.H. Dominiczak (Eds.), *Medical Biochemistry*, Mosby Publisher, London, 1999, pp.7-10.

[149] J. Plank, H. Bian, Method to assess the quality of casein used as superplasticizer in self-levelling compounds, *Cem Concr Res* 40 (2010) 710-715.

[150] D.S. Horne, Casein interactions: casting light on the black boxes, the structure in dairy products, *Int Dairy J* 8 (1998) 171-177.

[ 151 ] K.J. Cross, N.L. Huq, J.E. Palamara, J.W. Perich, E.C. Reynolds, Physicochemical characterization of casein phosphopeptide-amorphous calcium phosphate nanocomplexes, *J Biol Chem* 280 (2005) 15362-15369.

[152] D.J. McMahon R.J. Brown, Composition, structure, and integrity of casein micelles: a review 1, *J Dairy Sci* 67 (1984) 499-512.

[ 153 ] K.J. Cross, N.L. Huq, J.E. Palamara, J.W. Perich, E.C. Reynolds, Physicochemical characterization of casein phosphopeptide-amorphous calcium phosphate nanocomplexes, *J Biol Chem* 280 (2005) 15362-15369.

[154] S.H. Ashoor, R.A. Sair, N.F. Olson, T. Richards, Use of a papain superpolymer to elucidate the structure of bovine casein micelles, *Biochim Biophys Acta* 229 (1971) 423-430.

[155] A. Pitkowski, T. Nicolai, D. Durand, Stability of caseinate solutions in the presence of calcium, *Food Hydrocolloids*, 23 (2009) 1164-1168.

[156] A. Sahu, N. Kasoju, U. Bora, Fluorescence study of the curcumin#casein micelle complexation and its application as a drug nanocarrier to cancer cells, *Biomacromolecules*, 9 (2008) 2905-2912.

[157] K. Helstad, M. Rayner, T. van Vliet, M. Paulsson, P. Dejmek, Liquid droplet-like behaviour of whole casein aggregates adsorbed on graphite studied by nanoindentation with AFM, *Food Hydrocolloids* 21 (2007) 726-738.

[158] H. Mok, H.J. Kim, T.G. Park, Dissolution of biomacromolecules in organic solvents by nano-complexing with poly(ethylene glycol), *Int J Pharm* 356 (2008) 306-313.

[159] Veronique Vie, J. Moreno, S. Beaufils, E. Lesniewska, Interfacial behavior of

---

goat kappa casein: ellipsometry and atomic force microscopy study, *Single Mol* 3 (2002) 127-133.

[160] T. Yakhno, Salt-induced protein phase transitions in drying drops, *J Colloid Interface Sci* 318 (2008) 225-230.

[161] H. Ecroyd, D.C. Thorn, Y.Q. Liu, J.A. Carver, The dissociated form of  $\kappa$ -casein is the precursor to its amyloid fibril formation, *Biochem J* 429 (2010) 251-260.

[162] D.C. Thorn, H. Ecroyd, M. Sunde, S. Poon, J.A. Carver, Amyloid fibril formation by bovine milk  $\alpha$ 2-casein occurs under physiological conditions yet is prevented by its natural counterpart,  $\alpha$ 1-casein, *Biochemistry* 47 (2008) 3926-3936.

[163] M.J. Auld, B.J. Walsh, N.A. Thomson, Seasonal and lactational influences on bovine milk composition in New Zealand, *J Dairy Res* 65 (1998) 401-411.

[164] D.T. Davies, A.J.R. Law, Variation in the protein composition of bovine casein micelles and serum casein in relation to micellar size and milk temperature, *J Dairy Res* 50 (1983) 67-75.

[165] P.H. Risso, V.M. Relling, M.S. Armesto, M.S. Pires, C.A. Gatti, Effect of size, proteic composition, and heat treatment on the colloidal stability of proteolyzed bovine casein micelles, *Colloid Polym Sci* 285 (2007) 809-817.

[166] D. T. Davies, Andrew J. R. Law, Quantitative fractionation of casein mixtures by fast protein liquid chromatography, *J Dairy Res* 54 (1987) 369-376.

[167] Y. Igarashi, Separation of caseins by chemical procedures, *Int Dairy J* 9 (1999) 377-378.

[168] A.L. Andrews, D. Atkinson, M.T.A. Evans, E.G. Finer, J.P. Green, M.C. Philips, R.N. Robertson, The conformation and aggregation of bovine  $\beta$ -casein A. I. Molecular aspects of thermal aggregation, *Biopolymers* 18 (1979) 1105-1121.

[169] H. Singh, Heat stability of milk, *Int J Dairy Technol* 57 (2004) 111-119.

[170] S. Sandra, D.G. Dalgleish, Effects of ultra-high-pressure homogenization and heating on structural properties of casein micelles in reconstituted skim milk powder, *Int Dairy J* 15 (2005) 1095-1104.

[171] A. Raemy, R.F. Hurrell, J. Loeliger, Thermal behaviour of milk powders studied by differential thermal analysis and heat flow calorimetry, *Thermochimica Acta* 65 (1983) 81-92.

[172] H. Kato, M. Matsumura, F. Hayase, Chemical changes in casein heated with and without D-glucose in the powdered state or in an aqueous solution, *Food Chem* 7 (1981) 159-168.

---

[173] J. Bjarnason, K.J. Carpenter, Mechanisms of heat damage in proteins, *Br J Nutr* 23 (1969) 859-868.

[174] H. Meisel, H.B. Andersson, K. Buhl, H.F. Erbersdobler, E. Schlimme, Heat-induced changes in casein-derived phosphopeptides, *Z Ernahrungswiss* 30 (1991) 227-232.

[175] J. Belec, R. Jenness, Dephosphorization of casein by heat treatment. I. In caseinate solutions, *J Dairy Sci* 45 (1962) 12-19.

[176] N.V. Chuyen, T. Kurata, M. Fujimaki, Formation of N-[2(3-alkylpyrazin-2-on-1-yl)acyl]-amino acids or -peptides on heating tri- or tetra-peptides with glyoxal, *Agric Biol Chem* 37 (1973) 1613-1618.

[177] A.J.R. Law, D.S. Horne, J.M. Banks, J. Leaver, Heat-induced changes in the whey proteins and caseins, *Milchwissenschaft* 49 (1994) 125-129.